Enterococcus faecalis-derived lactic acid suppresses macrophage activation to facilitate persistent and polymicrobial wound infections

Ronni A. G. da Silva[1,2], Brenda Yin Qi Tien[2], Patrick Hsien Neng Kao[2], Haris Antypas[2], Cenk Celik[3], Ai Zhu Casandra Tan[2], Muhammad Hafiz Ismail[2], Guangan Hu[5], Kelvin Kian Long Chong[2], Guillaume Thibault[3,4], Jianzhu Chen[1,5], Kimberly A. Kline[1,2,6*]

[1] Singapore-MIT Alliance for Research and Technology Centre, Antimicrobial Resistance Interdisciplinary Research Group, Singapore

[2] Singapore Centre for Environmental Life Sciences Engineering, Nanyang Technological University, 60 Nanyang Drive, Singapore 637551.

[3] School of Biological Sciences, Nanyang Technological University, Singapore

[4] Mechanobiology Institute, National University of Singapore, Singapore

[5] Koch Institute for Integrative Cancer Research and Department of Biology, Massachusetts Institute of Technology, Cambridge, MA, United States of America

[6] Department of Microbiology and Molecular Medicine, Faculty of Medicine, University of Geneva, Switzerland

[*]Correspondence: Kimberly.Kline@unige.ch

Graphical Abstract

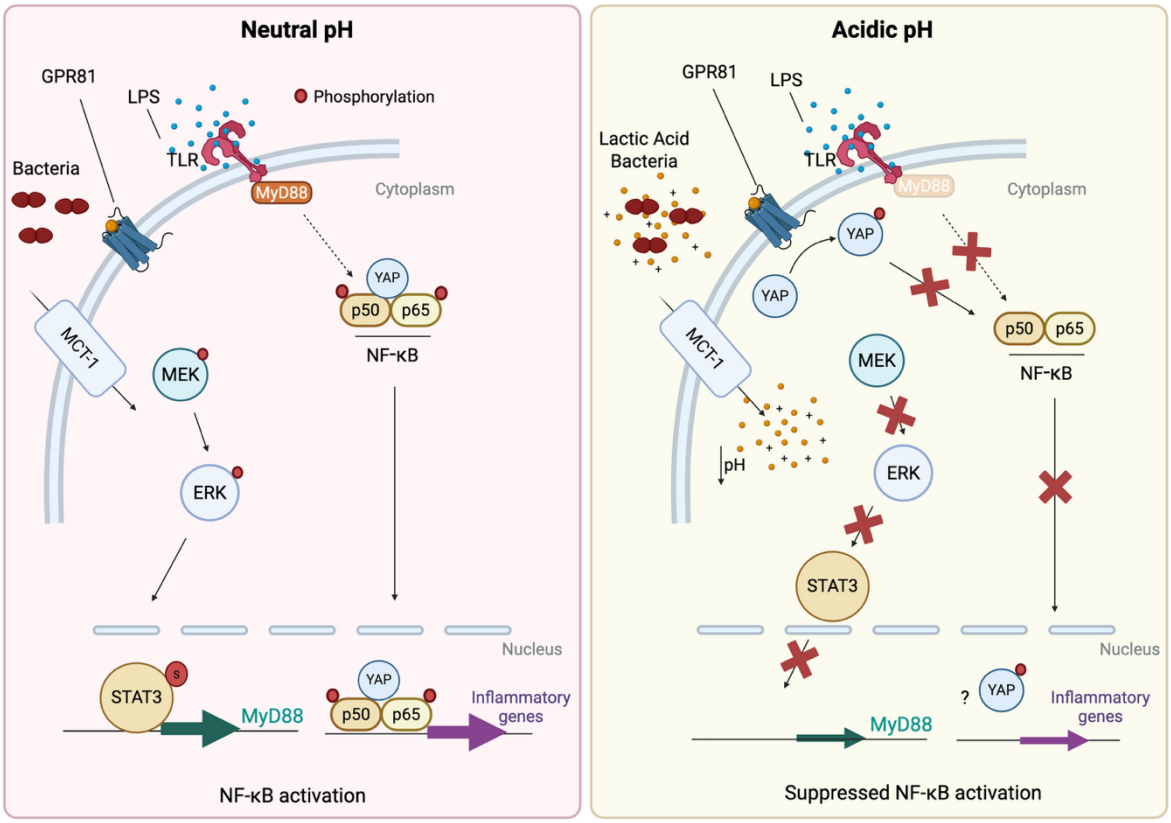

Highlights

- *E. faecalis* lactate dehydrogenase mutants fail to acidify the environment and cannot suppress NF-κB signaling.
- Lactic acid is necessary and sufficient to drive NF-κB suppression in macrophages.
- Lactic acid NF-κB suppression is relayed through two complementary routes: MCT-1 transport and the lactate sensor GPR81.
- MCT-1-dependent signaling blunts ERK/STAT3 phosphorylation, lowering MyD88 levels; whereas GPR81 drives YAP phosphorylation, reducing NF-κB activation.
- *E. faecalis*-derived lactic acid drives immunosuppression, potentiates persistence, and promotes multi-species wound infection *in vivo*.

Summary

Macrophage activation is essential for innate immunity, and its suppression enables pathogen persistence. We show that *Enterococcus faecalis* suppresses macrophage activation through lactic acid-mediated extracellular acidification. Mutants lacking lactate dehydrogenase (*ldh*), and thus unable to acidify the environment, fail to inhibit NF-κB. *E. faecalis*-derived lactic acid acts via MCT-1 and GPR81 through two distinct but complementary mechanisms that culminate in the reduction of NF-κB activity. Lactic acid acts through MCT-1 to inhibit ERK and STAT3 phosphorylation, leading to reduced STAT3 binding to the *Myd88* promoter, and reduced MyD88 protein levels. Lactic acid signaling to GPR81 mediates the phosphorylation of the transcriptional factor YAP, ultimately attenuating NF-κB signaling. In a murine wound infection model, this lactic acid-driven immunosuppressive niche enables prolonged *E. faecalis* persistence and enhances the fitness of co-infecting bacteria such as *Escherichia coli.* These findings reveal how bacterial lactic acid subverts innate immunity to support chronic and polymicrobial infections.

Introduction

Enterococcus faecalis are commensal, lactic acid producing, Gram-positive bacteria that are ubiquitous in the healthy human gastrointestinal tract [1]. *E. faecalis* are also opportunistic pathogens in the nosocomial environment, particularly among immunocompromised individuals, contributing to considerable morbidity and mortality in susceptible populations [2, 3]. *E. faecalis* infections are often polymicrobial in nature with two or more species present at an infection site, especially in catheter associated urinary tract infections (CAUTI) and wound infections [4-6]. Treatment of *E. faecalis* infections has become increasingly difficult due to their acquired antibiotic resistance,

antibiotic tolerance associated with their ability to form biofilm in the host, and intracellular survival [4, 7-9].

The nuclear factor kappa-light-chain-enhancer of activated B cells (NF-κB) pathway is a central regulator of the immune response to bacterial and viral infections [10-12]. Stimuli, such as lipopolysaccharide (LPS) or lipoteichoic acid (LTA), are recognized by co-receptors, including CD14 and pattern recognition Toll-like receptors (TLRs), inducing TLR dimerization and cargo internalization. This process, mediated by downstream adaptor proteins such as MyD88, initiates a signaling cascade that ultimately activates the IκB kinase (IKK) complex [13]. The IKK complex phosphorylates IκB, leading to its ubiquitin-dependent degradation and release of the NF-κB transcription factor (typically a p65/p50 dimer), which then translocates to the nucleus and subsequently drives the expression of genes involved in immunity, inflammation, and cell survival [10].

Recent work highlights the importance of host metabolic and epigenetic regulators in controlling inflammatory signaling [14, 15]. The monocarboxylate transporter 1 (MCT-1, encoded by *SLC16A1*) facilitates proton-coupled lactate transport, thereby influencing intracellular pH and redox balance [16]. MCT-1 activity can alter macrophage transcription and inflammatory responses [17]. Similarly, the G-protein-coupled lactate receptor GPR81 (also known as hydroxycarboxylic acid receptor 1, HCAR1) senses extracellular lactate to regulate AMPK–YAP signaling, which can suppress NF-κB-driven cytokine expression and dampen inflammation [18, 19]. In addition, histone deacetylases (HDACs) fine-tune NF-κB responses by deacetylating histones and NF-κB subunits such as p65/RelA, thereby influencing chromatin

accessibility and transcriptional activity [20, 21]. Together, these systems link metabolic cues, pH homeostasis, and epigenetic regulation to immune signaling control in macrophages.

To colonize and persist within the human host, *E. faecalis* deploys multiple strategies to evade immune clearance, including biofilm formation to hinder phagocytosis by immune cells, and prolonged survival within macrophages and neutrophils [8, 9, 22-28]. *E. faecalis* strains isolated from the gastrointestinal tract of healthy human infants can suppress mitogen-activated protein kinase (MAPK) and NF-κB signaling, as well as interleukin 8 (IL-8) expression in intestinal epithelial cells *in vitro* [29, 30]. We previously demonstrated that *E. faecalis* infection suppresses NF-κB signaling in RAW 264.7 macrophages at high multiplicities of infection (MOI 100) [31]. In addition, *E. faecalis* suppresses lipopolysaccharide (LPS) or lipoteichoic acid (LTA)-mediated NF-κB activation in the same cell line in a dose-dependent manner [31]. However, the *E. faecalis* and host factors involved in NF-κB suppression in macrophages were not reported.

In this study, we identified *E. faecalis* lactate dehydrogenase and its lactic acid product as critical factors in macrophage suppression. *E. faecalis*-derived lactic acid lowers the extracellular pH [39]. Lower extracellular pH increases the activity of MCT-1 to transport protons and lactate into the intracellular environment driving down the intracellular pH [16, 32, 33] which impairs STAT3-dependent transcription of *Myd88*, ultimately preventing signaling transduction leading to NF-κB activation. In parallel, low extracellular pH likely enhances GPR81 affinity for extracellular lactate, in turn triggering AMPK-LATS signaling, increasing inhibitory YAP phosphorylation [19, 34],

115 and limiting NF-κB activation. In addition, lactic acid-mediated immune suppression
116 promotes persistent *E. faecalis* wound infection and promotes *E. coli* growth during
117 mixed species wound infection. These findings advance our understanding of *E.*
118 *faecalis* pathogenesis and identify potential targets for immunotherapeutic strategies
119 aimed at improving treatment and prevention of recalcitrant infections.
120

121 ## Results

122 ### *E. faecalis* infection suppresses the antibacterial response of macrophages

123 We previously demonstrated that *E. faecalis* can suppress LPS- and LTA-mediated
124 NF-κB activation in RAW 264.7 macrophages in a dose-dependent manner without
125 causing host cell cytotoxicity [22]. To further investigate this immunosuppression, we
126 infected RAW 264.7 macrophages for 6 h with *E. faecalis* strain OG1RF in the
127 presence or absence of LPS followed by RNA sequencing. Gene set enrichment
128 analysis (GSEA) revealed that while *E. faecalis* infection at MOI 100 enriched for
129 pathways linked to the immune response to bacteria, *E. faecalis* suppressed pathways
130 associated with positive immune regulation and defense responses in LPS-treated
131 cells, **(Fig. 1A, SI 1-3)**. To explore how *E. faecalis* interferes with NF-κB signaling, we
132 examined transcripts of key genes in this pathway. LPS alone increased transcripts
133 that encode the LPS co-receptor CD14 [35] and the transcription factor p50 precursors
134 p100 and p105 **(Fig. 1B, Table S1, SI 4-6)**. *E. faecalis* significantly suppressed some
135 of these LPS-induced transcripts, with *Myd88* expression reduced by ~2-fold in MOI
136 100-infected LPS-untreated macrophages and nearly 4-fold in MOI 100-infected LPS-
137 treated macrophages **(Fig. 1B, Table S1)**. This suppression may explain why NF-κB
138 is inactive following MOI 100 infection, despite higher transcript levels of genes
139 encoding p100 and p105 compared to uninfected cells **(Fig. 1B, Table S1, SI 4-6)**.

140 Consistently, the levels of MyD88 protein were lower in MOI 100-infected
141 macrophages with or without LPS, as well as the downstream phosphorylated TAK1,
142 IKK, IκBα, and p65 but not the levels of the unphosphorylated TAK1, IKKα and p65
143 **(Fig. 1C and Fig. S1A)**.
144
145 Since MyD88 also activates AP-1 **(Fig. S1B)**, we investigated components of this
146 pathway, including ERK, c-Jun N-terminal kinases (JNK), p38, and AP-1 (c-Jun and
147 c-Fos). While LPS did not affect AP-1 pathway transcript levels **(Fig. 1B, Table S1)**,
148 MOI 100 infection reduced p38 transcripts compared to uninfected macrophages. In
149 LPS-treated cells, MOI 100 infection decreased *Fos* (encoding c-Fos) transcripts
150 relative to controls. Protein analysis showed significantly reduced phosphorylated
151 ERK at MOI 100, regardless of LPS presence **(Fig. 1C)**, while total and
152 phosphorylated levels of p38 and JNK, as well as total ERK levels were unaffected
153 **(Fig. 1C and S1C)**. Minimal changes in phosphorylated c-Jun and c-Fos at MOI 100
154 suggest that *E. faecalis* likely interferes with AP-1 activation to a lesser degree than
155 with NF-κB **(Fig. S1C)**.
156
157 To determine if *E. faecalis* affects other aspects of MyD88-related signaling, beyond
158 suppressing *Myd88* expression, we analyzed the RNA-seq data to include a wider
159 range of immune signaling genes. While *Tlr4* transcript levels remained unchanged by
160 *E. faecalis* infection, expression of *Cd14* was reduced following 6 h of infection of LPS-
161 treated cells, indicating that *E. faecalis* might also impact cargo internalization as
162 CD14 mediates the LPS-induced internalization of extracellular molecules [23] **(Fig.
163 1B and Table S1)**. Although there was a significant delay in CD14 internalization at
164 early times in *E. faecalis* infected cells, there was no marked difference in CD14

165 internalization at the end of the experiment, suggesting that *E. faecalis* infection-
166 mediated suppression of NF-κB cannot be explained by changes in CD14 levels and
167 internalization **(Fig. 1D)**. Similarly, *E. faecalis* infection had no effect on TLR2
168 internalization with or without LTA **(Fig. S1D)**. These data show that *E. faecalis*
169 infection suppresses NF-κB activation in macrophages by reducing MyD88 protein
170 levels and preventing the downstream phosphorylation cascade and leading to NF-κB
171 suppression.
172
173 **Lactate dehydrogenase-dependent lactic acid production by *E. faecalis* drives**
174 **suppression of macrophage NF-κB activation**
175 To investigate the bacterial factors involved in suppression of macrophage activation,
176 we screened a ~15,000 member *E. faecalis* mariner transposon library [36] for mutants
177 that failed to suppress LPS-induced NF-κB activation in RAW 264.7 macrophages.
178 We identified 151 transposon mutants in our primary screen **(Fig. S2A)** which were
179 then subjected to secondary analyses for growth defects, leading to a final list of 47
180 transposon mutants that failed to suppress NF-κB activation **(Fig. S2B, Table S2)**.
181 Bacterial growth in media containing a pH indicator showed that 18 of 47 mutants
182 failed to acidify the media as a function of growth as compared to wild type (WT) *E.*
183 *faecalis* **(Fig. S2B).** Among these was *ldh1* (OG1RF_10199), encoding lactate
184 dehydrogenase (LDH) **(Fig. S2B)**, which reduces pyruvate to L-lactate to generate
185 NAD^+ for ongoing glycolysis in *E. faecalis* [37, 38]. L-lactate is released from *E. faecalis*
186 in the form of lactic acid, which is subsequently deprotonated to L-lactate, releasing a
187 hydrogen ion (H^+) and in turn lowering the pH in the surrounding environment. Since
188 acidification is a defining feature of *E. faecalis* metabolism due to the release of lactic
189 acid [39], we further investigated the impact of LDH on NF-κB activation.

190

191 The *E. faecalis* genome contains two LDH genes, *ldh1* and *ldh2,* where LDH1 plays
192 the major role in lactic acid production under laboratory conditions as compared to
193 LDH2 [37]. As predicted, and confirming the result of the transposon screen, infection
194 of RAW 264.7 macrophages with Δ*ldh1* or the Δ*ldh1*Δ*ldh2* double mutant (hereafter
195 called Ldh), failed to suppress LPS-induced NF-κB activation as compared to WT *E.*
196 *faecalis*, Δ*ldh2,* or *ldh1* complementation strains **(Fig. 2A).** Immunofluorescence using
197 confocal laser scanning microscopy (CLSM) to investigate p65 nuclear localization
198 confirmed WT suppression and Ldh activation of NF-κB **(Fig. 2B and S3)**. Failure to
199 suppress macrophage activation was not due to a growth defect of the mutants,
200 whether grown in BHI or cell culture medium **(Fig. S4A-B)**. Lactic acid accumulated in
201 culture supernatants of WT *E. faecalis* infected cells in an MOI-dependent manner,
202 resulting in a pH decrease that is delayed for the Ldh mutant **(Fig. S4C-D)**. In contrast
203 to WT *E. faecalis*, macrophage infection with either the Δ*ldh1* or Ldh mutants produced
204 less lactic acid and, consequently, acidified the environment at a slower rate than WT
205 *E. faecalis,* in agreement with lesser suppression of NF-κB **(Fig. 2A and S4E-F)**.
206 Consistent with previous reports, Δ*ldh2* was not attenuated for lactate release [37, 40].
207

208 To confirm that LDH-mediated macrophage suppression was not specific to RAW
209 264.7 macrophages, we assessed the release of the NF-κB-regulated cytokine IL-6
210 from murine bone marrow-derived macrophages (BMDM) infected with Δ*ldh1* and Ldh
211 mutants compared to WT *E. faecalis* **(Fig. 2C)***.* Similar to RAW 264.7 macrophages,
212 infection with either WT or the Δ*ldh1* complemented strains had no effect on IL-6
213 release by BMDM, whereas infection of LPS-treated cells with either Δ*ldh1* or Ldh
214 stimulated IL-6 production **(Fig. 2C)**. qRT-PCR analysis of representative genes

215 showed that *E. faecalis* infection of BMDM, as in RAW264.7 cells, decreased *Myd88*
216 expression **(Fig. S5)**. Infection of BMDM or the human monocytic cell line THP-1 with
217 *E. faecalis* similarly showed an LDH-dependent decrease of MyD88, p-ERK, and p-
218 p65 levels **(Fig. S6A-B)**. Multiplex cytokine analysis of RAW264.7 cells also confirmed
219 an LDH-dependent reduction of pro-inflammatory cytokines (IL-6, IL-12 p70 and IFNγ)
220 and chemokines (CCL3, CCL4, CCL5, CSF2 and CSF3) for *E. faecalis*-infected
221 macrophages **(Fig. S6C)**. Furthermore, supplementation of macrophages infected
222 with the Ldh mutant with a minimum of 20 mM lactic acid restored suppression of LPS-
223 induced NF-κB activation to similar levels as WT *E. faecalis* **(Fig. 2D)**. In the absence
224 of infection, 40 mM lactic acid was sufficient to suppress LPS-induced NF-κB
225 activation **(Fig. 2E)** without compromising macrophage viability **(S6D)**. In addition, WT
226 *E. faecalis* suppressed LPS-induced NF-κB activation even in cells pre-activated with
227 LPS for 1 h prior to infection **(Fig. S6E-F)**. As expected, the Ldh mutant failed to
228 suppress NF-κB activation independent of LPS pre-exposure **(Fig. S6E-F)**. Overall,
229 these results demonstrate that *E. faecalis* suppression of NF-κB activation in
230 macrophages is mediated by LDH-derived lactic acid.
231

232 **Extracellular acidification, rather than lactate alone, underlies NF-κB**
233 **suppression during *E. faecalis* infection**

234 Among the 47 transposon mutants that failed to suppress macrophage activation, 18
235 did not acidify the medium to the same extent as WT *E. faecalis*, but only 11 produced
236 less lactate **(Fig. S2B)**, suggesting that pH reduction rather than lactic acid production
237 alone is the primary driver of NF-κB suppression. Indeed, supplementation with 40
238 mM lactic acid suppressed NF-κB activation, whereas 40 mM sodium L-lactate did not
239 **(Fig. 3A)**. To confirm this, we acidified filtered Ldh mutant supernatants to pH 6.4 (pH

240 equivalent to WT MOI 100) or neutralized WT supernatants to pH 7.8 (pH equivalent
241 to MOI 1). Acidified supernatants suppressed LPS-induced NF-κB activation across
242 all MOI in the absence of cytotoxicity, while neutralized supernatants failed to do so
243 **(Fig. 3B-C, S7A-E)**. Consistent with previous reports [41], acidifying cell culture media
244 to pH 6.4 using HCl or phosphoric acid (H_3PO_4) also suppressed LPS-induced NF-κB
245 activation without affecting macrophage viability **(Fig. 3D and S7F).** p-p65 levels were
246 also reduced in LPS-stimulated macrophages infected with the Ldh mutant when
247 supplemented either with lactic acid or HCl, compared to those without acid
248 supplementation **(Fig. S7G)**.
249
250 Since *E. faecalis* can persist and replicate within macrophages [9, 42], we investigated
251 whether intracellular *E. faecalis* contributed to NF-κB suppression. We therefore
252 infected macrophages with *E. faecalis* for 3 h, followed by antibiotic killing of
253 extracellular bacteria [9]. In the absence of extracellular *E. faecalis*-mediated
254 acidification of the medium, we observed increased NF-κB activation at all MOI during
255 intracellular infection, without significant cell death **(Fig. S8A-B).** In fact, *E. faecalis*
256 infection resulted in higher NF-κB activation than the LPS positive control **(Fig. 3E)**.
257 Heat and UV-killed *E. faecalis* similarly were not capable of suppressing NF-κB at high
258 MOI **(Fig. S8C-D)**. Together, our results suggest that extracellular acidification, rather
259 than lactate levels or intracellular infection, is important for *E. faecalis*-mediated
260 immune suppression in macrophages.
261
262 ***E. faecalis* suppresses MyD88 expression by pH-dependent STAT3 inactivation**
263 To understand the mechanism by which *E. faecalis*-mediated acidification impacts NF-
264 κB activation, we focused on the reduction of MyD88 levels, which would give rise to

265 the observed downstream signaling defects. STAT3 is a transcription factor that
266 regulates *Myd88* expression [43]. STAT3 activation depends on its phosphorylation by
267 ERK at serine 727 (S727) [44], preceded by ERK phosphorylation by MEK [45-47].
268 STAT3 activity can also be regulated by phosphorylation at tyrosine 705 (Y705) (34)
269 and inhibited by acetylation [43]. Consistent with reduced MyD88 level, WT *E. faecalis*
270 infection of macrophages also reduced the level of p-ERK, p-MEK and STAT3
271 phosphorylation at the S727 residue as compared to uninfected or Ldh-infected
272 macrophages **(Fig. 4A)**. Total STAT3 protein levels were slightly reduced in WT-
273 infected macrophages whereas total MEK protein levels were unchanged.
274
275 Since MEK enzymatic activity is pH sensitive [48], we measured the intracellular pH
276 and MEK activity in macrophages following *E. faecalis* infection. Using the pH-
277 sensitive fluorescent reporter BCECF-AM, we observed that the intracellular pH (pHi)
278 in macrophages infected with WT *E. faecalis* decreased to ~6.3, whereas it remained
279 between 6.9 and 7.2 in the Ldh-infected and non-infected cells, respectively **(Fig. S9A-**
280 **B)**. To determine whether reduced pHi could affect MEK-driven signal transduction,
281 we assessed MEK activity by immunoprecipitating MEK from WT-infected
282 macrophages and measuring its *in vitro* phosphorylation capacity of non-
283 phosphorylated ERK from cell lysates. We confirmed that MEK activity from infected
284 cells was reduced **(Fig. 4B-D)**. These findings support the hypothesis that *E. faecalis*-
285 induced changes in pHi ultimately disrupt the MEK–ERK–STAT3 signaling cascade,
286 consistent with report of MEK signaling in fibroblasts [48].
287
288 To evaluate whether *E. faecalis* infection reduces STAT3 binding to the *Myd88*
289 promoter, we performed chromatin immunoprecipitation (ChIP) followed by qPCR.

290 Using the Eukaryotic Promoter Database, we identified six potential STAT3 binding
291 sites near the *Myd88* transcription starting site that could be grouped and probed
292 based on their proximity: region 1 (R1; -1147 and -1065), region 2 (R2; -61 and -23)
293 and region 3 (R3; 386 and 488). STAT3 binding was reduced at these regions in WT
294 *E. faecalis*-infected macrophages treated with LPS, whereas Ldh-infected LPS-treated
295 macrophages showed no reduction **(Fig. 4E)**. Further, lactic acid alone was sufficient
296 to reduce STAT3 binding at these sites. Overexpressing *Myd88* in RAW264.7 cells
297 alleviated NF-κB suppression by *E. faecalis* **(Fig. S9G-H)**. Although
298 immunofluorescence of WT *E. faecalis* infected macrophages in the presence or
299 absence of LPS did not reveal major changes in STAT3 localization **(Fig. S9F)**,
300 subcellular fractionation revealed an absence of S727-phosphorylated STAT3 in the
301 nucleus of WT *E. faecalis* infected macrophages **(Fig. S9I)**, while Y705-
302 phosphorylated STAT3 was detected **(Fig. S9J).** These results suggest a mechanism
303 by which reduced STAT3 phosphorylation directly leads to reduced transcription of
304 Myd88 [49].
305
306 We also assessed whether STAT1 contributes to NF-κB activity in infected
307 macrophages [50]. As expected, inhibition of either MEK or STAT3 with Selumetinib
308 or Stattic, respectively, impaired NF-κB activation in the presence of LPS, regardless
309 of *E. faecalis* infection **(Fig. 4F, Fig. S10A)**. By contrast, STAT1 inhibition with
310 Fludarabine reduced, but did not completely abolish, NF-κB activation **(Fig. S10B)**.
311 Moreover, LPS-induced NF-κB activation was restored in *E. faecalis*-infected
312 macrophages that were treated with the STAT3 agonist ML115 but not with the STAT1
313 agonist 2NP **(Fig. 4G and Fig. S10C)**, indicating that STAT3 plays a central role in
314 NF-κB activation. Immunoblot of infected cell lysates treated with ML115 with or

315 without LPS confirmed increased in MyD88 expression **(Fig. S10D)**. Functionally,
316 treatment of macrophages with ML115 to overcome *E. faecalis*-mediated STAT3
317 suppression enhanced intracellular bacterial clearance by ~10 fold, whereas treatment
318 with 2NP did not **(Fig. 4H)**. Agonist and inhibitor concentrations did not cause
319 cytotoxicity **(Table S3)**. Collectively, these results show that *E. faecalis* interferes with
320 STAT3 activity to suppress *Myd88* transcription, thereby inhibiting NF-κB activation.
321

322 **MCT-1 and GPR81 mediate NF-κB suppression in *E. faecalis*-infected**
323 **macrophages**

324 Macrophages sense extracellular lactate and pH gradients via monocarboxylate
325 transporters and G-protein coupled receptors [34, 51]. To investigate their contribution
326 to *E. faecalis*-mediated immune suppression, we silenced the genes encoding MCT-
327 1, GPR81 (also known as hydroxycarboxylic acid receptor 1), and GPR65 in RAW
328 264.7 macrophages. Knockdown was confirmed by RT-PCR and viability of
329 knockdown cells remained >80% **(Fig. S11F-H and S12)**. Individual knockdowns
330 partially restored NF-κB activation, whereas combined *Mct-1+Gpr81*, or a triple
331 knockdown of *Mct-1+Gpr81+Gpr65*, fully restored NF-κB activation in the presence *E.*
332 *faecalis* and LPS, while non-targeting controls had no effect **(Fig. 5A-B, Fig. S11A-E)**.
333 These results identify MCT-1 and GPR81 as the main mediators of lactate/pH sensing
334 during *E. faecalis* infection.
335

336 To define the mechanism by which MCT-1 and GPR81 contribute to NF-κB regulation,
337 we focused on GPR81-YAP and MCT-1-pH signaling. We hypothesized that GPR81
338 activation by extracellular lactate promoted YAP phosphorylation, limiting its nuclear
339 cooperation with p65 [19], and thereby attenuating NF-κB activation. Consistent with

340 this, the YAP agonist PY60 increased NF-κB activity in *E. faecalis*-infected cells,
341 whereas the YAP inhibitor verteporfin blunted NF-κB activation **(Fig. S13A-B)**.
342 Although the lactate-driven YAP response is reported to be adenylyl-cyclase
343 independent [19], and lactate is reported to reduce cAMP and inhibit NF-κB [52],
344 infection did not alter intracellular cAMP **(Fig. S13C)**, supporting a possible
345 noncanonical GPR81-YAP pathway. Combining PY60 with the adenylyl cyclase
346 inhibitor MDL-12330A (MDL-12) further increased LPS-driven NF-κB activation,
347 independent of infection, suggesting that GPR81-mediated YAP phosphorylation
348 dominates during infection **(Fig. S13D)**. Immunofluorescence and subcellular
349 fractionation confirmed altered pYAP localization and increased nuclear YAP **(Fig. S9I**
350 **and Fig. S13E)**.
351
352 MCT-1 imports lactate in a proton-dependent manner, reducing intracellular pH [53].
353 At pH 6.4, NF-κB activation was suppressed in LPS-treated siRNA control cells, and
354 addition of lactate further enhanced suppression **(Fig. 5C)**. In *Gpr81*-silenced cells,
355 lactate did not increase suppression, indicating that MCT-1 alone can mediate NF-κB
356 inhibition under acidic conditions **(Fig. 5D)**. By contrast, *Mct-1* knockdown cells
357 showed stronger NF-κB suppression with increasing lactate at low pH, demonstrating
358 that GPR81 activity requires both acidity and lactate **(Fig. 5E)**. Notably, DMEM
359 supplemented with 10% FBS contains baseline lactate that may activate GPR81 under
360 low pH, contributing to NF-κB inhibition **(Fig. S14A)**. Finally, dual *Mct-1/Gpr81*
361 knockdown restored NF-κB activation, with any residual suppression likely mediated
362 by other pH sensors such as GPR65 **(Fig. 5F)**.
363

364 To further clarify the contribution of MCT-1 to NF-κB suppression, we used the MCT-
365 1/4 inhibitor α-cyano-4-hydroxycinnamate (CHC), the selective MCT-1 inhibitor
366 AZD3965, and the MCT inhibitor 7ACC2, either alone or in combination with the
367 adenylyl cyclase inhibitor MDL-12, in the presence or absence of *E. faecalis* and LPS
368 **(Fig. S14)**. MDL-12 was included to keep intracellular cAMP levels low, thereby ruling
369 out residual cAMP-driven effects and focusing on pH- and transport-dependent
370 mechanisms. Consistent with its role in NF-κB activation, MDL-12 alone reduced NF-
371 κB reporter activity under neutral pH conditions **(Fig. S14B)**. In infected macrophages,
372 MCT-1 inhibition modestly relieved suppression when using AZD3965 or 7ACC2, but
373 not CHC **(Fig. S14C-D)**. Importantly, combining MCT inhibitors with MDL-12 restored
374 NF-κB activation to levels comparable to LPS stimulation alone **(Fig. S14D-E)**. These
375 results support that MCT-1 activity contributes to NF-κB suppression and that the
376 effect is independent of canonical cAMP signaling, as blocking both lactate transport
377 and adenylyl cyclase eliminates the suppression phenotype.
378

379 **NF-κB suppression by *E. faecalis* occurs independently of HIF-1α, IL-10, and**
380 **HDAC pathways**

381 We also considered whether the pH sensor HIF-1α [54] was involved in *E. faecalis*
382 immunosuppression of macrophages. HIF-1α was stabilized in WT *E. faecalis*-infected
383 macrophages, enhancing IL-1β production **(Fig. S15A-D)**. Hypoxia response element
384 (HRE) reporter assays confirmed enhanced HIF-1α activity during infection and an IL-
385 1R reporter assay similarly confirmed bioactive IL-1β, which was reduced with HIF-1α
386 inhibition by LW6 and enhanced by the HIF-1α activator O-phenanthroline **(Fig. S15E-**
387 **G)**. However, NF-κB remained suppressed despite elevated IL-1β during infection **(Fig.**

388 **5G)**, in line with the ability of *E. faecalis* to disrupt MyD88 expression and thereby
389 impair IL-1β signaling, which depends on MyD88 **(Fig. S15H)**.
390
391 IL-10 activates IL-10R, triggering JAK1/TYK2-dependent STAT3 Y705
392 phosphorylation **(Fig. S16A)** [55]. Since IL-10 is produced during *E. faecalis* wound
393 infection regardless of strain **(Fig. S16B-D)**, we asked whether infection-derived IL-10
394 could contribute to NF-κB suppression during infection. We first exposed NF-κB
395 reporter cells ± LPS to 20 μL bacteria-free supernatants from WT *E. faecalis*-infected
396 macrophages. These supernatants activated NF-κB **(Fig. S16E-F)**, consistent with our
397 prior findings on IL-1β signaling, suggesting that infection-derived IL-1β overrides, or
398 that endogenous IL-10 is insufficient to drive macrophage suppression. By contrast,
399 supernatants from IL-10-supplemented infections suppressed LPS-driven NF-κB
400 activity, consistent with carry-over of exogenous IL-10, while blockade with anti-IL-10R
401 yielded a response similar to untreated supernatant **(Fig. S16F)**. Finally, we directly
402 infected NF-κB reporter cells with WT *E. faecalis* under all combinations of LPS, IL-10,
403 and αIL-10R. NF-κB suppression remained robust regardless of IL-10 modulation **(Fig.**
404 **5H)**. These results indicate that although IL-10 is produced during infection, it plays
405 little to no role in *E. faecalis*-mediated NF-κB suppression.
406
407 Finally, we measured HDAC contribution to lactic acid-mediated NF-κB suppression
408 in macrophages during *E. faecalis* infection. WT *E. faecalis* infection did not alter
409 global H3 acetylation, whereas the Ldh mutant reduced it **(Fig. S17A).** Pan HDAC
410 inhibition with trichostatin A (trichoA) partially restored NF-κB activation in LPS-treated,
411 *E. faecalis*-infected macrophages **(Fig S17B)** and HDAC6 inhibition with tubastatin A
412 (tubA) modestly relieved suppression, but inhibition of other isoforms had no effect

413 **(Fig S17C-G)**. Together these results show that *E. faecalis*-derived lactic acid
414 suppresses NF-κB primarily through MCT-1-mediated proton import and GPR81-
415 driven YAP phosphorylation, whereas HIF-1α/ IL-1β responses occur but do not
416 rescue NF-κB activation and HDAC activity contributes only marginally.
417
418 ***E. faecalis* LDH contributes to *E. faecalis* persistence in wound infections**
419 *E. faecalis* infection suppresses the immune response and impairs healing in a murine
420 model of wound infection [56]. We predicted that LDH-mediated immune modulation
421 is important for *E. faecalis* survival in wounds. To test this, wounds were inoculated
422 with either WT *E. faecalis* or the Ldh mutant. Both strains showed similar survival at
423 24 hpi **(Fig. 6A)**, despite LDH-dependent reduction of lactate in wound tissues at the
424 same time point **(Fig. S18A),** but in agreement with *in vitro* data that show no
425 difference between WT and Ldh survival in RAW264.7 cells and BMDMs 24 hpi **(Fig**
426 **S18B)**. By 7 dpi, however, Ldh CFU were ~1-log lower than WT **(Fig. 6B)**, indicating
427 that LDH primarily supports *E. faecalis* persistence rather than acute infection.
428 Supporting this, a modified killing assay maintaining extracellular acidosis revealed
429 reduced macrophage bactericidal capacity at low pH, independent of strain **(Fig. S18C)**
430 or the source of bacterial-free supernatant **(Fig. S18D)**. Importantly, combined
431 inhibition of MCT-1 with AZD3965 and YAP activation with PY-60 enhanced bacterial
432 killing in both RAW264.7 cells and BMDMs **(Fig. S18E)**.
433
434 To define how LDH influences immune signaling *in vivo*, we examined p-p65, p-ERK,
435 and MyD88 in wound tissues. WT *E. faecalis* infection, but not Ldh mutant, reduced
436 p-ERK at 24 hpi and all three proteins at 7 dpi **(Fig. 6C)**. Flow cytometry revealed that
437 macrophages expanded to ~80% of immune cells at 7 dpi in WT *E. faecalis* -infected

438 wounds versus ~25% at 1 dpi **(Fig. 6D, S18F)**, coinciding with the stronger reduction
439 in signaling proteins **(Fig. 6C)**. Direct analysis of macrophages confirmed marked
440 reductions in MyD88 and p-ERK at 7 dpi in WT *E. faecalis*-infected wounds compared
441 to uninfected or Ldh-infected wounds **(Fig. 6E-F)**. By contrast, topical application of
442 the STAT3 agonist ML115 on WT-infected wounds reduced *E. faecalis* CFU by 1.1-
443 log compared to PBS treatment **(Fig. 6G)**, further supporting the model that *E. faecalis*
444 suppresses macrophages killing via MyD88 downregulation. Altogether, these results
445 demonstrate that LDH contributes significantly to persistent *E. faecalis* wound infection
446 by promoting an acidic environment that impairs macrophage killing and dampens
447 immune signaling pathways.
448

449 ***E. faecalis* LDH-mediated immune suppression promotes *E. coli* survival during**
450 **mixed species infection**

451 We previously showed that co-infection with *E. faecalis* enhances *E. coli* virulence and
452 growth in a mouse wound infection model [57]. To test whether immune suppression
453 contributed to this phenotype, we co-infected RAW 264.7 macrophages with *E. coli*
454 and either WT or Ldh *E. faecalis* and observed higher NF-κB activation for the Ldh co-
455 infection compared to WT **(Fig. 7A)**. Similarly, WT *E. faecalis* supernatants
456 suppressed NF-κB activation by other species, including *E. faecium*, *P. aeruginosa*
457 (PA), *S. aureus* (USA300), *L. monocytogenes* (LM), and *S. Typhimurium* (ST),
458 highlighting the potential of *E. faecalis* to promote a variety of polymicrobial infections
459 **(Fig. 7B)**. With the exception of the *E. faecalis* Ldh mutant, *P. aeruginosa* PAO1, and
460 *L. monocytogenes* ATCC19115, each of these species also acidified the medium to
461 below pH 7 **(Fig. S19A)**. However, only enterococci and *S. aureus* produced

462 detectable amounts of lactic acid **(Fig. S19B)** and suppressed LPS-induced NF-κB
463 activation at high MOI **(Fig. S19C)** in the absence of marked cytotoxicity **(Fig. S19D)**.
464 In a murine wound model, co-inoculation with *E. coli* and either WT *E. faecalis* or the
465 Ldh mutant yielded similar *E. faecalis* CFU at 24 hpi **(Fig. 7C)**, whereas *E. coli* growth
466 was significantly enhanced during co-infection with WT, not the mutant **(Fig. 7D)**. To
467 exclude *E. faecalis*-derived lactate as a nutrient source for *E. coli*, we tested *E. coli*
468 growth *in vitro* with increasing lactate concentrations and observed no enhancement
469 **(Fig. S19E)**. Altogether, these findings demonstrate that LDH-dependent lactic acid
470 production by *E. faecalis* suppresses host NF-κB signaling, thereby facilitating *E. coli*
471 proliferation during wound infection. Lactic acid-driven immune suppression may thus
472 represent a conserved strategy among certain lactic-acid producing species to
473 modulate host responses and promote polymicrobial persistence.
474

475 ## Discussion

476 *E. faecalis* is among the top pathogens associated with hospital acquired infections
477 including CAUTI, central line-associated bloodstream infection, and surgical site
478 infection [4, 58]. While previous studies focused on host inflammatory responses at
479 lower MOI [29, 59], we and others have shown that *E. faecalis* exhibits
480 immunomodulatory properties at higher MOI via mechanisms and bacterial factors that
481 were previously unclear [30, 31, 60]. Here we demonstrate that *E. faecalis* infection at
482 MOI 100 suppresses macrophage activation by interfering with STAT3 and YAP
483 activity, resulting in reduced MyD88 levels and inhibition of downstream signaling
484 events required for NF-κB activation. Additionally, we identify *E. faecalis* lactate
485 dehydrogenase (LDH) and its lactic acid product as critical factors for macrophage

486 suppression and persistence in wounds, as well as for promoting *E. coli* growth during
487 co-infection.
488
489 Lactic acid production is a metabolic hallmark of *E. faecalis* fermentation [61]. *E.*
490 *faecalis* LDH catalyzes the reduction of pyruvate to L-lactate, which is exported as
491 lactic acid and deprotonates into L-lactate at physiological pH, reducing the local pH.
492 Here we show that *ldh1* is necessary, and its byproduct (lactic acid) is sufficient, to
493 suppress LPS-induced NF-κB activation. This may be why LDH-deficient *E. faecalis*
494 exhibit reduced virulence in systemic murine infections [38]. Similarly, LDH is
495 important for virulence of *S. aureus* in a murine sepsis model [62]. Lactic acid-induced
496 immunosuppression appears widespread; other lactic acid bacteria, such as
497 *Lactobacillus*, suppress NF-κB activation in macrophages and myometrial cells [63,
498 64]. While we focused on the role of LDH in this study, we identified additional mutants
499 that failed to suppress LPS-induced NF-κB activation despite acidifying the
500 environment, suggesting additional immune suppressive mechanisms. Beyond
501 infection, lactic acid contributes to immune suppression in tumor microenvironments,
502 inducing tissue acidosis that suppresses NF-κB activity, through mechanisms
503 involving pH changes and histone acetylation [17, 65-75]. Here we show that *E.*
504 *faecalis* lactic acid-mediated suppression of MyD88 levels and downstream signaling
505 events can be mimicked by acidic conditions, driven by pH effects rather than
506 phosphorylation changes. These mechanisms may be context dependent and warrant
507 further study.
508
509 The MEK-ERK-STAT3 axis is disrupted by *E. faecalis*-derived lactic acid, reducing
510 STAT3 phosphorylation and binding to the *Myd88* promoter, consistent with previous

511 reports [43]. While other bacterial infections activate the MEK/ERK cascade for
512 oxidative and nitrosative bursts, endosomal trafficking, and proinflammatory
513 macrophage polarization [76-78], *E. faecalis* subverts this defense [79, 80].
514 *Salmonella typhimurium* and *Helicobacter pylori*, for example, induce STAT3
515 phosphorylation via secreted factors to alter immune responses [79]. We show that
516 pH sensitive kinases, including MEK and ERK, are disrupted at lower intracellular pH,
517 inhibiting STAT3 activity in alignment with previous studies [81]. Indeed, pH 6.2-6.4
518 also reduces MEK and ERK phosphorylation in fibroblasts and prevent NF-kB
519 activation in macrophages [48, 82].
520
521 How then does extracellular *E. faecalis*-derived lactic acid exert these pH-driven
522 intracellular effects? We identified the host lactate transporter MCT-1 and the lactate
523 sensor GPR81 as mediators of NF-κB suppression during *E. faecalis* infection. MCT-
524 1 import of lactate, other metabolites and protons was previously shown to mediate
525 the inhibition of HDAC11 activity that leads to the activation of HDAC6 to promote IL-
526 10 release [83]. Here we show that MCT-1 transport of protons is driving intracellular
527 pH down which disrupts the MEK-ERK-STAT3 phosphorylation signaling cascade
528 leading to lower MyD88 expression. At the same time, GPR81 sensing of extracellular
529 lactate prevents the activation of the transcription factor YAP and, ultimately, leads to
530 NF-κB suppression [19, 83]. Classically, lactate activates GPR81 to lower cAMP,
531 whereas lower cAMP via PKA activates LATS1/2 to phosphorylate YAP and retain it
532 in the cytoplasm. Therefore, logically, a simple drop in cAMP would be expected to
533 decrease, not increase, YAP phosphorylation leading to greater NF-κB activation [84].
534 However, lactate-GPR81 signaling increases YAP phosphorylation in macrophages
535 likely in an adenylyl cyclase-dependent manner, consistent with the hypothesis that

536 GPR81 can drive AMPK-LATS signaling pathway to rather inactivate YAP and
537 dampen NF-κB [19]. In line with this model, *E. faecalis* infection did not measurably
538 reduce intracellular cAMP in our system, and the adenylyl-cyclase inhibitor MDL-12
539 reduced rather than increased NF-κB activation in uninfected and infected
540 macrophages. Interestingly, we also detected nuclear pYAP signal, although Ser127
541 phosphorylation typically promotes cytoplasmic retention, suggesting non-canonical
542 nuclear YAP pools during infection.
543
544 Expression of the genes encoding MCT-1 and GPR81 is pH-dependent [25-27].
545 Moreover, both MCT-1 and GPR81 may be activated at lower pH [34, 85]. Lactate
546 supplementation alone did not replicate *E. faecalis* LDH-mediated immune
547 suppression, suggesting that MCT-1/GPR81 activation is indeed pH dependent.
548 Initially, our study seems to contrast a study showing that lactic acid can induce
549 phosphorylation of ERK in rat hepatocyte RLN-10 cells via GPR81 sensing [86].
550 However, that study was conducted under adjusted neutral pH, excluding the potential
551 effect of pH on ERK phosphorylation. Similarly, studies showing increased MEK and
552 ERK phosphorylation via GPR81 used sodium lactate, which does not lower pH in
553 their experiments [87, 88]. Conversely, others have observed that acidosis (pH 4-5)
554 can activate ERK2, but not ERK1, in human epidermoid squamous carcinoma A431
555 cells [89], whereas pH 6.6 can increase the phosphorylation of ERK after 2 h of
556 incubation but gradually inhibit phosphorylation after 4 h in human prostate carcinoma
557 epithelial 22Rv1 cells [90]. Similarly, pH 6.3 was observed to inhibit ERK
558 phosphorylation in Jurkat cells after 24 h [91]. These studies are consistent with our
559 model that pH affects the phosphorylation status of these kinases.
560

561 *E. faecalis* wound infections are immune suppressive and delay wound healing [42].
562 We show that *E. faecalis* LDH activity drives immune suppression, *E. faecalis*
563 persistence in wounds, as well as the growth of *E. coli* during co-infection. Given the
564 prevalence of infections caused by lactic acid-producing bacteria [92, 93], as well as
565 their beneficial contributions to healthy microbiomes, further studies are needed to
566 delineate how extracellular pH and lactate mechanistically shape polymicrobial
567 interactions. We found that several bacterial species can acidify their environment,
568 often through metabolites other than lactate, although many exhibited cytotoxicity at
569 higher MOI. At lower MOI, when these species activated NF-κB, *E. faecalis*
570 supernatant alone was sufficient to suppress this activation. Together, these findings
571 reveal *E. faecalis* as a paradigm for metabolic immune modulation, demonstrating how
572 bacterial acidification can reprogram host signaling to foster interspecies coexistence
573 and persistence within infected tissues. Importantly, compounds that override this
574 suppression and activate macrophage NF-κB signaling during *E. faecalis* infection
575 enhance macrophage intracellular killing of bacteria [94, 95]. Here, we observed that
576 the STAT3 agonist ML115 was also effective both *in vitro* and *in vivo* to reduce the
577 bacterial burden of *E. faecalis* infection, further highlighting the therapeutic potential
578 of immunomodulation for immunosuppressive bacterial infections. Overall, a
579 comprehensive understanding of the immunological pathways affected by *E. faecalis*
580 infection could inform new strategies to mitigate persistent infections.
581

582 ## Materials and Methods

583 ### Bacterial strains and growth conditions

584 *E. coli* strains used in this study were grown overnight in Luria-Bertani (LB) (Difco)
585 broth or agar at 37°C under static conditions. *E. faecalis* strain OG1RF or *ldh* mutants

586 and other bacterial strains **(Table S4)** were grown statically in brain heart infusion
587 (BHI) (Becton, Dickinson, USA) broth or agar at 37°C overnight. Overnight cultures of
588 bacteria were centrifuged at 6,000 *g* for 5 minutes and resuspended in PBS at OD_{600}
589 0.7 (2 x 10^8 CFU/mL) for *E. faecalis* and at OD_{600} 0.4 (2 x 10^8 CFU/mL) for *E. coli*.
590

591 **Genetic manipulations**

592 To create deletion mutants, we used a thermosensitive shuttle plasmid pCGP213
593 which was isolated using the Monarch Plasmid Miniprep Kit (New England BioLabs
594 Inc., USA) following the manufacturer's instruction [96]. OG1RF genomic DNA is
595 isolated using Wizard Genomic DNA Purification Kit (Promega, USA) and Phusion
596 DNA polymerase (Thermo Fisher Scientific, Singapore) was used to amplify
597 approximately 1 kb upstream and downstream of the gene of interested according to
598 the manufacturer's protocol. Primers used in the study are listed in **Table S5**.
599 Subsequently, the amplified products were sewn together using the primers
600 dLDH1_For, dLDH1_Rev, dLDH2_For and dLDH2_Rev. *ldh1* and *ldh2* constructs
601 were then subcloned individually into pGCP213 using In-Fusion HD Cloning Kit using
602 (Clontech, Takara, Japan) following manufacturer's instruction. Deletion constructs
603 were then transformed into *E. coli* and correct transformants were selected at 37°C
604 under erythromycin (Sigma-Aldrich, St Louis, MO) pressure 500 µg/mL. The amplified
605 plasmids were then purified from *E. coli* using the Monarch Plasmid Miniprep Kit. The
606 plasmids were then transformed into OG1RF using electroporation, and the correct
607 transformants were selected at 30°C under erythromycin pressure 25 µg/mL.
608 Chromosomal integrations were selected by passaging 37°C in the absence of
609 erythromycin. The loss of *ldh1* or *ldh2* is then verified by PCR using primer pairs
610 LDH1_F, LDH1_R, LDH2_F and LDH2_R. Δ*ldh1*Δ*ldh2* was created by subcloning the

611 pGCP213-*ldh1* deletion construct into Δ*ldh2*. All deletion constructs were
612 subsequently confirmed using whole genomic sequence to ensure that only the gene
613 of interest is deleted in the absence of any spontaneous mutation.
614
615 **Growth kinetics and pH curve**

616 Bacterial cultures were grown as described above and overnight cultures were
617 normalized to obtain a final concentration of 10^3 cells/mL before inoculating at 1:25
618 ratio into 200 µL of either BHI or DMEM supplemented with 10% FBS. Subsequently,
619 growth rates were measured by recording OD 600 over 20 h at 37°C using a microplate
620 reader (Tecan infinite M200 Pro, Switzerland).
621
622 For pH measurements, bacterial cultures were grown and normalized to 3.4 x 10^7
623 cells/mL (assuming MOI 100 for 10^6 macrophages) in DMEM supplemented with 10%
624 FBS. The pH was then measured at 1-h interval for up to 6 h, and subsequently
625 measured at 8 h and 24 h using a digital pH meter (Sartorius, Germany).
626
627 **Cell culture**

628 RAW 264.7 cells derived from RAW 264.7 macrophages (Invivogen, USA), containing
629 a plasmid encoding a secreted embryonic alkaline phosphatase (SEAP) reporter
630 under transcriptional control of an NF-κB-inducible promoter, were cultivated in
631 Dulbecco Modified Eagle medium (DMEM) containing 4500 mg/L high glucose (1X)
632 with 4.0 nM L-glutamine, without sodium pyruvate (Gibco, Thermo Fisher Scientific,
633 Singapore) and supplemented with 10% fetal bovine serum (FBS; PAA) supplemented
634 with 200 µg/mL Zeocin (Gibco, Thermo Fisher Scientific, Singapore), at 37°C in 5%
635 CO_2. For MyD88 rescue experiments and HIF-1α reporter assays cells were

636 transduced with pCMV3-mMYD88 (Sino Biological) and pGL4.42[luc2P/HRE/Hygro]
637 (Promega), respectively, using the Lipofectamine LTX with Plus Reagent (Thermo
638 Fisher Scientific) following the manufacturer's instructions at least 1 day before the
639 assays were performed. HEK-Blue IL1R cells (Invivogen), which is a HEK 293 reporter
640 cells for human and murine IL-1α & IL-1β cytokines, were cultured in DMEM (Gibco)
641 supplemented with 10% (v/v) heat-inactivated fetal bovine serum, 100 U/mL penicillin,
642 100 μg/mL streptomycin, and 1x HEK-Blue selection (Invivogen) at 37°C in a
643 humidified incubator with 5% CO_2. Cells were passaged when they reached 80%
644 confluency. For passaging or harvesting cells for assays, cells were washed and
645 incubated in PBS for 2 min at 37°C, followed by vigorous pipetting of PBS over the cell
646 monolayer to detach the cells.

647

648 **Bone marrow-derived macrophages (BMDM) isolation and cultivation**

649 BMDMs were harvested according to previously published protocol [97]. Briefly,
650 femurs were harvested from 6 to 10 weeks old C57BL/6J mice (InVivos Pte. Ltd.,
651 Singapore). Following euthanasia, the legs were first sprayed with 70% ethanol before
652 dissection and removing the skin and muscles. The bone was then placed in 70%
653 ethanol and transferred into a sterile flow hood. Subsequently, the bone was cut using
654 scissor and bone marrow was flushed out with cell culture media (containing DMEM
655 with 10% FBS and supplemented with 100 U/mL penicillin and 100 μg/mL
656 streptomycin (Gibco, Thermo Fisher Scientific, Singapore) using a 26G needle into a
657 sterile falcon tube (Becton, Dickinson and Company, Franklin Lakes, NJ).
658 Subsequently, cell suspension was centrifuged at 500 G for 5 min and the supernatant
659 was removed. The cell pellet was then resuspended in 1X RBC Lysis Buffer
660 (eBioscience, Thermo Fisher Scientific, Singapore) for lysis of erythrocytes. After 5

661 mins, PBS was added to inactivate the lysis buffer before centrifuging the cell
662 suspension. Supernatant was discarded, and cell pellet was resuspended in cell
663 culture media supplemented with 100 ng/mL macrophage colony-stimulating factor
664 (M-CSF) (Biolegend, San Diego, USA), 100 U/mL penicillin and 100 µg/mL
665 streptomycin. Cells were adjusted to 2 x 10^6 cells/mL and seeded into T175 flask (Nunc,
666 Thermo Fisher Scientific, China) and incubated at 37°C with 5% CO_2. After 2-3 days,
667 cells were washed, and fresh cell culture media supplemented with 100 ng/mL M-CSF
668 was added. Macrophages are fully differentiated after 6 to 7 days, ready for
669 experimental use.
670
671 **RAW 264.7 macrophage or BMDM infection**
672 RAW 264.7 cells and BMDM were seeded into 96-well and 6-well microtiter plates
673 (Nunc, Thermo Fisher Scientific, Singapore) with cell density of 1 x 10^5 or 1 x 10^6
674 cells/well respectively in antibiotic free media (DMEM with 10% heat inactivated FBS)
675 and incubated overnight at 37°C with 5% CO_2 when necessary. Following overnight
676 incubation, the cells were washed once with PBS and fresh media was added. The
677 SEAP reporter assay was established by empirically defining the minimal agonist LPS
678 concentration that induced the maximum SEAP activity in the absence of cell death.
679 Cells were stimulated using LPS purified from *E. coli* O111:B4 (Sigma-Aldrich, St
680 Louis, MO) (100 ng/mL) as positive control, or media alone as a negative control. RAW
681 264.7 cells were infected with *E. faecalis* (at MOI of 100:1, 10:1 and 1:1) for 6 h with
682 or without TLR agonists. Variations of this assay included lowering the pH to 6.4 with
683 lactic acid, H_3PO_4 or HCl, and also neutralizing acidic supernatants to pH 7.8 with Tris.
684 For co-infection experiments, RAW 264.7 cells were simultaneously infected with
685 *E. coli* UTI89 (MOI of 0.125:1) and *E. faecalis* (MOI of 100:1). For killing assays, cells

686 were infected at a multiplicity of infection (MOI) of 10 or 100 for up to 6 hours. Following
687 infection, the medium was aspirated, and the cells were washed three times in PBS
688 and incubated with gentamicin (150 µg/mL) (Sigma-Aldrich) and vancomycin (20
689 µg/mL) (Sigma-Aldrich) to kill extracellular bacteria in complete DMEM for up to 24 h
690 to selectively kill extracellular bacteria. The antibiotic-containing medium was then
691 removed, and the cells were washed three times in PBS before addition of 2% Triton
692 X-100 (Sigma-Aldrich) PBS solution to lyse the cells for enumeration of the intracellular
693 bacteria. Variations of this assay included lowering the pH to 6.4 with wither LA or HCl,
694 pretreatment of mammalian cells for 30 min, before bacterial infection, with AZD3965
695 (10µM), PY60 (10 µM) or both followed by antibiotic treatment also containing these
696 compounds.
697
698 **Fluorescent staining and microscopy**
699 Cells were seeded at 2 × 10^5 cells/well in a 24-well plate with 10 mm coverslips and
700 allowed to attach overnight at 37 °C and 5% CO_2. Infection and LPS treatment were
701 performed for 6 h prior to fixation with 4% PFA at 4 °C for 15 min. Cells were then
702 blocked for 1 h with PBS supplemented with 0.1% saponin and 2% bovine serum
703 albumin (BSA). For antibody labelling, antibody solutions were diluted in PBS with 0.1%
704 saponin at a 1:100 dilution for anti-p65 (Cell Signaling Technology), anti-STAT3 (Cell
705 Signaling Technology) and anti-p-Yap (Cell Signaling Technology) and incubated
706 overnight at 4°C. The following day, coverslips were washed 3 times in 1× PBS with
707 0.1% saponin and incubated with a 1:100 dilution of goat anti-Rabbit IgG (H+L) Alexa
708 Fluor 568 secondary antibody (Thermo Fisher Scientific) for 1 h at room temperature.
709 For actin labeling, the phalloidin-Alexa Fluor 647 conjugate (Thermo Fisher Scientific)
710 was diluted 1:40 in blocking solution and incubated for 1 h. Coverslips were then

711 washed three times in PBS with 0.1% saponin. For nuclei staining, Hoechst 33342
712 was added in a dilution of 1:1000 for 5 min. Coverslips were then subjected to a final
713 wash with PBS thrice. Finally, the coverslips were mounted with SlowFade Diamond
714 Antifade (Thermo Fisher Scientific) and sealed. Confocal images were then acquired
715 on a 63×/NA1.4, Plan Apochromat oil objective fitted onto an Elyra PS.1 with an LSM
716 780 confocal unit (Carl Zeiss), using the Zeiss Zen Black 2012 FP2 software suite.
717 Laser power and gain were kept constant between the experiments. Z-stacked images
718 were processed by using Zen 2.1 (Carl Zeiss). Acquired images were visually
719 analyzed using ImageJ.
720
721 **Intracellular pH measurement**
722 BCECF AM (Thermo Fisher Scientific) was used to measure intracellular pH as per
723 manufacturer's instructions. Cells were loaded with 1 mM BCECF AM for 30 min prior
724 to infection. After 6 h of infection, fluorescence at excitation 440 nm and emission 535
725 nm was measured using a plate reader. To calibrate intracellular fluorescence ratio to
726 pH, the CCCP technique was used [98]. Cells were first loaded with BCECF AM, then
727 treated with 2 mM CCCP for 30 min following addition of pH-defined medium and
728 fluorescence measurement.
729
730
731 **ChIP-qPCR and histone H3 acetylation assay**
732 For each sample, chromatin immunoprecipitated DNA was captured using a STAT3
733 Rabbit mAb (D3Z2G; CST) and a high-sensitivity ChIP kit (Cat. #ab185913; Abcam)
734 according to the manufacturer's instructions and as inspired by [83] .The captured and
735 purified DNA was prepared for ChIP-qPCR, and specific primers (**Table S5**) were

736 designed for the sites that we identified as potential STAT3 binding sites near the
737 *Myd88* transcriptional starting site (TSS). The prediction of STAT3 binding sites
738 around the *Myd88* TSS was made using the Eukaryotic Promoter Database
739 (https://epd.expasy.org/epd/). We identified six potential STAT3 binding sites near the
740 *Myd88* TSS (-1147, -1065, -61, -23, 386 and 488). We named them region 1 (R1, -
741 1147 and -1065), region 2 (-61 and -23), and region 3 (386 and 488). For R1, we
742 designed primers that covered from region -100 to 0; for R2 from -1030 to -1182 and
743 R3 from 362 to 464 **(Table S5)**. qPCR was performed for each primer set. Amplification
744 was performed with KAPA SYBR Fast (Kapa Biosystems) with specific primers **(Table**
745 **S5)** and detected by StepOnePlus Real-Time PCR machine (Applied Biosystems).
746 Relative quantification was performed using the delta-delta method [99] with calibrator
747 primers that interrogate the *Gapdh* gene. Positive control was established for an RNA
748 polymerase binding site for the *Gapdh* gene. To measure the levels of histone H3
749 acetylation of samples infected with *E. faecalis*, the histone H3 acetylation assay Kit
750 (#ab115102, Abcam) was used as per the manufacturer's instructions.
751
752 **Flow cytometry**
753 To assess CD14 and TLR2 surface levels, flow cytometry was performed as described
754 in [35, 95]. RAW 264.7 cells were either infected or treated with LPS (1 μg/mL) or LTA
755 (10 μg/mL) alone or in combination for 30 min to 120 min before CD14 (LPS) and
756 TLR2 (LTA) endocytoses were examined by flow cytometry. Cells (10^7 per sample)
757 were then incubated with 1 μL of Fc-blocker (anti-CD16/CD32 antibody; BioLegend)
758 for 30 min, followed by incubation with a CD14 and TLR2 marker-conjugated with
759 BV605 and PE, respectively, antibodies (BioLegend) (1:100 dilution) for 30 min at
760 room temperature. Cells were then centrifuged at 500 *g* for 5 min at 4°C and washed

761 in FACS buffer (2% FBS and 0.2 mM ethylenediaminetetraacetic acid (EDTA) in PBS
762 (Gibco, Thermo Fisher Scientific). Following which, cells were analyzed using the BD
763 LSRFortessa X-20 Cell Analyzer (Becton Dickinson). The samples were gated on side
764 scatter area (SSC-A) versus forward scatter area (FSC-A) to select the RAW264.7
765 population. The RAW264.7 population was subsequently gated on side scatter width
766 (SSC-W) versus SSC-A to exclude doublets. The resulting single-cell population was
767 then assessed for CD14 and TLR2 fluorescent marker. Data was calculated relative
768 to uninfected untreated cells which were set as 100% levels for the examined
769 receptors.
770
771 For wound samples, flow cytometry was performed as described in [9]. Excised skin
772 samples were placed in 1.5 mL Eppendorf tubes containing 2.5 U/ml liberase prepared
773 in DMEM with 500 µg/mL of gentamicin and penicillin G (Sigma-Aldrich). The mixture
774 was then transferred into 6-well plates and incubated for 1 h at 37 °C in a 5% CO_2-
775 humidified atmosphere with constant agitation. Dissociated cells were then passed
776 through a 70 µm cell strainer to remove undigested tissues and spun down at 1350
777 rpm for 5 min at 4 °C. The enzymatic solution was then aspirated, and cells were
778 blocked in 500 µL of FACS buffer (2% FBS and 0.2 mM ethylenediaminetetraacetic
779 acid (EDTA) in PBS (Gibco, Thermo Fisher Scientific). 10^7 cells per sample were then
780 incubated with 1 µL of Fc-blocker (anti-CD16/CD32 antibody, Biolegend) for 30 min,
781 followed by incubation with an antimouse CD45, CD11b, and F4/80 (macrophages)
782 plus MyD88 (ProteinTech) and p-ERK (Biolegend) markers conjugated with PE-Cy5,
783 PE-Cy7, BV605, FITC and APC, respectively, antibodies (1:100 dilution) for 30 min at
784 room temperature. Cells were then centrifuged at 500*g* for 5 min at 4 °C and washed
785 in FACS buffer. Cells were fixed in 4% PFA for 15 min at 4 °C, before a final wash in

786 FACS buffer and final resuspension in this buffer. Following which, cells were analyzed
787 using a BD LSRFortessa X-20 Cell Analyzer (Becton Dickinson). Samples were first
788 gated on side scatter area (SSC-A) versus forward scatter area (FSC-A) to identify the
789 wound cell population. This population was then gated on forward scatter height (FSC-
790 H) versus FSC-A to exclude doublets. The resulting single-cell population was
791 analyzed for CD45 expression to identify immune cells, followed by assessment of
792 CD11b and F4/80 fluorescence to define the macrophage population. Compensation
793 was done using AbC Total Antibody Compensation Bead Kit (Thermo Fisher Scientific)
794 as per manufacturer's instructions.
795
796 **siRNA transfection**
797 Silencer select pre-designed siRNA (Thermo Fisher Scientific) against *Slc16a1 (Mct-*
798 *1)*, *Hcar1 (Gpr81), Gpr65, Gapdh* and NT siRNA were used. RAW264.7 cells were
799 seeded at 40% density the day before transfection in 6-well plates, and siRNA
800 transfections were performed with Silencer™ siRNA Transfection II Kit (Invitrogen)
801 according to the manufacturer's instructions. Cells were used for experiments after 48
802 h and also harvested at the same time point after transfection to verify successful gene
803 silencing by RT-PCR.
804
805 **Collection of bacteria cell-free culture supernatants**
806 Bacteria were grown in cell culture media for 6 h, and bacteria-free culture
807 supernatants were collected after centrifugation (6,000 *g*) followed by filtration (using
808 a 0.2 µm syringe filter). Alternatively, supernatants were collected after infecting
809 macrophages with bacteria at various MOI and then filtered by using a 0.2 µm syringe

810 filter. Sterility of bacteria-free culture supernatants were verified by the absence of
811 viable bacteria when plated on BHI agar.
812
813 **NF-κB reporter assay**
814 Post-infection, 20 µL of supernatant was added to 180 µL of QUANTI-Blue reagent
815 (Invivogen) and incubated overnight at 37 ˚C. SEAP levels were determined at 640 nm
816 using a TECAN M200 microplate reader. All experiments were performed in biological
817 triplicate.
818
819 **IL-1 reporter assay**
820 After RAW264.7 infection, bacteria were pelleted and supernatants were filter-
821 sterilized. 20 µl of bacterial supernatant filtrate were added to 50,000 HEK-Blue IL-1R
822 cells (Invivogen) in 180 µl DMEM supplemented with 10% FBS and 100 U/mL
823 Penicillin-Streptomycin in a 96-well plate. As negative control, DMEM was used
824 instead of bacterial supernatants. DMEM supplemented with human mature IL-1β (100
825 pg/mL) served as a positive control. Some RAW264.7 cells were pre-treated with HIF-
826 1α inhibitor LW6 (10 µM) or HIF-1α activator O-phenanthroline (5 µM) for 30 min prior
827 to the beginning of the assay. Samples were incubated for 6 h at 37°C. Next, 20 µl of
828 HEK-Blue IL-1R cell supernatants were transferred to 180 µl of QUANTI-Blue Solution
829 (invivogen) in a 96-well plate and incubated at 37°C for 1 h, followed by absorbance
830 at 640 nm in a plate reader (TECAN).
831
832 **Cell viability assay**
833 Simultaneously with supernatant collection for SEAP determination, culture
834 supernatants were collected from each well to measure lactate dehydrogenase (LDH)

835 release, using an LDH cytotoxicity assay (Clontech) according to manufacturer's
836 instructions. Background LDH activity was determined using mock (PBS) treated RAW
837 264.7 cells. Maximal LDH activity was determined by lysing cells with 1% Triton-X.
838 Each condition was assayed in triplicate. Percentage cytotoxicity was calculated as
839 follows: (sample absorbance-background absorbance)/(maximal absorbance-
840 background absorbance) x 100.
841
842 **Transposon library screen**
843 The transposon library was kindly provided by Professor Dunny Gary [100]. To screen
844 the library, the mutants were first inoculated into DMEM for 24 h and 20 μL of the
845 bacteria suspension will be transferred to previously seeded RAW 264.7 cells with 180
846 μL fresh DMEM in the presence of 100 ng/mL of LPS in 96 well microtitre plate.
847 Macrophages were stimulated for 6 h before the supernatant was collected and tested
848 with SEAP assay to determine the NF-κB activity. LPS-only group was used as
849 positive control for reporter activity and signals higher than the means of LPS-only
850 group minus 1 standard deviation was considered positive hits and non-suppressing
851 mutants. Growth kinetics of the selected mutants were performed to exclude the
852 mutants that grow poorly in DMEM. In addition, pictures of the overnight cultures were
853 taken to record the acidifying ability of each mutant by phenol red, a color indicator in
854 DMEM.
855
856 Mutants that grew similarly to *E. faecalis* WT further underwent a secondary screening,
857 where they were normalized to MOI 100 and infected the RAW 264.7 cells in the
858 presence of LPS. For the secondary screen, WT was used as control and signals
859 higher than means of WT group plus 2 standard deviations were considered weak-

860 suppressing mutants and validated hits. To measure the acidification ability of the
861 validated hits, 10^8 CFU of bacteria were inoculated into 5 mL of DMEM for indicated
862 time, and the pH value was determined by pH meter.
863
864 **Lactate and cAMP levels measurement**
865 Bacteria were grown in DMEM supplemented with 10% FBS for 6 h in the absence of
866 macrophages before collecting the supernatant and storing it at -80°C until
867 assessment by the L-Lactate Assay Kit (Abcam), according to manufacturer's
868 recommendations. All samples were assessed using the same kit lot and at the same
869 time to avoid inter-assay variability. Alternatively, blood gas analysis using abl90 flex
870 series analyser (Radiometer Medical) or or QuantiQuik L-Lactic acid quick test strips
871 (BioAssay Systems) were used to quantify lactate concentration. Intracellular levels of
872 cAMP were assessed using cAMP Direct Immunoassay Kit (Abcam) according to the
873 manufacturer's instructions.
874
875 **IL-6, IL-1β and IL-10 quantification**
876 Wound lysates from 24 hpi and supernatants collected from RAW 264.7 cells 6 hpi
877 were stored at -80 °C until assessment by the ELISA MAX Deluxe Set Mouse for IL-
878 6, IL-1β and IL-10 assay kit (Biolegend), according to manufacturer's
879 recommendations. All samples were assessed using the same kit lot and at the same
880 time to avoid inter-assay variability.
881
882 **Cytokine Luminex xMAP analysis**

883 Supernatants were collected from RAW 264.7 cells 6 hpi and stored at -80°C until
884 assessment by the Bio-Plex ProTM mouse cytokine 23-plex assay kit (Bio-Rad
885 Laboratories), according to manufacturer's recommendations. All samples were
886 assessed using the same kit lot and at the same time to avoid inter-assay variability.

887

888 **Mouse model of wound infection**

889 Bacterial cultures, prepared as described above, were used to infect wounds in 7 to 8
890 weeks old, 20 to 23 g female C57BL/6J mice (InVivos). Wounds were prepared as
891 previously described [57]. Briefly, mice were anesthetized with isoflurane (3%) and the
892 dorsal hair was trimmed. After trimming, remaining fine hairs were removed by first
893 applying Nair Cream (Church and Dwight) and shaving using a scalpel. Next, the skin
894 was first disinfected using 70% ethanol and a 6 mm biopsy punch (Integra Miltex) was
895 used to create a fill-thickness wound and inoculated with bacteria subsequently.
896 Inoculum volumes of 10 µL, containing a bacterial suspension of either single or
897 polymicrobial species prepared in PBS: (i) 10^2 CFU of *E. coli* strain UTI89 with 10^6
898 CFU *E. faecalis* WT, and (ii) 10^2 CFU of *E. coli* strain UTI89 with 10^6 CFU *E. faecalis*
899 Ldh. Single species controls (10^2 CFU of *E. coli* strain UTI89, 10^6 CFU *E. faecalis*
900 OG1RF, or 10^6 CFU *E. faecalis* Ldh) were performed alongside polymicrobial
901 infections. The wound site was then sealed with a sterile transparent dressing
902 (Tegaderm 3M, St Paul Minnesota, USA). After 24 h, animals were euthanized by
903 carbon dioxide inhalation and cervical dislocation and a 1 cm by 1 cm squared piece
904 of skin surrounding the wound was excised and homogenized in 1 mL PBS for CFU
905 enumeration by serial dilution on MacConkey agar (Becton, Dickinson and Company)
906 or BHI agar supplemented with 10 µg/mL colistin (Sigma-Aldrich) and 10 µg/mL
907 nalidixic acid (BHI-CNA) (Sigma-Aldrich) to isolate *E. coli* or *E. faecalis*, respectively.

908

909 **RNA extraction**

910 After 6 hpi with *E. faecalis* at various MOI in the presence or absence of LPS (100
911 ng/mL), cells were washed once with the tissue culture grade 1X PBS (Gibco, Thermo
912 Fisher Scientific) prior to RNA extraction. 1 mL of Trizol (Invitrogen, Thermo Fisher)
913 per well and was stored at -80°C until RNA extraction using Direct-zol RNA Miniprep
914 Plus kit (Zymo Research) according to manufacturer's protocol. Briefly, 200 µL of
915 chloroform (Sigma Aldrich) was first added to 1 mL of Trizol extracted samples, mixed
916 vigorously for 2 min and allowed to stand at room temperature for minimum 10 min.
917 The samples were centrifuged at 12,000 *g* for 15 min at 4°C and the top layer (aqueous
918 phase) was transferred to 500 µL of ethanol (Fisher Scientific, Canada) before loading
919 into the Zymo-Spin IIICG Column. Subsequently, RNA extraction was performed
920 according to manufacturer's protocol for Direct-zol RNA Miniprep Plus kit. Next,
921 extracted RNA samples were further cleaned and concentrated using RNA Clean &
922 Concentrator-5 (Zymo Research) following the manufacturer's protocol.

923

924 RNA samples were first screened using TapeStation (Aligent Technologies) to obtain
925 RIN value and concentration. Qubit analysis was also performed to measure the DNA
926 and RNA concentration using Qubit dsDNA HS Assay Kit (Invitrogen, Thermo Fisher
927 Scientific) and Qubit RNA BR Assay Kit (Invitrogen, Thermo Fisher Scientific), before
928 storage at -80°C until sequencing using an Illumina Hiseq®2500 v.2 (Illumina), 150 bp
929 paired-end.

930

931 **qRT-PCR**

932 To quantify the levels of RNA transcripts, total RNA was extracted from noninfected or
933 WT-infected RAW264.7 cells in presence or absence of LPS (100 ng/mL) with the
934 RNeasy MinElute Kit (QIAGEN) and reverse-transcribed using SuperScript III First-
935 Strand Synthesis SuperMix (Thermo Fisher Scientific), followed by amplification with
936 KAPA SYBR Fast (Kapa Biosystems) and detected by StepOnePlus Real-Time PCR
937 machine (Applied Biosystems). Relative quantification of gene expression was
938 performed using the comparative CT method [101], where the CT values were
939 normalized with the housekeeping gene glyceraldehyde phosphate dehydrogenase
940 (GAPDH) for comparison.

941

942 **Protein extraction and immunoblot**

943 Following infection with *E. faecalis* as described previously, proteins were harvested
944 using 2x Laemmli buffer (Bio-rad, Hercules) containing 50 mM dithiothreitol (Sigma
945 Aldrich) and denatured at 99°C for 10 min. 30 µL of protein samples were loaded and
946 subjected to Sodium Dodecyl Sulfate-Polyacrylamide Gel Electrophoresis (SDS-
947 PAGE) using NuPAGE 4-12% Bis-Tris Gel (Invitrogen, Thermo Fisher Scientific) in 1
948 x NuPAGE MOPS SDS Running Buffer (Invitrogen, Thermo Fisher Scientific). The
949 protein samples were transferred to polyvinylidene fluoride (PVDF) membrane using
950 iBlot® Gel Transfer Device (Invitrogen, Thermo Fisher Scientific, USA) as per
951 manufacturer's instructions. The PVDF membrane was then blocked using 5% BSA in
952 Tris-buffered saline (20 mM Tris-HCl pH 7.4, 150 mM NaCl) containing 0.1% Tween-
953 20 (Sigma Aldrich) at room temperature for 1 h. Subsequently, primary antibodies such
954 as MyD88, TAK1, phospho-TAK1, IKKα, IKKβ, phospho-IKKα/β, IκBα, phospho- IκBα,
955 p65, phospho-p65, SAPK/JNK, p38 MAPK, phospho-p38, p44/p42 MAPK (ERK1/2),
956 phospho-p44/p42 MAPK, c-Jun, phospho-c-Jun, c-Fos, phospho-cFos and GADPH

957 (Cell Signalling Technology) were used for probing overnight at 4 °C. The membranes
958 were washed with Tris-buffered saline and incubated with 1:3000 diluted anti-rabbit
959 IgG antibodies conjugated with horseradish peroxidase (Invitrogen, Thermo Fisher
960 Scientific, USA) at room temperature for 1 h. Following which, membranes were
961 washed, and proteins were detected using SuperSignal West Femto Maximum
962 Sensitivity Substrate (Invitrogen, Thermo Fisher Scientific) and autoradiography films
963 (Kodak).

964

965 **Subcellular Protein Fractionation**

966 The subcellular protein fractionation kit for cultured cells (Thermo Fisher Scientific)
967 was used as per manufacturer's instructions. Briefly, after infection cells were washed
968 and harvested, then gently plasma membrane permeabilized to collect the cytosolic
969 proteins. Cellular membranes were solubilized to remove membrane-associated
970 proteins while keeping nuclei intact. Nuclear proteins were then extracted using
971 nuclear buffer. Collected samples were then used for immunoblot.

972

973 ***In vitro* MEK activity assay**

974 *In vitro* MEK activity assay was performed using the MEK Activity Assay Kit (Sigma,
975 code CS0490) instructions with some modifications. MEK was immunoprecipitated
976 from samples with anti-MEK antibody (Thermo Fisher Scientific) and Protein A/G
977 magnetic beads (Abcam). The immunoprecipitated MEK was used to phosphorylate
978 the non-phosphorylated ERK substrate from cells that were treated with Selumetinib
979 (1 μM) for 6h and further depleted of MEK via IP. The level of ERK phosphorylation
980 was detected by immunoblotting using anti-p-ERK.

981

982 **Transcriptomics analysis**

983 Sequencing data are available at NCBI's BioProject (accession no. GSE188916). The
984 sequencing was performed at the Singapore Centre for Environmental Life Sciences
985 Engineering High Throughput Sequencing Unit, NTU, Singapore. Following quality
986 control (FastQC v0.11.9), trimming (cutadapt v4.2) and pre-processing using
987 TrimGalore (v0.6.6), the reads were mapped to the Gencode Mouse Release M32
988 (GRCm39) using Salmon (v.1.10.0). Differentially expressed gene analysis was
989 conducted in DESeq2 (v1.38.3) from raw counts. For over-representation and gene
990 set enrichment analysis (GSEA), we utilised clusterProfiler (v 4.6.0), enrichplot (v
991 1.18.3) and DOSE (v 3.24.2) packages for Gene Ontology (GO) analyses. The
992 workflow can be found at https://github.com/cenk-celik/daSilva_et_al.

993

994 **Statistical Analysis**

995 Statistical analysis was performed utilizing GraphPad Prism V6 and V10.4.1 software
996 (GraphPad Software). One-way ANOVA (Analysis of Variance) were used to compare
997 between median and the different conditions. Statistical significance for multiplex
998 immunoassay was determined using Kruskal-Wallis statistical analysis. CFU titers
999 were compared using the non-parametric Mann-Whitney U test. *P*-values less than
1000 0.05 were deemed significant. Unless otherwise stated, values represented means ±
1001 SEM derived from at least 3 independent experiments.

1002

1003 **Ethics Statement**

1004 All animal experiments were performed with approval from the Institutional Animal
1005 Care and Use Committee (IACUC) in Nanyang Technological University (NTU),

School of Biological Sciences under protocols ARF-SBS/NIE-A18061, A19061 and A24066.

Funding: R.A.G.d.S. and part of this work were supported by the National Research Foundation, Prime Minister's Office, Singapore, under its Campus for Research Excellence and Technological Enterprise (CREATE) program, through core funding of the Singapore-MIT Alliance for Research and Technology (SMART) Antimicrobial Resistance Interdisciplinary Research Group (AMR IRG). This work was also supported by the National Research Foundation and Ministry of Education Singapore under its Research Centre of Excellence Programme (to the Singapore Centre for Environmental Life Sciences Engineering, SCELSE), by the Singapore Ministry of Education under its Tier 2 program (MOE2019-T2-2-089) and a Swiss National Science Foundation project grant (310030_212262), both awarded to K.A.K. The funders had no role in study design, data collection and analysis, decision to publish, or preparation of the manuscript.

Author contributions: R.A.G.d.S., B.Y.Q.T., and K.A.K. designed the experiments. R.A.G.d.S., B.Y.Q.T., P.H.N.K., H.A., A.Z.C.T., and K.K.L.C. performed experiments. R.A.G.d.S., B.Y.Q.T., P.H.N.K., C.C., M.H.I., and G.H. analyzed data. R.A.G.d.S., B.Y.Q.T. and K.A.K. interpreted the results. B.Y.Q.T. and K.A.K. conceived the project. G.T., J.C., and K.A.K. supervised, acquired funding, and provided resources. R.A.G.d.S., B.Y.Q.T. and K.A.K. wrote the manuscript. All authors reviewed and approved the final manuscript.

1031

1032 **Reference**

1033 1. Gilmore, M.S., et al., *Enterococci: From commensals to leading causes of drug*
1034 *resistant infection*. 2014, Boston: Massachusetts Eye and Ear Infirmary. .
1035 2. Arias, C.A. and B.E. Murray, *The rise of the Enterococcus: beyond vancomycin*
1036 *resistance.* Nat Rev Microbiol, 2012. **10**(4): p. 266-78.
1037 3. Schmidt-Hieber, M., et al., *Intensified strategies to control vancomycin-resistant*
1038 *enterococci in immunocompromised patients.* Int J Hematol, 2007. **86**(2): p. 158-62.
1039 4. Hidron, A.I., et al., *NHSN annual update: antimicrobial-resistant pathogens*
1040 *associated with healthcare-associated infections: annual summary of data reported to*
1041 *the National Healthcare Safety Network at the Centers for Disease Control and*
1042 *Prevention, 2006-2007.* Infect Control Hosp Epidemiol, 2008. **29**(11): p. 996-1011.
1043 5. Sievert, D.M., et al., *Antimicrobial-resistant pathogens associated with healthcare-*
1044 *associated infections: summary of data reported to the National Healthcare Safety*
1045 *Network at the Centers for Disease Control and Prevention, 2009-2010.* Infect
1046 Control Hosp Epidemiol, 2013. **34**(1): p. 1-14.
1047 6. Dombrádi, Z., et al., *A case report of vancomycin-resistant Enterococcus faecalis*
1048 *colonization of a femoral wound in central europe*, in *Open Medicine*. 2009. p. 259.
1049 7. Hollenbeck, B.L. and L.B. Rice, *Intrinsic and acquired resistance mechanisms in*
1050 *enterococcus.* Virulence, 2012. **3**(5): p. 421-33.
1051 8. Archambaud, C., et al., *Enterococcus faecalis: an overlooked cell invader.* Microbiol
1052 Mol Biol Rev, 2024. **88**(3): p. e0006924.
1053 9. da Silva, R.A.G., et al., *Enterococcus faecalis alters endo-lysosomal trafficking to*
1054 *replicate and persist within mammalian cells.* PLoS Pathog, 2022. **18**(4): p.
1055 e1010434.
1056 10. Oeckinghaus, A., M.S. Hayden, and S. Ghosh, *Crosstalk in NF-kappaB signaling*
1057 *pathways.* Nat Immunol, 2011. **12**(8): p. 695-708.
1058 11. Tato, C.M. and C.A. Hunter, *Host-pathogen interactions: subversion and utilization*
1059 *of the NF-kappa B pathway during infection.* Infect Immun, 2002. **70**(7): p. 3311-7.
1060 12. Oeckinghaus, A. and S. Ghosh, *The NF-kappaB family of transcription factors and its*
1061 *regulation.* Cold Spring Harb Perspect Biol, 2009. **1**(4): p. a000034.
1062 13. Li, D. and M. Wu, *Pattern recognition receptors in health and diseases.* Signal
1063 Transduct Target Ther, 2021. **6**(1): p. 291.
1064 14. Chen, S., et al., *Epigenetic regulation of macrophages: from homeostasis*
1065 *maintenance to host defense.* Cell Mol Immunol, 2020. **17**(1): p. 36-49.
1066 15. Fang, Y., et al., *Emerging roles of lactate in acute and chronic inflammation.* Cell
1067 Commun Signal, 2024. **22**(1): p. 276.
1068 16. Halestrap, A.P., *The monocarboxylate transporter family--Structure and functional*
1069 *characterization.* IUBMB Life, 2012. **64**(1): p. 1-9.
1070 17. Shi, W., et al., *Lactic acid induces transcriptional repression of macrophage*
1071 *inflammatory response via histone acetylation.* Cell Rep, 2024. **43**(2): p. 113746.
1072 18. Hoque, R., et al., *Lactate reduces liver and pancreatic injury in Toll-like receptor-*
1073 *and inflammasome-mediated inflammation via GPR81-mediated suppression of*
1074 *innate immunity.* Gastroenterology, 2014. **146**(7): p. 1763-74.
1075 19. Yang, K., et al., *Lactate Suppresses Macrophage Pro-Inflammatory Response to LPS*
1076 *Stimulation by Inhibition of YAP and NF-kappaB Activation via GPR81-Mediated*
1077 *Signaling.* Front Immunol, 2020. **11**: p. 587913.
1078 20. Ashburner, B.P., S.D. Westerheide, and A.S. Baldwin, Jr., *The p65 (RelA) subunit of*
1079 *NF-kappaB interacts with the histone deacetylase (HDAC) corepressors HDAC1 and*

HDAC2 to negatively regulate gene expression. Mol Cell Biol, 2001. **21**(20): p. 7065-77.

21. Zhang, S.Y., et al., *Histone deacetylases and their inhibitors in inflammatory diseases.* Biomed Pharmacother, 2024. **179**: p. 117295.
22. Baldassarri, L., et al., *Glycosaminoglycans mediate invasion and survival of Enterococcus faecalis into macrophages.* J Infect Dis, 2005. **191**(8): p. 1253-62.
23. Gentry-Weeks, C.R., et al., *Survival of Enterococcus faecalis in mouse peritoneal macrophages.* Infection and Immunity, 1999. **67**(5): p. 2160-2165.
24. Rakita, R.M., et al., *Enterococcus faecalis bearing aggregation substance is resistant to killing by human neutrophils despite phagocytosis and neutrophil activation.* Infect Immun, 1999. **67**(11): p. 6067-75.
25. Roilides, E., et al., *How Biofilms Evade Host Defenses.* Microbiol Spectr, 2015. **3**(3).
26. Zou, J. and N. Shankar, *Enterococcus faecalis infection activates phosphatidylinositol 3-kinase signaling to block apoptotic cell death in macrophages.* Infect Immun, 2014. **82**(12): p. 5132-42.
27. Zou, J. and N. Shankar, *The opportunistic pathogen Enterococcus faecalis resists phagosome acidification and autophagy to promote intracellular survival in macrophages.* Cellular Microbiology, 2016. **18**(6): p. 831-843.
28. Stocks, C.J., et al., *Enterococcus faecalis persists and replicates intracellularly within neutrophils.* bioRxiv, 2025: p. 2025.07.03.662968.
29. Wang, S., et al., *Enterococcus faecalis from healthy infants modulates inflammation through MAPK signaling pathways.* PLoS One, 2014. **9**(5): p. e97523.
30. Wang, S., et al., *Infant intestinal Enterococcus faecalis down-regulates inflammatory responses in human intestinal cell lines.* World journal of gastroenterology : WJG, 2008. **14**(7): p. 1067-76.
31. Tien, B.Y.Q., et al., *Enterococcus faecalis Promotes Innate Immune Suppression and Polymicrobial Catheter-Associated Urinary Tract Infection.* Infection and immunity, 2017. **85**(12): p. e00378-17.
32. Birsoy, K., et al., *MCT1-mediated transport of a toxic molecule is an effective strategy for targeting glycolytic tumors.* Nat Genet, 2013. **45**(1): p. 104-8.
33. Morris, M.E. and M.A. Felmlee, *Overview of the proton-coupled MCT (SLC16A) family of transporters: characterization, function and role in the transport of the drug of abuse gamma-hydroxybutyric acid.* AAPS J, 2008. **10**(2): p. 311-21.
34. Certo, M., et al., *Understanding lactate sensing and signalling.* Trends Endocrinol Metab, 2022. **33**(10): p. 722-735.
35. Zanoni, I., et al., *CD14 controls the LPS-induced endocytosis of Toll-like receptor 4.* Cell, 2011. **147**(4): p. 868-80.
36. Kristich, C.J., et al., *Development and use of an efficient system for random mariner transposon mutagenesis to identify novel genetic determinants of biofilm formation in the core Enterococcus faecalis genome.* Appl Environ Microbiol, 2008. **74**(11): p. 3377-86.
37. Jönsson, M., et al., *Construction and characterization of three lactate dehydrogenase-negative Enterococcus faecalis V583 mutants.* Applied and environmental microbiology, 2009. **75**(14): p. 4901-4903.
38. Rana, N.F., et al., *Redox Balance via Lactate Dehydrogenase Is Important for Multiple Stress Resistance and Virulence in Enterococcus faecalis.* Infection and Immunity, 2013. **81**(8): p. 2662.
39. Harold, F.M. and E. Levin, *Lactic acid translocation: terminal step in glycolysis by Streptococcus faecalis.* J Bacteriol, 1974. **117**(3): p. 1141-8.

1129 40. Mehmeti, I., et al., *Transcriptome, proteome, and metabolite analyses of a lactate*
1130 *dehydrogenase-negative mutant of Enterococcus faecalis V583.* Applied and
1131 environmental microbiology, 2011. **77**(7): p. 2406-2413.
1132 41. Heming, T.A., et al., *Post-transcriptional effects of extracellular pH on tumour*
1133 *necrosis factor-alpha production in RAW 246.7 and J774 A.1 cells.* Clin Sci (Lond),
1134 2001. **100**(3): p. 259-66.
1135 42. Gentry-Weeks, C.R., et al., *Survival of Enterococcus faecalis in mouse peritoneal*
1136 *macrophages.* Infect Immun, 1999. **67**(5): p. 2160-5.
1137 43. Mondello, P., et al., *Panobinostat acts synergistically with ibrutinib in diffuse large B*
1138 *cell lymphoma cells with MyD88 L265P mutations.* JCI Insight, 2017. **2**(6): p. e90196.
1139 44. Rebe, C., et al., *STAT3 activation: A key factor in tumor immunoescape.* JAKSTAT,
1140 2013. **2**(1): p. e23010.
1141 45. Lee, H.K., et al., *Extracellular Signal-regulated Kinase Activation Is Required for*
1142 *Serine 727 Phosphorylation of STAT3 in Schwann Cells in vitro and in vivo.* Korean J
1143 Physiol Pharmacol, 2009. **13**(3): p. 161-8.
1144 46. Chung, J., et al., *STAT3 serine phosphorylation by ERK-dependent and -independent*
1145 *pathways negatively modulates its tyrosine phosphorylation.* Mol Cell Biol, 1997.
1146 **17**(11): p. 6508-16.
1147 47. Chang, F., et al., *Signal transduction mediated by the Ras/Raf/MEK/ERK pathway*
1148 *from cytokine receptors to transcription factors: potential targeting for therapeutic*
1149 *intervention.* Leukemia, 2003. **17**(7): p. 1263-93.
1150 48. Balgi, A.D., et al., *Regulation of mTORC1 signaling by pH.* PLoS One, 2011. **6**(6): p.
1151 e21549.
1152 49. Villarino, A.V., Y. Kanno, and J.J. O'Shea, *Mechanisms and consequences of Jak-*
1153 *STAT signaling in the immune system.* Nat Immunol, 2017. **18**(4): p. 374-384.
1154 50. Wu, M., et al., *Hepatitis B virus polymerase inhibits the interferon-inducible MyD88*
1155 *promoter by blocking nuclear translocation of Stat1.* J Gen Virol, 2007. **88**(Pt 12): p.
1156 3260-3269.
1157 51. Hajjar, S. and X. Zhou, *pH sensing at the intersection of tissue homeostasis and*
1158 *inflammation.* Trends Immunol, 2023. **44**(10): p. 807-825.
1159 52. Liu, C., et al., *Lactate inhibits lipolysis in fat cells through activation of an orphan G-*
1160 *protein-coupled receptor, GPR81.* J Biol Chem, 2009. **284**(5): p. 2811-2822.
1161 53. Felmlee, M.A., et al., *Monocarboxylate Transporters (SLC16): Function, Regulation,*
1162 *and Role in Health and Disease.* Pharmacol Rev, 2020. **72**(2): p. 466-485.
1163 54. Kappler, M., et al., *The real face of HIF1alpha in the tumor process.* Cell Cycle,
1164 2012. **11**(21): p. 3932-6.
1165 55. Saraiva, M., P. Vieira, and A. O'Garra, *Biology and therapeutic potential of*
1166 *interleukin-10.* J Exp Med, 2020. **217**(1).
1167 56. Chong, K.K.L., et al., *Enterococcus faecalis Modulates Immune Activation and Slows*
1168 *Healing During Wound Infection.* J Infect Dis, 2017. **216**(12): p. 1644-1654.
1169 57. Keogh, D., et al., *Enterococcal Metabolite Cues Facilitate Interspecies Niche*
1170 *Modulation and Polymicrobial Infection.* Cell Host Microbe, 2016. **20**(4): p. 493-503.
1171 58. Weiner, L.M., et al., *Antimicrobial-Resistant Pathogens Associated With Healthcare-*
1172 *Associated Infections: Summary of Data Reported to the National Healthcare Safety*
1173 *Network at the Centers for Disease Control and Prevention, 2011-2014.* Infect
1174 Control Hosp Epidemiol, 2016. **37**(11): p. 1288-1301.
1175 59. Zou, J. and N. Shankar, *Roles of TLR/MyD88/MAPK/NF-κB signaling pathways in*
1176 *the regulation of phagocytosis and proinflammatory cytokine expression in response*
1177 *to E. faecalis infection.* PLoS ONE, 2015. **10**(8): p. e0136947.

1178 60. Zou, J., et al., *A TIR domain protein from E. faecalis attenuates MyD88-mediated*
1179 *signaling and NF-kappaB activation.* PLoS One, 2014. **9**(11): p. e112010.
1180 61. Ramsey, M., A. Hartke, and M. Huycke, *The Physiology and Metabolism of*
1181 *Enterococci*, in *Enterococci: From Commensals to Leading Causes of Drug Resistant*
1182 *Infection*, M.S. Gilmore, et al., Editors. 2014: Boston.
1183 62. Richardson, A.R., S.J. Libby, and F.C. Fang, *A Nitric Oxide–Inducible Lactate*
1184 *Dehydrogenase Enables Staphylococcus aureus to Resist Innate*
1185 *Immunity.* Science, 2008. **319**(5870): p. 1672.
1186 63. Esvaran, M. and P.L. Conway, *Lactobacilli can attenuate inflammation in mouse*
1187 *macrophages exposed to polyethylene particles in vitro.* BMC research notes, 2018.
1188 **11**(1): p. 567-567.
1189 64. Kim, B., O. Shynlova, and S. Lye, *Probiotic Lactobacillus rhamnosus GR-1 is a*
1190 *unique prophylactic agent that suppresses infection-induced myometrial cell*
1191 *responses.* Scientific reports, 2019. **9**(1): p. 4698-4698.
1192 65. Colegio, O.R., et al., *Functional polarization of tumour-associated macrophages by*
1193 *tumour-derived lactic acid.* Nature, 2014. **513**(7519): p. 559-563.
1194 66. Dietl, K., et al., *Lactic acid and acidification inhibit TNF secretion and glycolysis of*
1195 *human monocytes.* J Immunol, 2010. **184**(3): p. 1200-9.
1196 67. Husain, Z., et al., *Tumor-Derived Lactate Modifies Antitumor Immune Response:*
1197 *Effect on Myeloid-Derived Suppressor Cells and NK Cells.* The Journal of
1198 Immunology, 2013. **191**(3): p. 1486.
1199 68. Morrot, A., et al., *Metabolic Symbiosis and Immunomodulation: How Tumor Cell-*
1200 *Derived Lactate May Disturb Innate and Adaptive Immune Responses.* Frontiers in
1201 oncology, 2018. **8**: p. 81-81.
1202 69. Mu, X., et al., *Tumor-derived lactate induces M2 macrophage polarization via the*
1203 *activation of the ERK/STAT3 signaling pathway in breast cancer.* Cell Cycle, 2018.
1204 **17**(4): p. 428-438.
1205 70. Romero-Garcia, S., et al., *Lactate Contribution to the Tumor Microenvironment:*
1206 *Mechanisms, Effects on Immune Cells and Therapeutic Relevance.* Frontiers in
1207 immunology, 2016. **7**: p. 52-52.
1208 71. Bidani, A., et al., *Evidence for pH sensitivity of tumor necrosis factor-alpha release*
1209 *by alveolar macrophages.* Lung, 1998. **176**(2): p. 111-21.
1210 72. Grabowski, J., et al., *Tumor necrosis factor expression is ameliorated after exposure*
1211 *to an acidic environment.* The Journal of surgical research, 2012. **173**(1): p. 127-134.
1212 73. Mogi, C., et al., *Involvement of Proton-Sensing TDAG8 in Extracellular*
1213 *Acidification-Induced Inhibition of Proinflammatory Cytokine Production in*
1214 *Peritoneal Macrophages.* The Journal of Immunology, 2009. **182**(5): p. 3243.
1215 74. Fernandez, S.F., et al., *Low pH Environmental Stress Inhibits LPS and LTA-*
1216 *Stimulated Proinflammatory Cytokine Production in Rat Alveolar Macrophages.*
1217 BioMed Research International, 2013. **2013**: p. 742184.
1218 75. Gerry, A.B. and D.S. Leake, *Effect of low extracellular pH on NF-κB activation in*
1219 *macrophages.* Atherosclerosis, 2014. **233**(2): p. 537-544.
1220 76. Rao, K.M., *MAP kinase activation in macrophages.* J Leukoc Biol, 2001. **69**(1): p. 3-
1221 10.
1222 77. Traves, P.G., et al., *Relevance of the MEK/ERK signaling pathway in the metabolism*
1223 *of activated macrophages: a metabolomic approach.* J Immunol, 2012. **188**(3): p.
1224 1402-10.
1225 78. Rosenberger, C.M. and B.B. Finlay, *Macrophages inhibit Salmonella typhimurium*
1226 *replication through MEK/ERK kinase and phagocyte NADPH oxidase activities.* J
1227 Biol Chem, 2002. **277**(21): p. 18753-62.

1228 79. Panagi, I. and T.L. Thurston, *Ready, STAT3, Go! Bacteria in the race for M2*
1229 *macrophage polarisation.* Curr Opin Microbiol, 2023. **73**: p. 102285.
1230 80. Hwang, J.T., et al., *Lactococcus lactis KR-050L inhibit IL-6/STAT3 activation.* J Appl
1231 Microbiol, 2017. **122**(5): p. 1412-1422.
1232 81. Casey, J.R., S. Grinstein, and J. Orlowski, *Sensors and regulators of intracellular pH.*
1233 Nat Rev Mol Cell Biol, 2010. **11**(1): p. 50-61.
1234 82. Wu, Z., et al., *Regulation of inflammatory responses by pH-dependent transcriptional*
1235 *condensates.* Cell, 2025.
1236 83. Heim, C.E., et al., *Lactate production by Staphylococcus aureus biofilm inhibits*
1237 *HDAC11 to reprogramme the host immune response during persistent infection.* Nat
1238 Microbiol, 2020. **5**(10): p. 1271-1284.
1239 84. Kim, M., et al., *cAMP/PKA signalling reinforces the LATS-YAP pathway to fully*
1240 *suppress YAP in response to actin cytoskeletal changes.* EMBO J, 2013. **32**(11): p.
1241 1543-55.
1242 85. Loike, J.D., et al., *Lactate transport in macrophages.* J Immunol, 1993. **150**(5): p.
1243 1951-8.
1244 86. Nonaka, M., et al., *Lactic acid induces HSPA1A expression through ERK1/2*
1245 *activation.* Biosci Biotechnol Biochem, 2023. **87**(2): p. 191-196.
1246 87. Falck Miniotis, M., et al., *MEK1/2 inhibition decreases lactate in BRAF-driven*
1247 *human cancer cells.* Cancer Res, 2013. **73**(13): p. 4039-49.
1248 88. Ohno, Y., et al., *Lactate increases myotube diameter via activation of MEK/ERK*
1249 *pathway in C2C12 cells.* Acta Physiol (Oxf), 2018. **223**(2): p. e13042.
1250 89. Xue, L. and J.M. Lucocq, *Low extracellular pH induces activation of ERK 2, JNK,*
1251 *and p38 in A431 and Swiss 3T3 cells.* Biochem Biophys Res Commun, 1997. **241**(2):
1252 p. 236-42.
1253 90. Chen, B., et al., *ERK-mediated NF-kappaB activation through ASIC1 in response to*
1254 *acidosis.* Oncogenesis, 2016. **5**(12): p. e279.
1255 91. Hirata, S., et al., *Extracellular acidic environments induce phosphorylation of ZAP-70*
1256 *in Jurkat T cells.* Immunol Lett, 2008. **115**(2): p. 105-9.
1257 92. Aguirre, M. and M.D. Collins, *Lactic acid bacteria and human clinical infection.* J
1258 Appl Bacteriol, 1993. **75**(2): p. 95-107.
1259 93. Rossi, F., et al., *Lactobacilli Infection Case Reports in the Last Three Years and*
1260 *Safety Implications.* Nutrients, 2022. **14**(6).
1261 94. da Silva, R.A.G., et al., *Bosutinib Stimulates Macrophage Survival, Phagocytosis, and*
1262 *Intracellular Killing of Bacteria.* ACS Infect Dis, 2024. **10**(5): p. 1725-1738.
1263 95. da Silva, R.A.G., et al., *Mitoxantrone targets both host and bacteria to overcome*
1264 *vancomycin resistance in Enterococcus faecalis.* Sci Adv, 2023. **9**(8): p. eadd9280.
1265 96. Paulsen, I.T., et al., *Role of mobile DNA in the evolution of vancomycin-resistant*
1266 *Enterococcus faecalis.* Science, 2003. **299**(5615): p. 2071-4.
1267 97. Weischenfeldt, J. and B. Porse, *Bone Marrow-Derived Macrophages (BMM):*
1268 *Isolation and Applications.* CSH Protoc, 2008. **2008**: p. pdb.prot5080.
1269 98. James-Kracke, M.R., *Quick and accurate method to convert BCECF fluorescence to*
1270 *pHi: calibration in three different types of cell preparations.* J Cell Physiol, 1992.
1271 **151**(3): p. 596-603.
1272 99. Pfaffl, M.W., *A new mathematical model for relative quantification in real-time RT-*
1273 *PCR.* Nucleic Acids Res, 2001. **29**(9): p. e45.
1274 100. Kristich, C.J., et al., *Development and use of an efficient system for random mariner*
1275 *transposon mutagenesis to identify novel genetic determinants of biofilm formation in*
1276 *the core Enterococcus faecalis genome.* Applied and environmental microbiology,
1277 2008. **74**(11): p. 3377-3386.

101. Livak, K.J. and T.D. Schmittgen, *Analysis of relative gene expression data using real-time quantitative PCR and the 2(-Delta Delta C(T)) Method.* Methods, 2001. **25**(4): p. 402-8.
102. Dunny, G.M., B.L. Brown, and D.B. Clewell, *Induced cell aggregation and mating in Streptococcus faecalis: evidence for a bacterial sex pheromone.* Proc Natl Acad Sci U S A, 1978. **75**(7): p. 3479-83.
103. Bourgogne, A., et al., *Large scale variation in Enterococcus faecalis illustrated by the genome analysis of strain OG1RF.* Genome Biol, 2008. **9**(7): p. R110.
104. Blattner, F.R., et al., *The complete genome sequence of Escherichia coli K-12.* Science, 1997. **277**(5331): p. 1453-62.
105. Totsika, M., et al., *Insights into a multidrug resistant Escherichia coli pathogen of the globally disseminated ST131 lineage: genome analysis and virulence mechanisms.* PLoS One, 2011. **6**(10): p. e26578.
106. Chen, S.L., et al., *Identification of genes subject to positive selection in uropathogenic strains of Escherichia coli: a comparative genomics approach.* Proc Natl Acad Sci U S A, 2006. **103**(15): p. 5977-82.
107. McDougal, L.K., et al., *Pulsed-field gel electrophoresis typing of oxacillin-resistant Staphylococcus aureus isolates from the United States: establishing a national database.* J Clin Microbiol, 2003. **41**(11): p. 5113-20.
108. Judicial Commission Of The International Committee On Systematics Of, P., *The type species of the genus Salmonella Lignieres 1900 is Salmonella enterica (ex Kauffmann and Edwards 1952) Le Minor and Popoff 1987, with the type strain LT2T, and conservation of the epithet enterica in Salmonella enterica over all earlier epithets that may be applied to this species. Opinion 80.* Int J Syst Evol Microbiol, 2005. **55**(Pt 1): p. 519-520.
109. Hentzer, M., et al., *Inhibition of quorum sensing in Pseudomonas aeruginosa biofilm bacteria by a halogenated furanone compound.* Microbiology (Reading), 2002. **148**(Pt 1): p. 87-102.
110. Zhang, X., et al., *RNA-seq and Tn-seq reveal fitness determinants of vancomycin-resistant Enterococcus faecium during growth in human serum.* BMC Genomics, 2017. **18**(1): p. 893.
111. Lam, M.M., et al., *Comparative analysis of the first complete Enterococcus faecium genome.* J Bacteriol, 2012. **194**(9): p. 2334-41.
112. Seeliger, H.P., *Listeriosis--history and actual developments.* Infection, 1988. **16 Suppl 2**: p. S80-4.

Figures

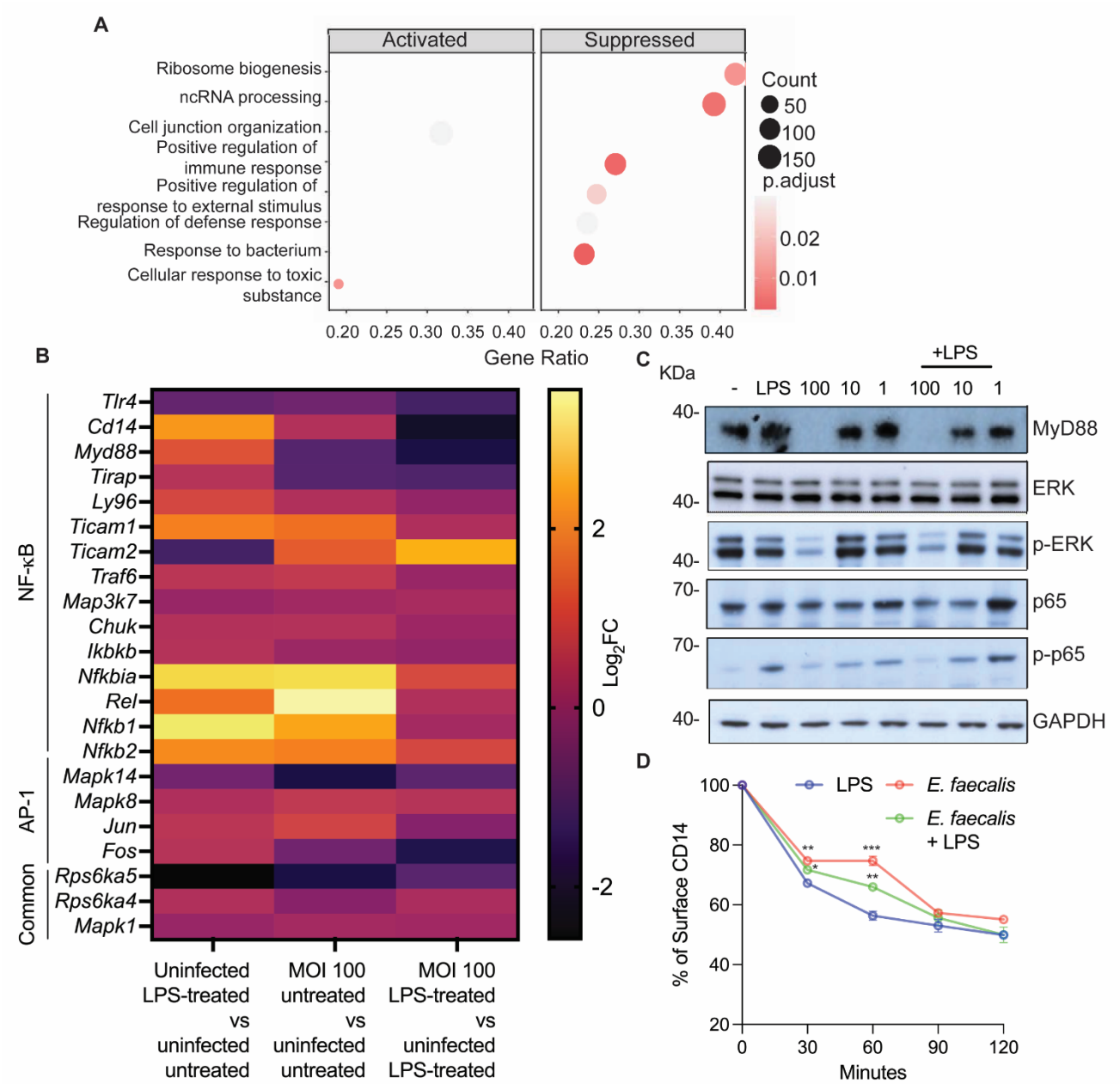

Figure 1 – *E. faecalis* modulates the macrophage response to bacteria by reducing MyD88 protein levels and preventing ERK and p65 phosphorylation. **(A)** GSEA using gene ontology biological process gene sets showing significantly enriched pathways in RAW 264.7 macrophages infected with *E. faecalis* OG1RF for 6 h at MOI 100 in the presence of LPS (100 ng/mL) compared to uninfected LPS-treated macrophages. Activated and suppressed pathways were determined based on genes that are over and under expressed in the analyzed pathways. The size of the circle

1353 indicates the number of genes in each pathway gene set that are up- or down-
1354 regulated. **(B)** Heatmap of differentially expressed NF-κB/ AP-1-related genes. **(C)**
1355 Immunoblots performed on protein extracted from RAW 264.7 macrophages infected
1356 with *E. faecalis* for 6 h at the indicated MOI (100, 10, 1) with or without LPS and probed
1357 with antibodies specific for MyD88, ERK, p-ERK, p65, p-p65 and GAPDH. The two
1358 bands for ERK and p-ERK immunoblots represent ERK isoforms 1 and 2. Data shown
1359 are representative of at least 3 independent experiments. **(D)** RAW 264.7 cells were
1360 either infected or treated with LPS alone or in combination for the times indicated
1361 before CD14 endocytosis was examined by flow cytometry. Data (mean ± SEM) are a
1362 summary of three independent experiments and calculated relative to uninfected
1363 untreated cells which were set as 100% levels for the examined receptor. Statistical
1364 analysis was performed using ordinary one-way ANOVA followed by Dunnett's
1365 multiple comparison test *$p<0.05$, **$p<0.01$ and ***$p<0.001$.
1366
1367
1368
1369

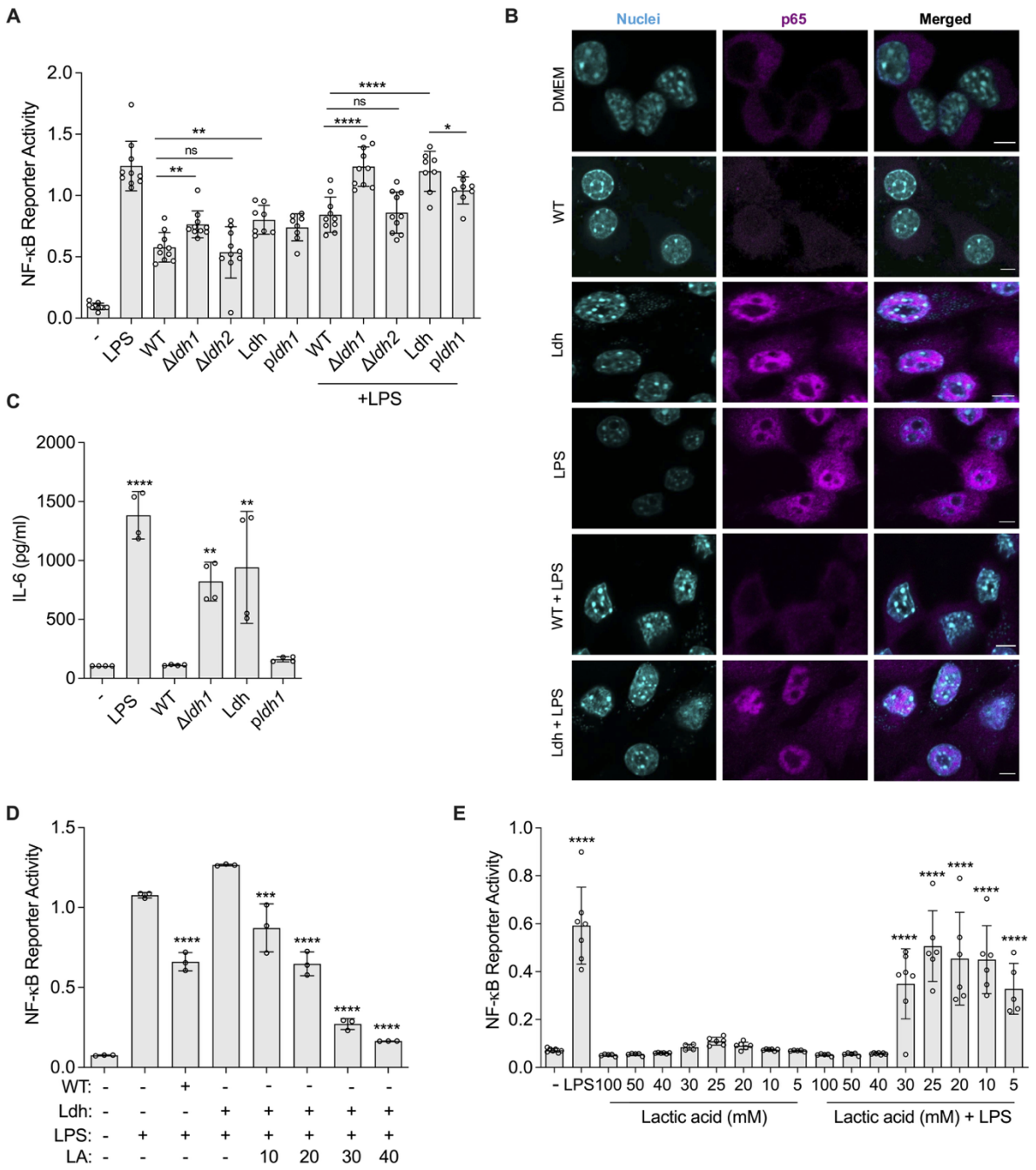

Figure 2 – *E. faecalis* LDH is essential for suppression of NF-κB activation in macrophages.

(A) RAW 264.7 macrophages were infected with WT, Δ*ldh1,* Δ*ldh2,* Ldh, or *ldh1* complementation strains alone or concurrently with LPS at MOI 100 for 6 h prior to measurement of NF-κB-driven SEAP reporter activity. **(B)** Immunofluorescence of p65 in RAW264.7 cells at 6 hpi infection with WT or Ldh in the presence or absence of

1377 LPS. Magenta, p65 and cyan, dsDNA stained with Hoechst 33342. Images are
1378 representative of 2 independent experiments. Scale bar: 5 μm. **(C)** BMDMs were
1379 infected with Δ*ldh1,* Ldh, or *ldh1* complemented strain for 6 h prior to measurement of
1380 IL-6 production. **(D)** RAW 264.7 cells were infected with WT *E. faecalis* or Ldh
1381 supplemented with lactic acid (LA) at various concentration (mM) for 6 h prior to
1382 measurement of NF-κB-driven SEAP reporter activity. 25 mM lactic acid best
1383 approximates the lactate concentration measured in MOI 100 supernatants in
1384 Fig. S4C. **(E)** RAW 264.7 cells were incubated with cell culture media supplemented
1385 with lactic acid at various concentrations for 6 h prior to measurement of NF-κB-driven
1386 SEAP reporter activity. Data (mean ± SEM) are a summary of at least three
1387 independent experiments. Statistical analysis was performed using one-way ANOVA
1388 with Fisher's LSD in **(B)** or Tukey's multiple comparison test where *$p<0.05$, **$p<0.01$,
1389 ***$p<0.001$ and ****$p<0.0001$ as indicated or as compared to media alone for **(C)** and
1390 **(E)**, and LPS for **(D)**.
1391
1392
1393
1394
1395
1396
1397
1398

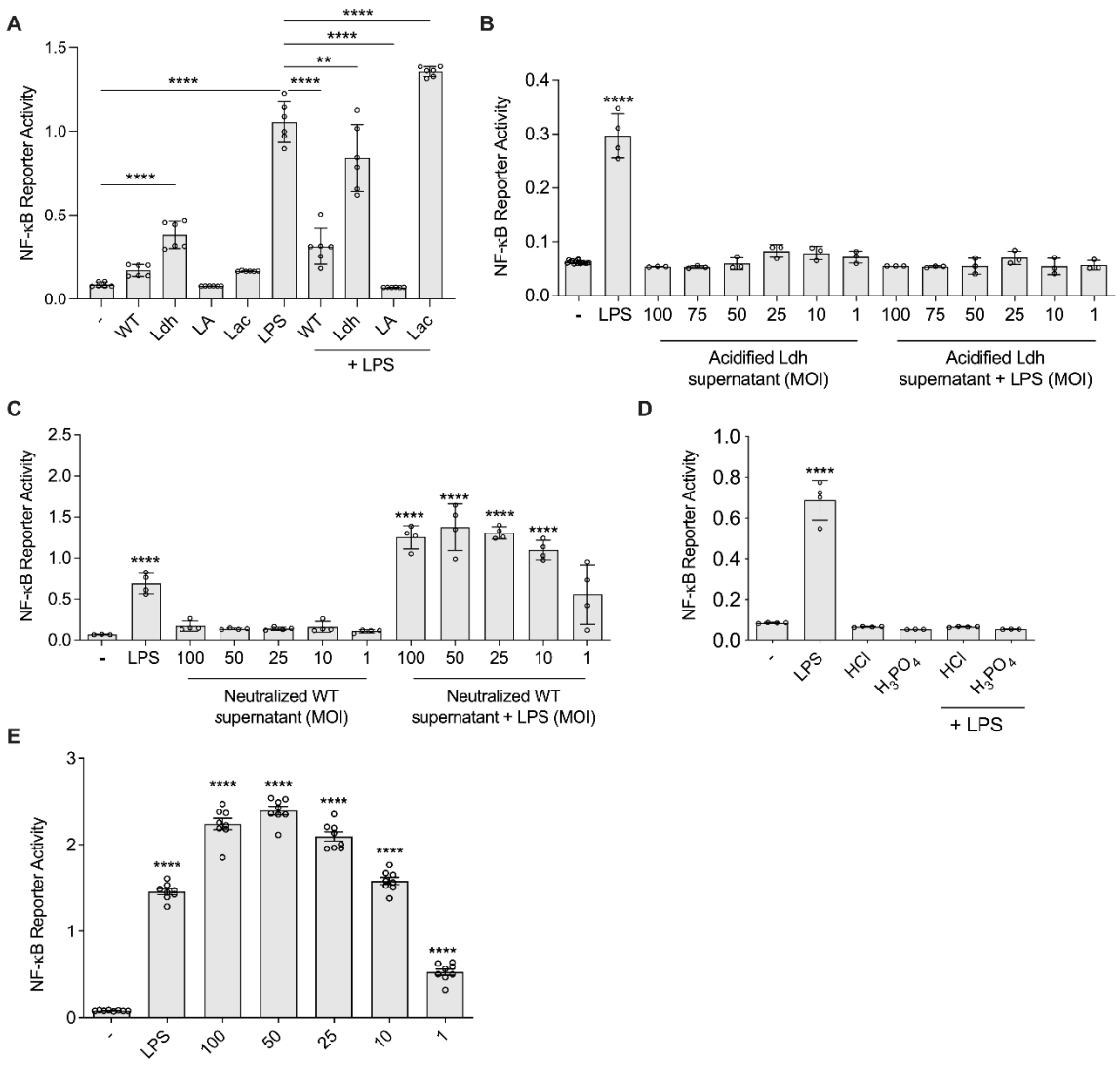

Figure 3 – Acidification is necessary and sufficient for *E. faecalis* suppression of macrophage activation.

(A) RAW 264.7 macrophages were infected with WT or Ldh or incubated with cell culture media supplemented with lactic acid (LA) or sodium lactate (Lac) (40 mM) in the presence or absence of LPS for 6 h prior to measurement of NF-κB-driven SEAP reporter activity. RAW 264.7 macrophages were incubated with **(B)** lactic acid-acidified, **(C)** neutralised bacterial-free supernatant (equivalent to shown MOI starting bacterial culture grown for 6 h in cell culture media in the absence of macrophages) and **(D)** HCl and H_3PO_4 acidified media for 6 h prior to measurement of NF-κB-driven SEAP reporter activity. **(E)** RAW 264.7 macrophages were incubated with *E. faecalis* WT

1410 (MOI 100, 50, 25, 10, 1) 3 h and treated with 500 μg/mL of gentamicin with penicillin
1411 G overnight at 37˚C prior to measurement of NF-κB-driven SEAP reporter activity. **(A-**
1412 **E)** Data (mean ± SEM) are a summary of at least three independent experiments.
1413 Statistical analysis was performed using one-way ANOVA with Tukey's multiple
1414 comparison tests where NS indicates $p > 0.05$, **$p<0.01$, ***$p<0.001$ and ****$p<0.0001$
1415 as compared to media alone unless otherwise indicated.

1416
1417
1418
1419
1420

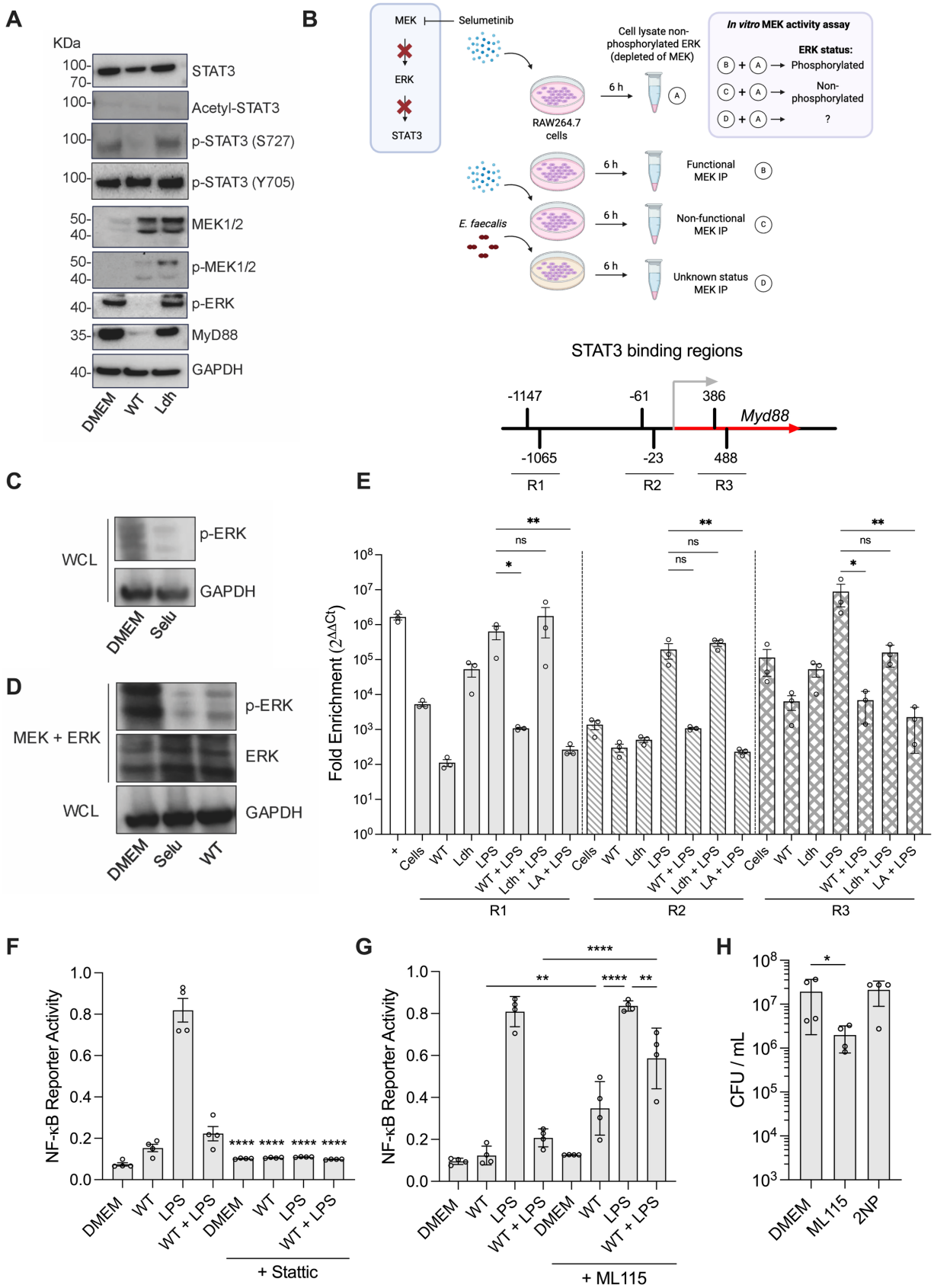

Figure 4 – *E. faecalis* infection reduces MyD88 expression by inhibiting STAT3 activity in macrophages. (A) Immunoblot of STAT3, acetyl-STAT3, p-STAT3 (S727),

1424 p-STAT3 (Y705), MEK1/2, p-MEK1/2, p-ERK, MyD88 and GAPDH with protein
1425 extracted from RAW 264.7 macrophages infected with WT *E. faecalis* or Ldh mutant.
1426 **(B)** *In vitro* MEK activity assay. **(C-D)** pERK immunoblot of whole cell lysate (WCL) of
1427 cells treated with Selu demonstrating Selu effectively diminishes ERK phosphorylation
1428 **(C).** ERK and pERK Immunoblot post *in vitro* MEK activity assay using
1429 immunoprecipitated MEK of WT infected WCL. GAPDH immunoblot shows initial
1430 reaction input were equal **(D)**. Immunoblot images represent two independent
1431 experiments **(C-D)**. **(E)** ChIP–qPCR for STAT3 of the three regions at the MyD88
1432 transcriptional starting site in purified DNA of RAW 264.7 cells that were infected with
1433 WT *E. faecalis* or Ldh mutant with or without LPS treatment for 6 h. Treatment with LA
1434 in the presence of LPS was also included. A depiction of the three regions relative to
1435 the transcriptional starting site (gray arrow) of *Myd88* is shown. *Myd88* coding
1436 sequence is represented in red. The positive control was established for an RNA
1437 polymerase binding site for the *Gapdh* gene. Replicates from 3 independent
1438 experiments are shown. Statistical analysis was performed using Kruskal-Wallis test
1439 followed by uncorrected Dunn's multiple comparison tests where ns, $p > 0.05$; *$p \leq 0.05$
1440 and **$p<0.01$. **(F-G)** RAW 264.7 macrophages were infected with the WT *E. faecalis*
1441 and incubated with cell culture media in the presence or absence of LPS and **(F)** Stattic
1442 (10 μM) and **(G)** ML115 (1 μM) for 6 h prior to measurement of NF-κB-driven SEAP
1443 reporter activity. Stattic and ML115 were added 30 min before the beginning of the
1444 experiment. Data (mean ± SEM) are a summary of at least three independent
1445 experiments. Statistical analysis was performed using one-way ANOVA with Tukey's
1446 multiple comparison tests where ns, $p > 0.05$, **$p<0.01$, ***$p<0.001$ and $p<0.0001$ as
1447 compared to LPS unless otherwise indicated. **(H)** RAW264.7 cells were infected with
1448 *E. faecalis* for 3 h, followed by 1 h of antibiotic treatment to kill extracellular bacteria.

1449 The antibiotic-containing medium was removed, cells were washed, and fresh medium
1450 with antibiotics was added together with ML115 (1 μM) and 2NP (45 μM). Viable
1451 intracellular CFU were enumerated after 18 h incubation. Data (mean ± SEM) are a
1452 summary of at least three independent experiments. Statistical analysis was
1453 performed using ordinary one-way ANOVA followed by Tukey's multiple comparison
1454 test ns, p>0.05; *p≤0.05.
1455
1456

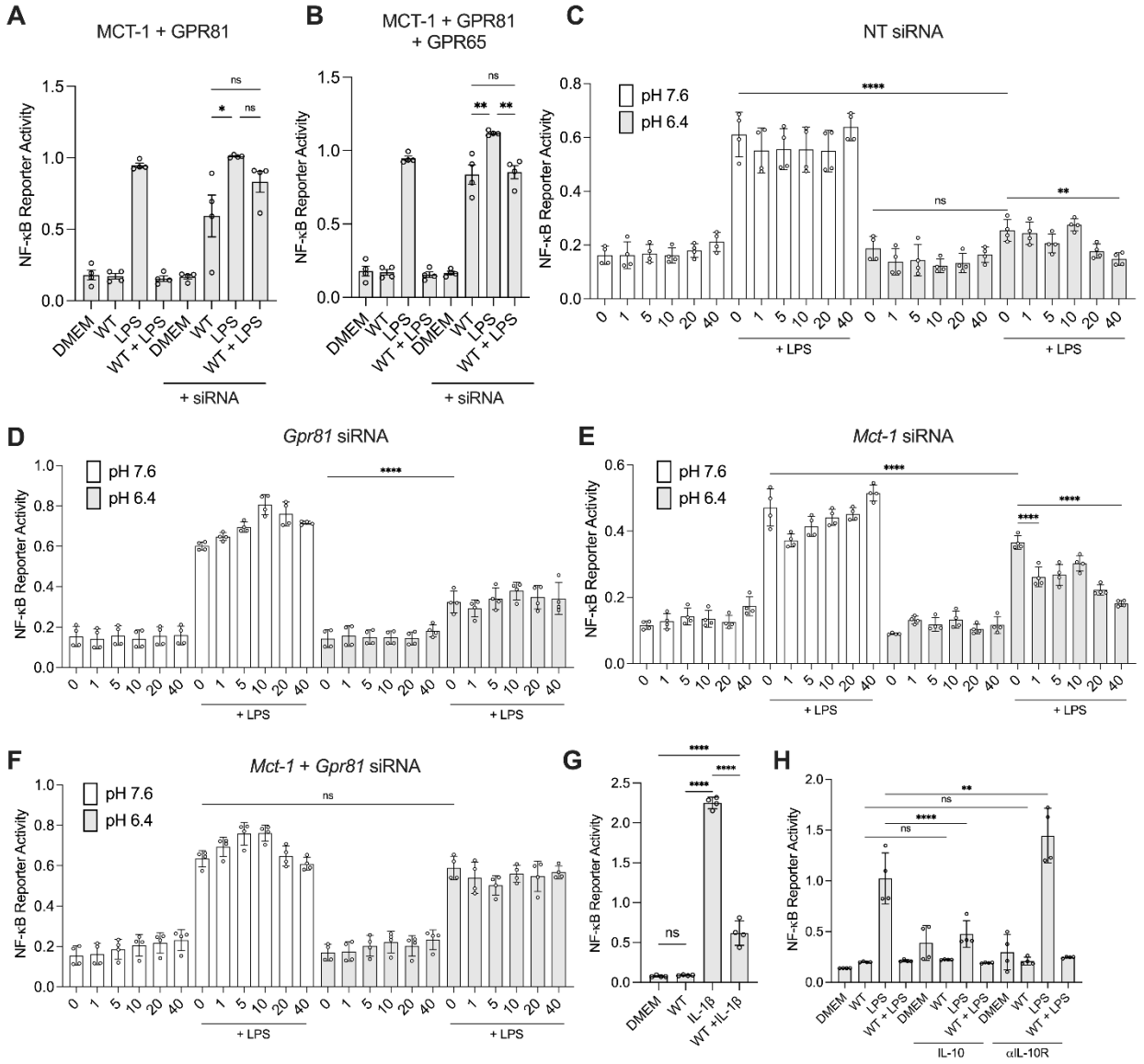

1457
1458

1459 **Figure 5 – The pH-sensitive lactate transporter MCT-1 and lactate sensor GPR81**
1460 **mediate suppression of NF-κB by *E. faecalis*.**
1461 **(A-B)** RAW 264.7 macrophages, with or without siRNA-silenced lactate transporters
1462 and sensors, were infected with *E. faecalis* in the presence or absence of LPS for 6 h
1463 prior to measurement of NF-κB-driven SEAP reporter activity. **(C-F)** Non-targeting,
1464 *Gpr81* (*Hcar1*), *Mct-1* (*Slc16a1*) siRNA alone or combined were used to silence RAW
1465 264.7 cells in pH 7.6 or pH 6.4 in the presence or absence of LPS, in increasing
1466 concentrations of lactate, for 6 h prior to measurement of NF-κB-driven SEAP reporter
1467 activity. **(G)** RAW 264.7 macrophages were infected with the WT *E. faecalis* and
1468 incubated in cell culture media in presence or absence of IL-1β for 6 h prior to
1469 measurement of NF-κB-driven SEAP reporter activity. **(H)** NF-κB reporter activity
1470 assay with RAW 264.7 cells uninfected or 6 h WT infected that were left untreated or
1471 treated with LPS. RAW 264.7 cells were pre-treated with IL-10 or antibody αIL-10R for
1472 30 min prior to the beginning of the assay. Data (mean ± SEM) represent at least two
1473 independent experiments. Statistical analysis was performed using ordinary one-way
1474 ANOVA followed by Tukey's multiple comparison test **(A-B and D-G)** or Fisher's LSD
1475 **(C and H),** ns, $p>0.05$; *$p\leq0.05$; **$p<0.01$ and ****$p<0.0001$.
1476
1477

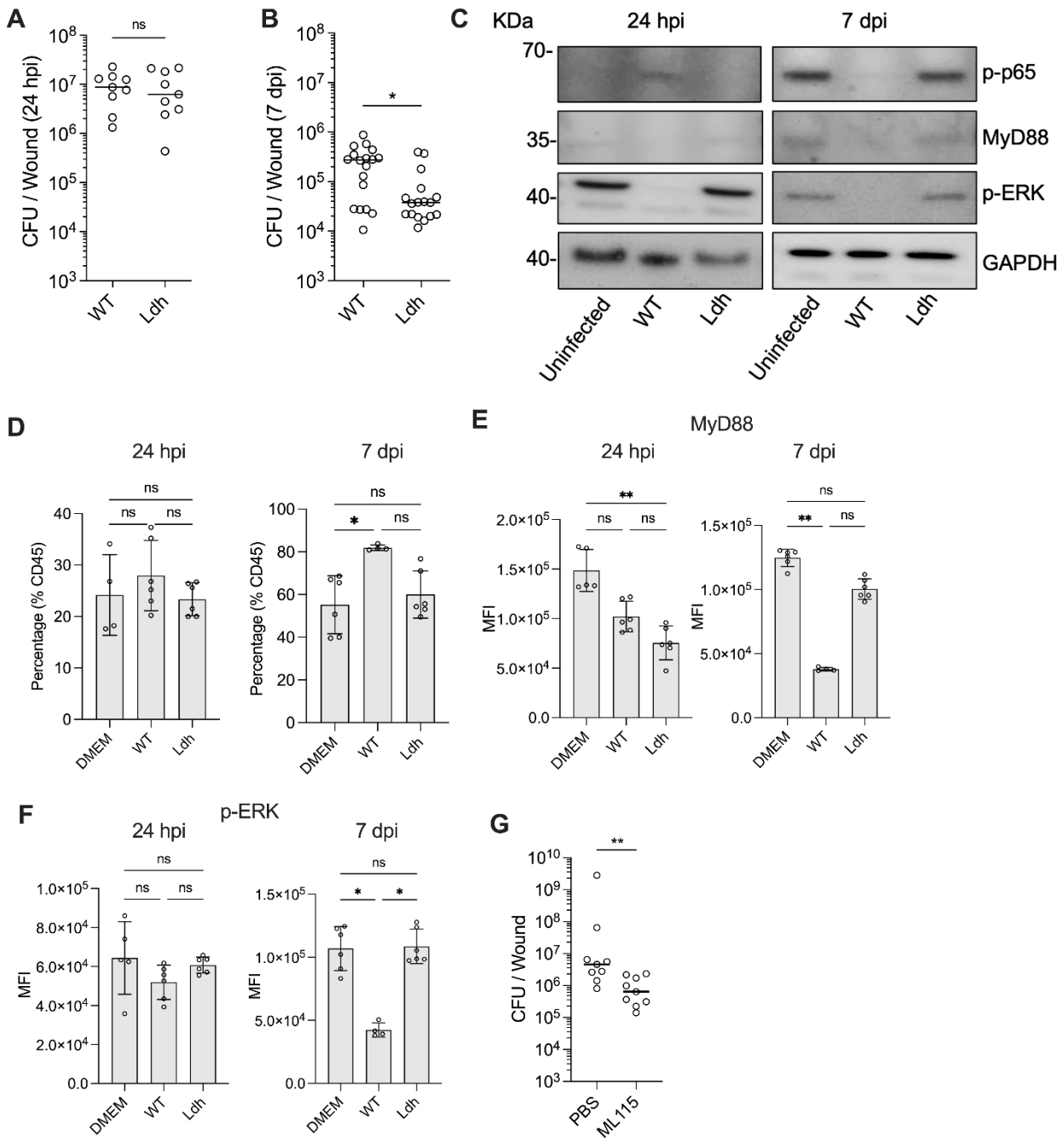

Figure 6 – *E. faecalis* LDH activity contributes to persistence in the wound. (A-B) Using a wound model, mice were infected with 10^6 CFU each of WT or Ldh mutant and CFU were enumerated at 24 hpi and 7 dpi. Each symbol represents one mouse with the median indicated by the horizontal line. Data are from at least 2 independent experiments with three to five mice per experiment. Statistical analysis was performed using the nonparametric Mann-Whitney test to compare ranks; ns, $p>0.05$, $*p\leq0.05$. **(C)** Immunoblot performed on protein extracted from harvested wound lysates of WT

1486 or Ldh infections 24 hpi or 7 dpi and probed with antibodies against p-p65, MyD88, p-
1487 ERK and GAPDH. **(D)** Percentage of $CD11b^+$ $F4/80^+$ macrophages recovered from
1488 uninfected or infected wounds with WT or Ldh after 24 hpi or 7 dpi. Comparison of
1489 mean fluorescence intensity (MFI) of MyD88 **(E)** and p-ERK **(F)** staining gating on
1490 $CD11b^+$ $F4/80^+$ macrophages recovered from uninfected or infected wounds with WT
1491 or Ldh after 24 hpi or 7 dpi. **(D-F)** Each dot represents one mouse. Data (mean ± SEM)
1492 are a summary of at least two independent experiments with two to four mice per
1493 experiment. Statistical analysis was performed using Kruskal-Wallis test with Dunn's
1494 posttest; ns, $p>0.05$; *$p \leq 0.05$; and **$p \leq 0.01$. **(G)** Mouse wounds were infected with
1495 10^6 CFU of WT *E. faecalis* and CFU were enumerated at 24 hpi after treatment with
1496 either PBS or 10 μL of ML115 (100 μM). Each symbol represents one mouse with the
1497 median is indicated by the horizontal line. Data are from at least 2 independent
1498 experiments with three to five mice per experiment. Statistical analysis was performed
1499 using the nonparametric Mann-Whitney test to compare ranks; **$p<0.01$.
1500
1501
1502

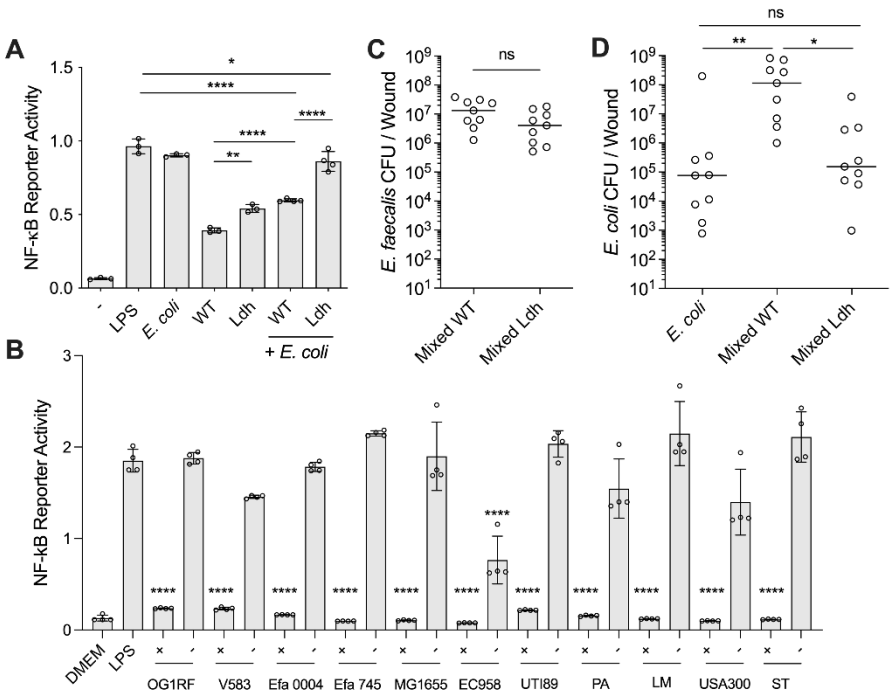

1503

1504 **Figure 7 – *E. faecalis* LDH-mediated immune suppression promotes *E. coli***

1505 **growth during polymicrobial infection.**

1506 **(A)** RAW 264.7 macrophages were infected with *E. coli* strain UTI89 at MOI 0.125,

1507 WT *E. faecalis* or Ldh mutant at MOI 100 in single species (control) or mixed species

1508 infection for 6 h prior to measurement of NF-κB-driven SEAP reporter activity. **(B)**

1509 RAW 264.7 macrophages were infected with different bacterial species as indicated

1510 at MOI 1 for 6 h in the presence or absence of WT supernatant prior to measurement

1511 of NF-κB-driven SEAP reporter activity. **(A-B)** Data (mean ± SEM) are summary from

1512 at least 3 independent experiments. Statistical analysis was performed using ordinary

1513 one-way ANOVA, followed by Tukey's multiple comparison test; ns, $p>0.05$;

1514 ***$p \leq 0.001$; and ****$p \leq 0.0001$. Mouse wounds were infected with 10^2 CFU/wound *E.*

1515 *coli* UTI89 or 10^6 CFU each of WT *E. faecalis* or Ldh mutant in single-species control

1516 for UTI89 or mixed species infections. 24 hpi CFU enumeration was performed for **(B)**

1517 *E. faecalis* and **(C)** *E. coli*. Each symbol represents one mouse with the median

1518 indicated by the horizontal line. Data are from at least 2 independent experiments with

1519 four to five mice per experiment. Statistical analysis was performed using the
1520 nonparametric Mann-Whitney test to compare ranks **(B)** and using Kruskal-Wallis test
1521 with Dunn's posttest **(C)**; ns, $p>0.05$; *$p \leq 0.05$; and **$p \leq 0.01$.

1522
1523
1524
1525
1526
1527
1528
1529
1530
1531
1532
1533
1534
1535
1536
1537
1538
1539
1540
1541
1542
1543
1544

1545 **Supplementary Figures**

1546

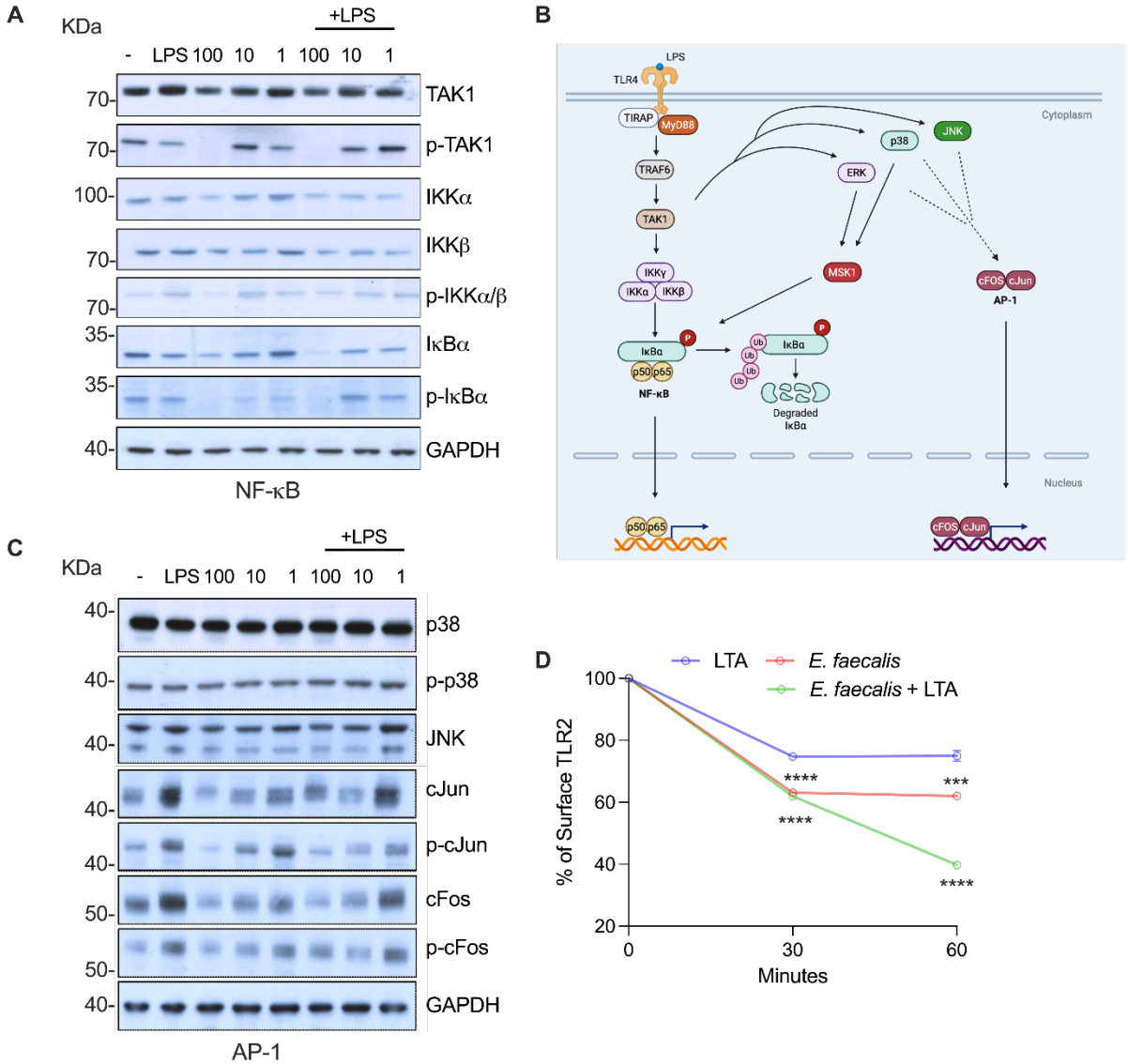

1547

1548 **Figure S1 – *E. faecalis* infection modulates macrophage response to bacteria by**

1549 **affecting the production and phosphorylation status of different proteins of the**

1550 **NF-κB pathway.**

1551 **(A)** Immunoblot performed on protein extracted from RAW 264.7 macrophages

1552 infected with WT *E. faecalis* at the indicated MOI (100, 10, 1) with or without LPS (100

1553 ng/mL) for 6 h and probed with antibodies specific for TAK1, phospho-TAK1, IKKα,

1554 IKKβ, phospho-IKKα/β, IκBα, phospho-IκBα, p65, phospho-p65 and GAPDH. M

1555 represents uninfected macrophages. GAPDH was used as an internal control for

1556 loading control. **(B)** TLR-NF-κB signaling pathway and cross-talk between NF-κB and

1557 AP-1 are shown. **(C)** Immunoblot performed on protein extracted from RAW 264.7
1558 macrophages infected with WT *E. faecalis* at the indicated MOIs (100, 10, 1) with or
1559 without LPS for 6 h and probed with antibodies specific for p38, phospho-p38, JNK,
1560 ERK, c-Jun, phospho c-Jun, c-Fos, phospho c-Fos and GAPDH. **(D)** RAW 264.7 cells
1561 were either infected or treated with LTA (10 μg/mL) for the times indicated before TLR2
1562 endocytosis was examined by flow cytometry. Data (mean ± SEM) are a summary of
1563 three independent experiments and calculated relative to uninfected untreated cells
1564 which were set as 100% levels for the examined receptor. Statistical analysis was
1565 performed using ordinary one-way ANOVA followed by Dunnett's multiple comparison
1566 test ***$p<0.001$ and ****$p<0.0001$.
1567
1568
1569
1570
1571

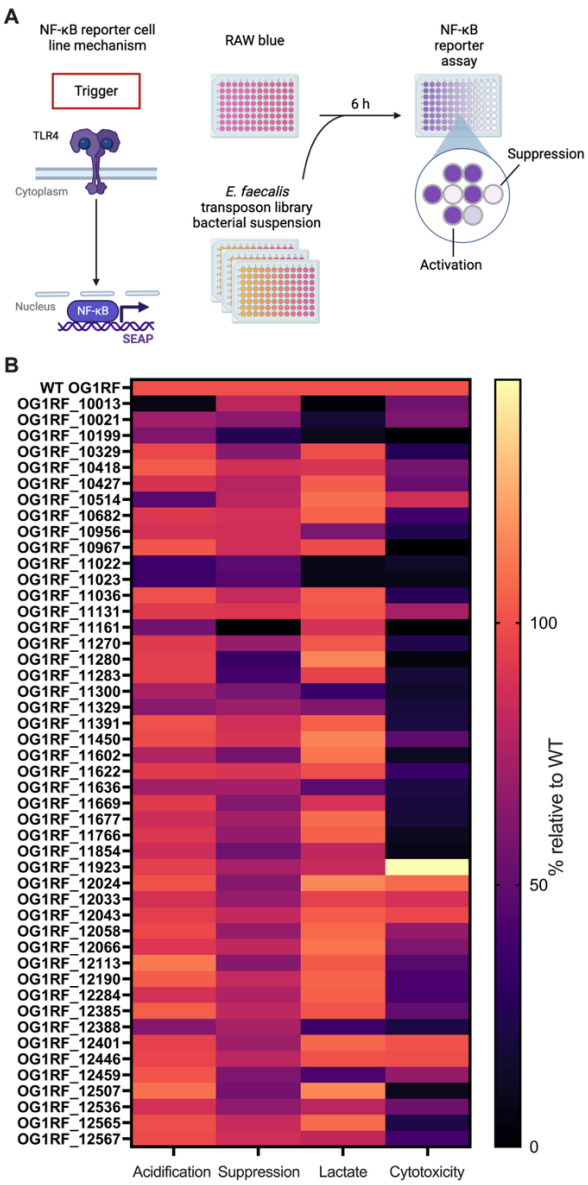

Figure S2 – Methodology for transposon library screen to identify bacterial factor(s) important in macrophage suppression.

(A) Screening workflow: all mutants were inoculated in DMEM + 10% FBS for 24 h before 20 μL of the bacteria suspension was transferred to RAW 264.7 cell culture. The macrophages were stimulated in the presence of LPS for 6 h and supernatant was collected for SEAP assay. Mutants showed significant higher NF-κB activity were identified as weak-suppressing mutants. **(B)** Bacterial genes identified in a transposon library screen for genes important in macrophage suppression at MOI 100. The heat map shows the degree of NF-κB suppression, medium acidification, lactate production,

1582 and cytotoxicity in RAW 264.7 macrophages infected at MOI 100 at 6 hpi relative to

1583 WT levels set to 100%.

1584

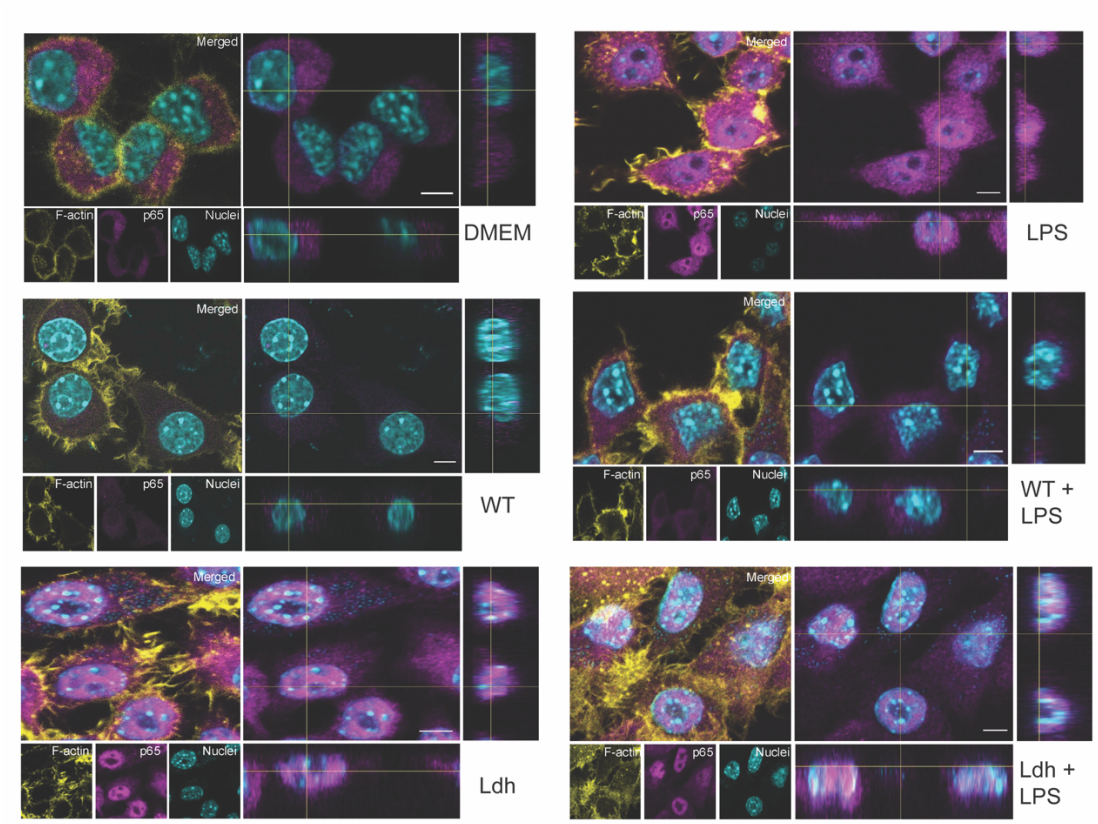

1585

1586 **Figure S3 – *E. faecalis* infection prevents p65 nuclear translocation.** CLSM

1587 orthogonal view of RAW 264.7 macrophages at 6 hpi with WT or Ldh strains in

1588 presence or absence of LPS. Magenta, p65; cyan, dsDNA stained with Hoechst 33342;

1589 yellow, F-actin stained with phalloidin. Images are representative of 2 independent

1590 experiments. Scale bar: 5 µm.

1591

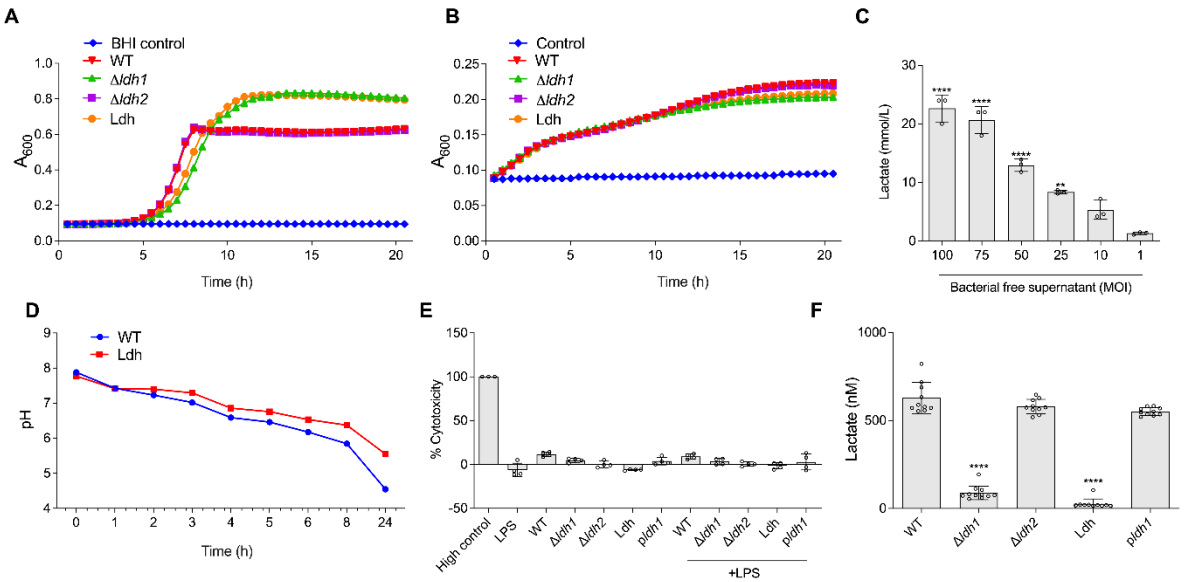

Figure S4 – LDH mutant does not have growth defects and acidifies the environment weakly.

Growth curve for *E. faecalis* strains grown overnight in either **(A)** BHI or **(B)** cell culture media supplemented with 10% FBS. **(C)** Lactate present in bacterial-free supernatant was quantified via blood gas analysis. **(D)** pH for *E. faecalis* strains grown in cell culture media measured over a time course. **(E)** RAW 264.7 macrophages infected with WT OG1RF or Ldh mutant supplemented with lactic acid at various concentration for 6 h prior to measurement of cytotoxicity. **(F)** Lactate concentration was measured using 6 hpi bacterial free supernatant. Statistical analysis was performed using one-way ANOVA with Tukey's multiple comparison test where $p<0.0001$ among all the different *E. faecalis* strains as compared to WT.

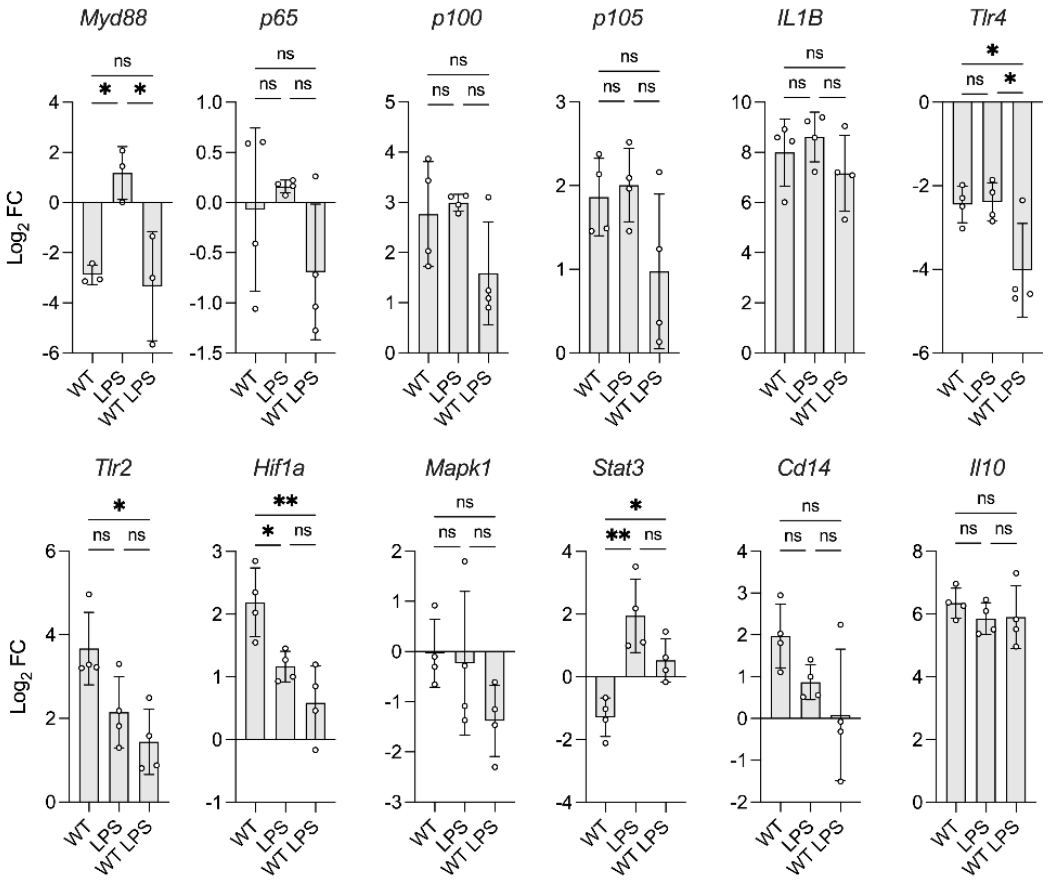

1604

1605 **Figure S5 – *E. faecalis* infection affect transcription of immune response genes**

1606 **in BMDM.** qRT-PCR analysis of NF-κB-related genes transcript level in RAW 264.7

1607 cells that were infected with WT *E. faecalis* for 6 h in the presence or the absence of

1608 LPS. Each dot represents one biological replicate. Statistical analysis was performed

1609 using ordinary one-way ANOVA, followed by Tukey's multiple comparison test, NS p

1610 > 0.05; *p≤0.05; and **p<0.01.

1611

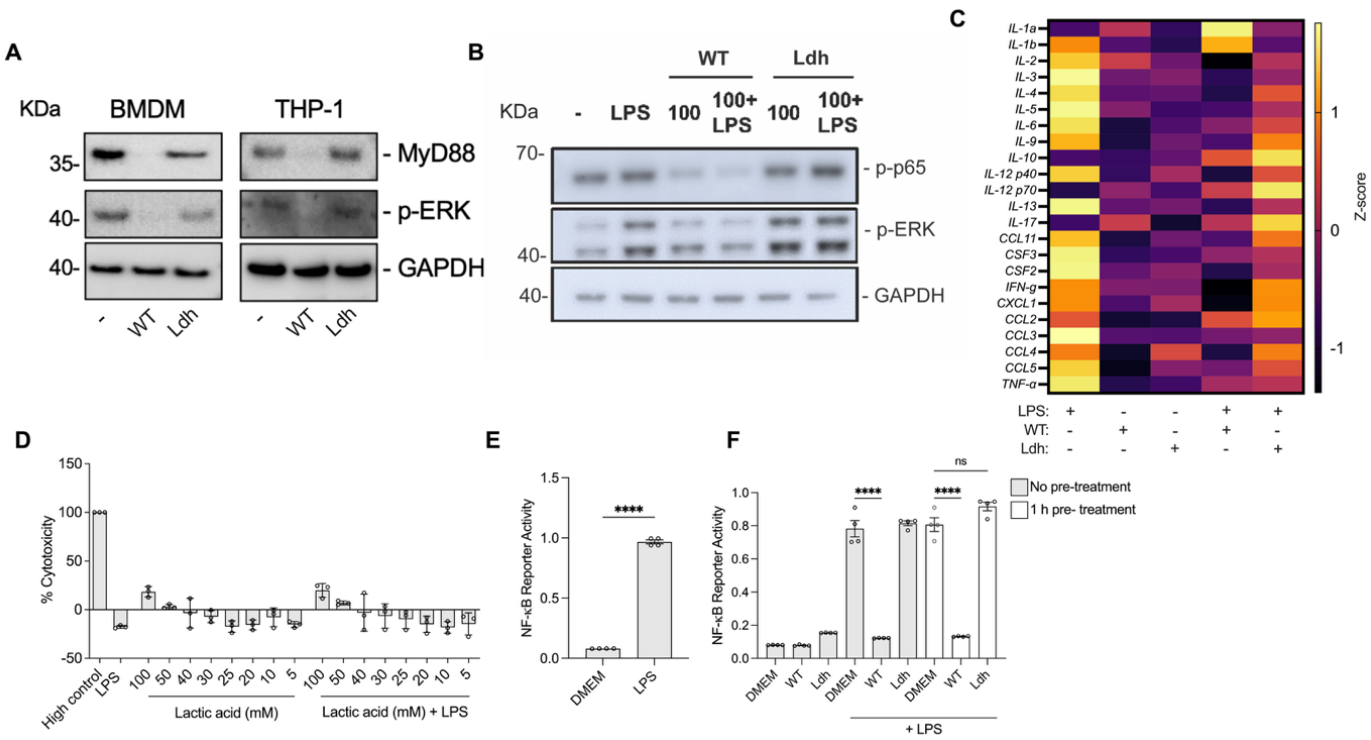

Figure S6 – *E. faecalis*-derived lactic acid suppresses NF-κB activation in LPS pre-treated cells.

Immunoblot performed on proteins extracted from BMDMs, THP-1s and RAW 264.7 macrophages infected with *E. faecalis* MOI 100 for 6 h and probed with antibodies specific for **(A)** MyD88, p-ERK and GAPDH, and **(B)** p-p65, p-ERK and GAPDH. Samples in **(B)** are with or without LPS. Data (mean ± SEM) are a summary of at least two independent experiments. **(C)** Heatmap showing $\log_2$-transformed, row-scaled fold changes in cytokine, chemokine, and growth factor expression relative to uninfected controls, detected in filtered supernatants at 6 hpi from WT *E. faecalis* and the Ldh mutant. The scale bar represents z-scores (mean = 0, SD = 1). **(D)** RAW 264.7 macrophages were incubated with cell culture media supplemented with lactate at various concentrations for 6 h prior to measurement of cytotoxicity. **(E)** RAW 264.7 cells were pre-treated for 1 h with LPS prior to measurement of NF-κB-driven SEAP reporter activity. **(F)** RAW 264.7 cells infected with WT *E. faecalis* or Ldh mutant for 6

h prior to measurement of NF-κB-driven SEAP reporter activity were either pre-treated or not with LPS for 1 h prior to infection. Data (mean ± SEM) are a summary of at least three independent experiments. Statistical analysis was performed using one-way ANOVA with Tukey's multiple comparison test where NS, p>0.05 and ****p<0.0001.

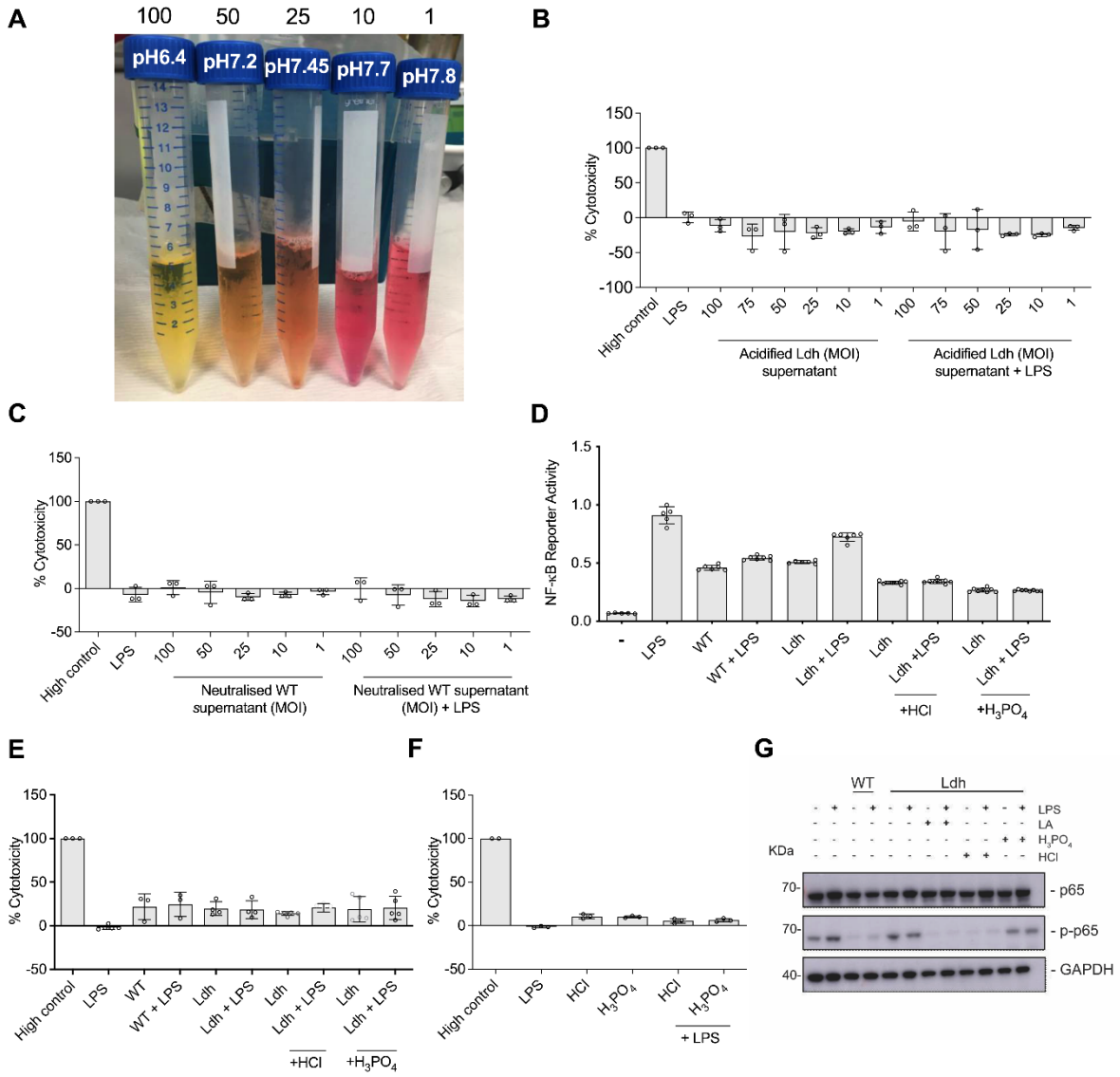

Figure S7 – pH adjusted medium does not affect macrophage viability.

(A) Picture of bacterial-free supernatant at indicated MOI. The color indicator in the cell culture medium turns yellow upon acidification. RAW 264.7 macrophages were incubated with **(B)** acidified bacterial-free Ldh supernatant, **(C)** neutralized bacterial-

1638 free WT supernatant, **(D-E)** WT *E. faecalis* or Ldh deletion mutant treated concurrently
1639 with LPS at specific MOI for 6 h, and **(F)** acidified cell media in the absence of bacteria,
1640 prior to measurement of NF-κB activity or cytotoxicity. **(B-C, E-F)** Triton-X treatment
1641 served as a positive control (high control) for cell death. **(D-E)** RAW 264.7
1642 macrophages incubated with WT or Ldh mutant were also supplemented with different
1643 acids to acidify the pH for the duration of the experiment prior to measurement of NF-
1644 κB-driven SEAP reporter activity and LDH activity. **(B-F)** Data (mean ± SEM) are a
1645 summary of at least three independent experiments. **(G)** Immunoblots were performed
1646 on protein extracted from RAW 264.7 macrophages infected with WT or Ldh that were
1647 incubated in acidified cell culture media in the presence or absence of LPS for 6 h and
1648 probed with antibodies specific for p65, p-p65, and GAPDH. Cell culture media was
1649 acidified to pH 6.4 with lactic acid and with the inorganic acids H_3PO_4 and HCl. Data
1650 shown are representative of at least 3 independent experiments.

1651
1652
1653
1654
1655
1656
1657
1658
1659
1660
1661
1662
1663

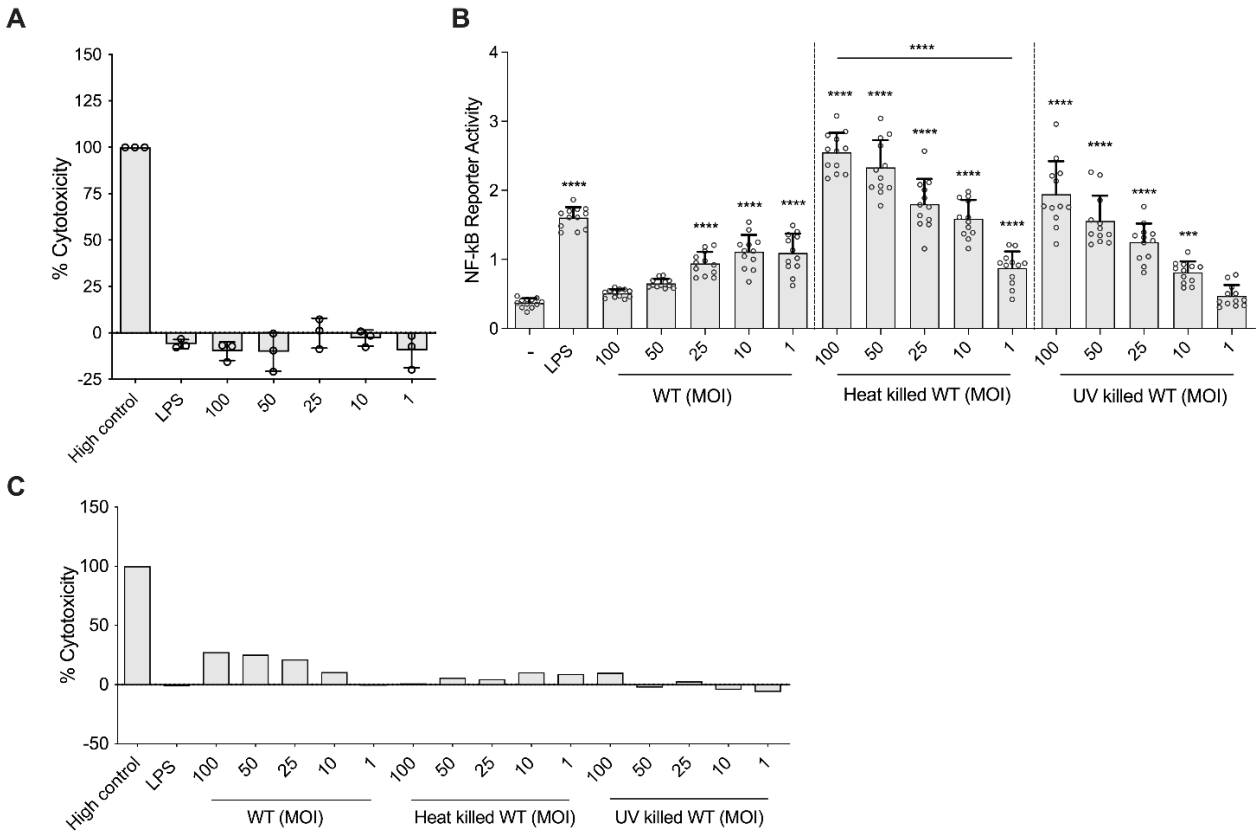

Figure S8 – Intracellular, heat or UV killed *E. faecalis* do not contribute to NF-κB suppression in macrophages.

RAW 264.7 macrophages were incubated with *E. faecalis* WT (MOI 100, 50, 25, 10, 1) for 3 h and treated with 500 µg/mL of gentamicin with penicillin G overnight at 37˚C **(A)** and were incubated with live, heat killed or UV killed WT (MOI 100, 50, 25, 10, 1) for 6 h **(B)** prior to measurement of NF-κB-driven SEAP reporter activity and **(A and C)** measurement of cytotoxicity. **(A-C)** Data (mean ± SEM) are a summary of at least three independent experiments. Statistical analysis was performed using one-way ANOVA with Tukey's multiple with comparison where ***p<0.001 and ****p<0.0001 as compared to media control.

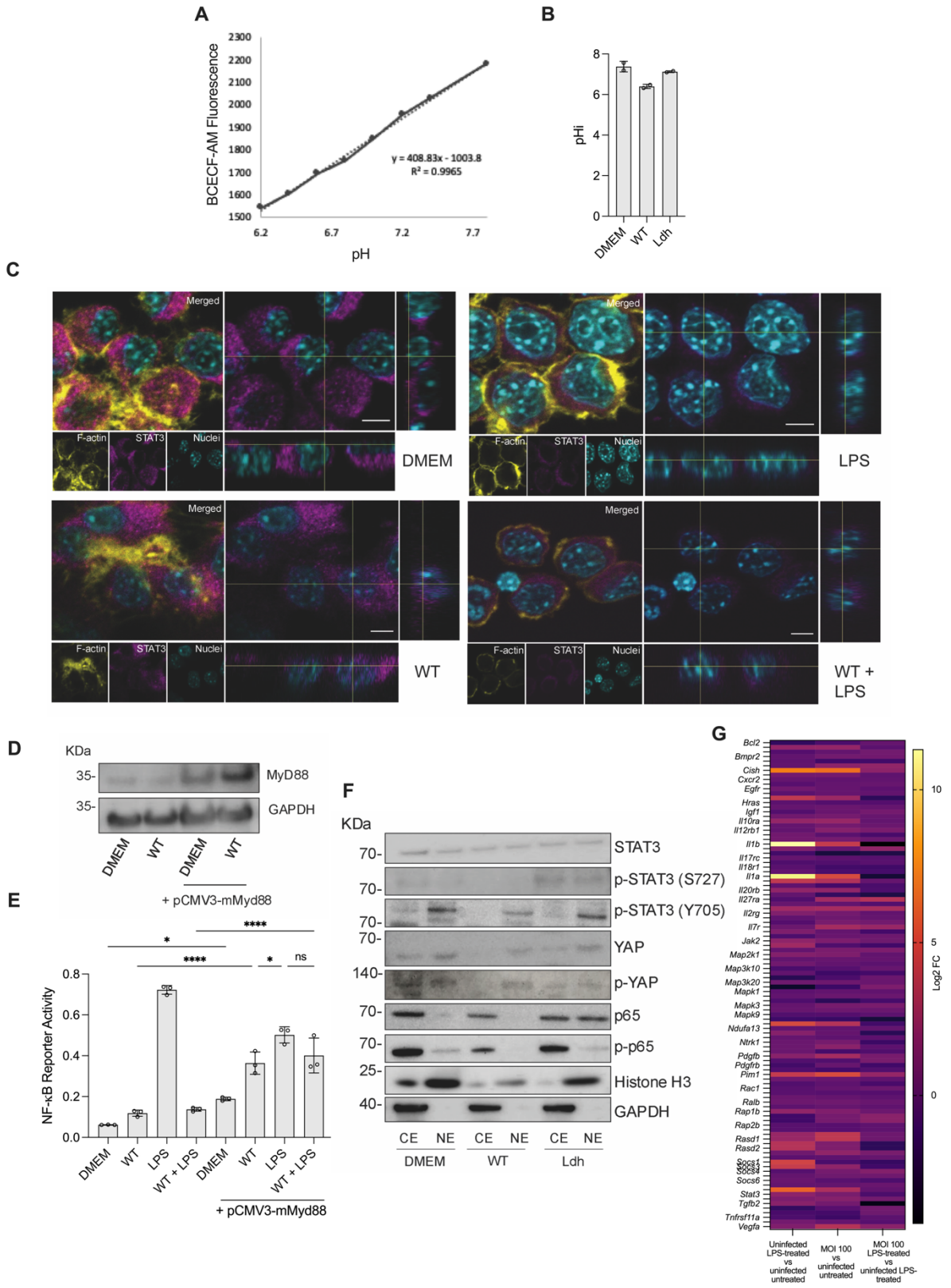

Figure S9 - Low pH during *E. faecalis* infection prevents ERK phosphorylation. **(A)** BCECF-AM calibration curve used in the BCECF-AM experiments. **(B)** pHi in non-infected, WT or Ldh infected RAW264.7 6 hpi using BCECF-AM. **(C)** CLSM orthogonal

1685 view of RAW264.7 macrophages at 6 hpi with WT in the presence or absence of LPS.
1686 Magenta, STAT3; cyan, dsDNA stained with Hoechst 33342; yellow, F-actin stained
1687 with phalloidin. Images are representative of 2 independent experiments. Scale bar: 5
1688 μm. **(D-E)** MyD88 rescue experiment using the mammalian expression vector pCMV3-
1689 mMyd88. A representative MyD88 immunoblot of successfully transduced RAW264.7
1690 cells that were uninfected or infected with *E. faecalis* is shown **(D)**. **(E)** Cells were
1691 transduced 24 h prior to performing NF-κB reporter assay. Data (mean ± SEM)
1692 represent three independent experiments. Statistical analysis was performed using
1693 ordinary one-way ANOVA followed by Tukey's multiple comparison test**,** ns, $p>0.05$;
1694 *$p\leq0.05$; and ****$p<0.0001$. **(F)** Immunoblot was performed on proteins from RAW
1695 264.7 macrophages subcellular fractions after WT or Ldh mutant infection for 6 h and
1696 probed with antibodies raised against STAT3, p-STAT3 (S727), p-STAT3 (Y705), YAP,
1697 p-YAP, p65, p-p65, histone H3 and GAPDH. CE and NE stand for cellular and nuclear
1698 extract, respectively. Immunoblot images represent two independent experiments **(D**
1699 **and F)**. **(G)** Heatmap of differentially expressed STAT3-related genes.

1700
1701
1702

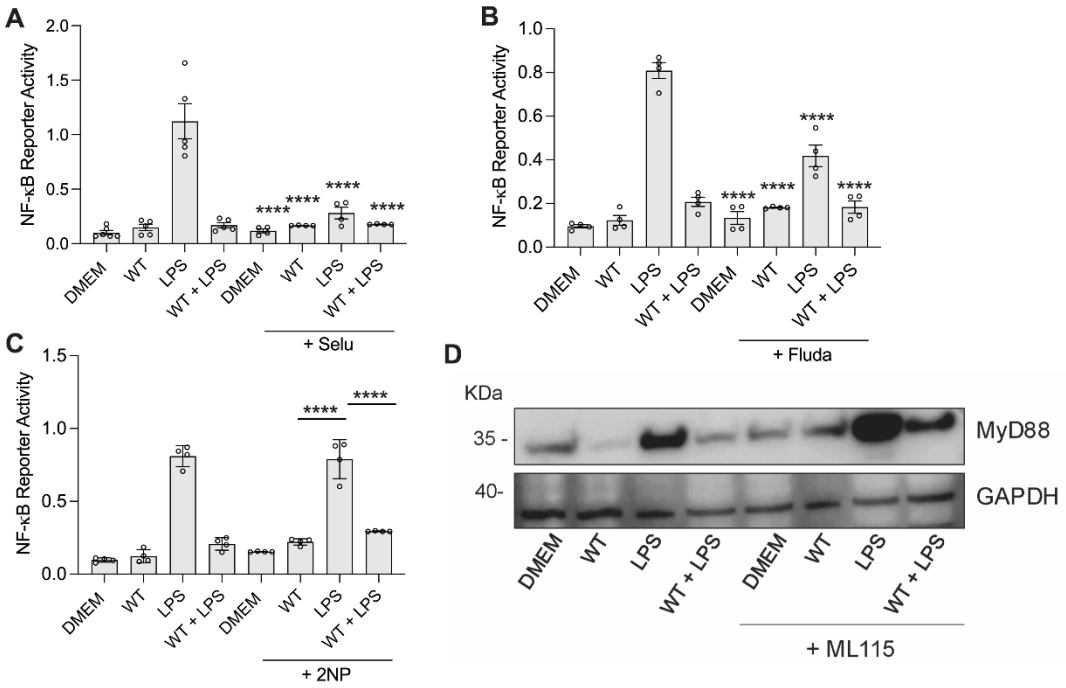

Figure S10 – STAT1 does not play a role in suppressing NF-κB in *E. faecalis*-infected macrophages.

RAW 264.7 macrophages were infected with the WT *E. faecalis* and incubated with cell culture media in presence or absence of LPS and **(A)** Selu (1 μM) and **(B)** Fluda (10 μM) and **(C)** 2NP (45 μM) for 6 h prior to measurement of NF-κB-driven SEAP reporter activity. The compounds were added 30 min before the beginning of the experiment. Data (mean ± SEM) are a summary of at least three independent experiments. Statistical analysis was performed using one-way ANOVA with Tukey's multiple comparison tests where ****$p<0.0001$ as compared to LPS unless otherwise indicated. (D) Immunoblot was performed on proteins from RAW 264.7 macrophages uninfected or infected with WT in presence or absence of ML115 (± LPS) for 6 h and probed with antibodies raised against MyD88 and GAPDH.

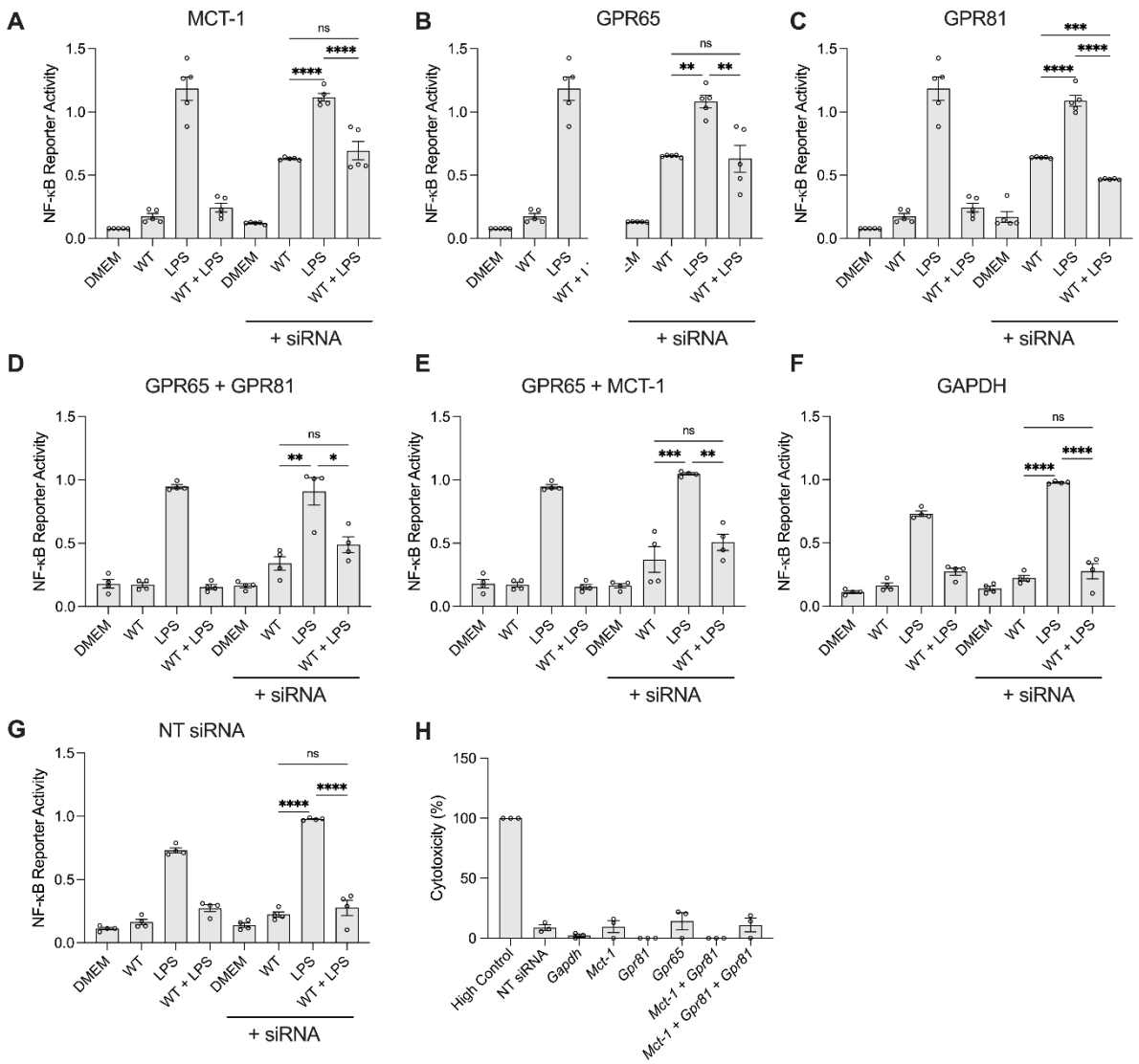

Figure S11 – The lactate transporters MCT-1 and GPR81 are redundant in their role in the suppression of NF-κB activation of *E. faecalis* infection. (A-G) RAW 264.7 macrophages, with successfully silenced lactate transporters as indicated, were infected with the WT *E. faecalis* and incubated with cell culture media in the presence or absence of LPS for 6 h prior to measurement of NF-κB-driven SEAP reporter activity. Silencing the expression of *Mct-1*, *Gpr81* and *Gpr65* alone or in combination was achieved by siRNA. Data (mean ± SEM) are a summary of at least two independent experiments. NT siRNA was used so was *Gapdh* siRNAs controls for adverse effects of the technique. Statistical analysis was performed using ordinary one-way ANOVA followed by Tukey's multiple comparison test ns, $p>0.05$; *$p\leq0.05$; and **$p<0.01$;

***p<0.001 and ****p<0.0001. (H) Ldh assay was performed to evaluate potential cytotoxicity of the technique under the different siRNAs used.

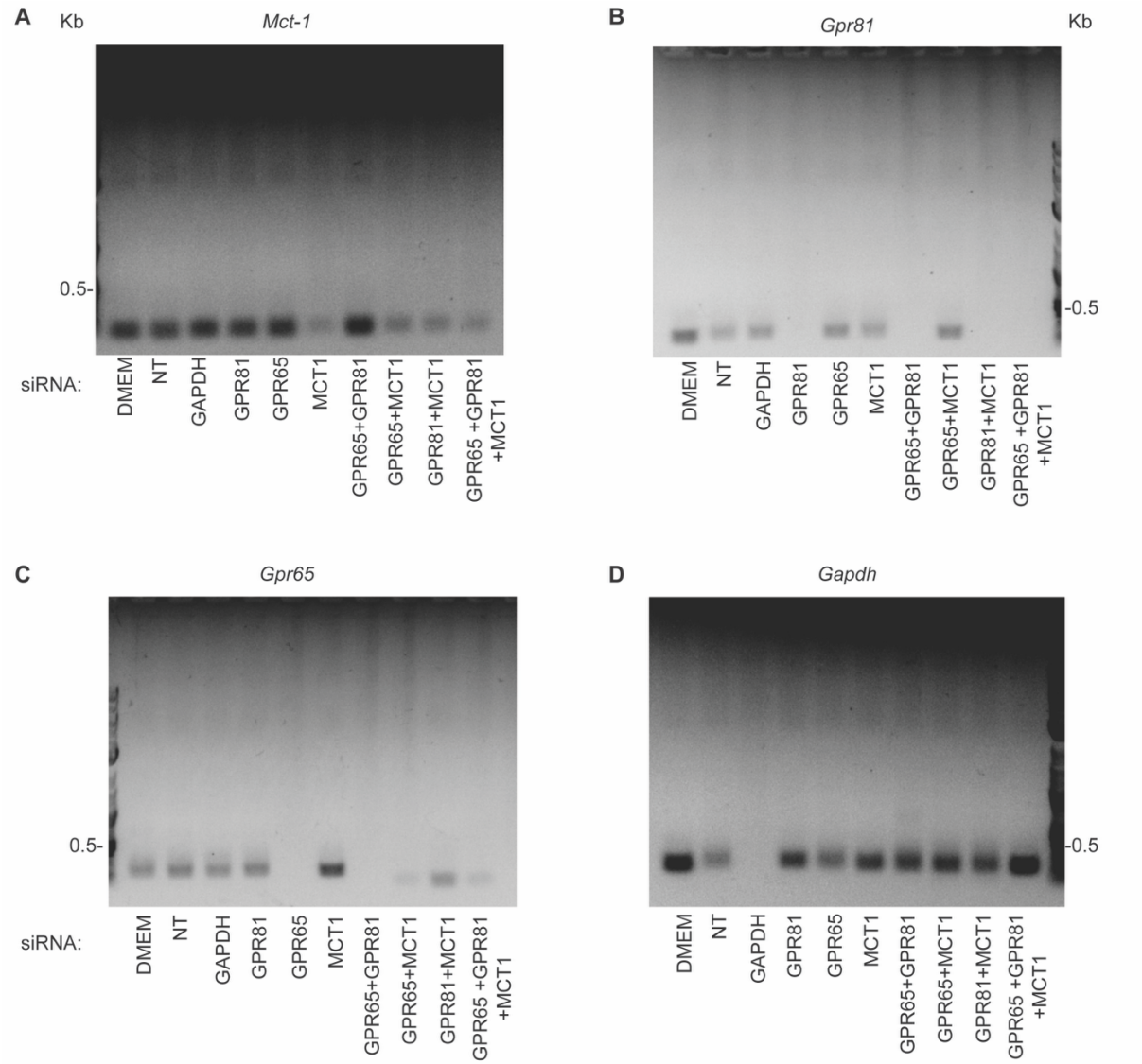

Figure S12 – Successful knockdown of lactate transporters of interest was verified with RT-PCR. (A-D) Transcript levels of the silenced genes of interest were assessed with specific primers for each target. Negative control (NT) used was the Silencer Select Negative Control siRNAs that contain siRNAs with sequences that do not target any gene product.

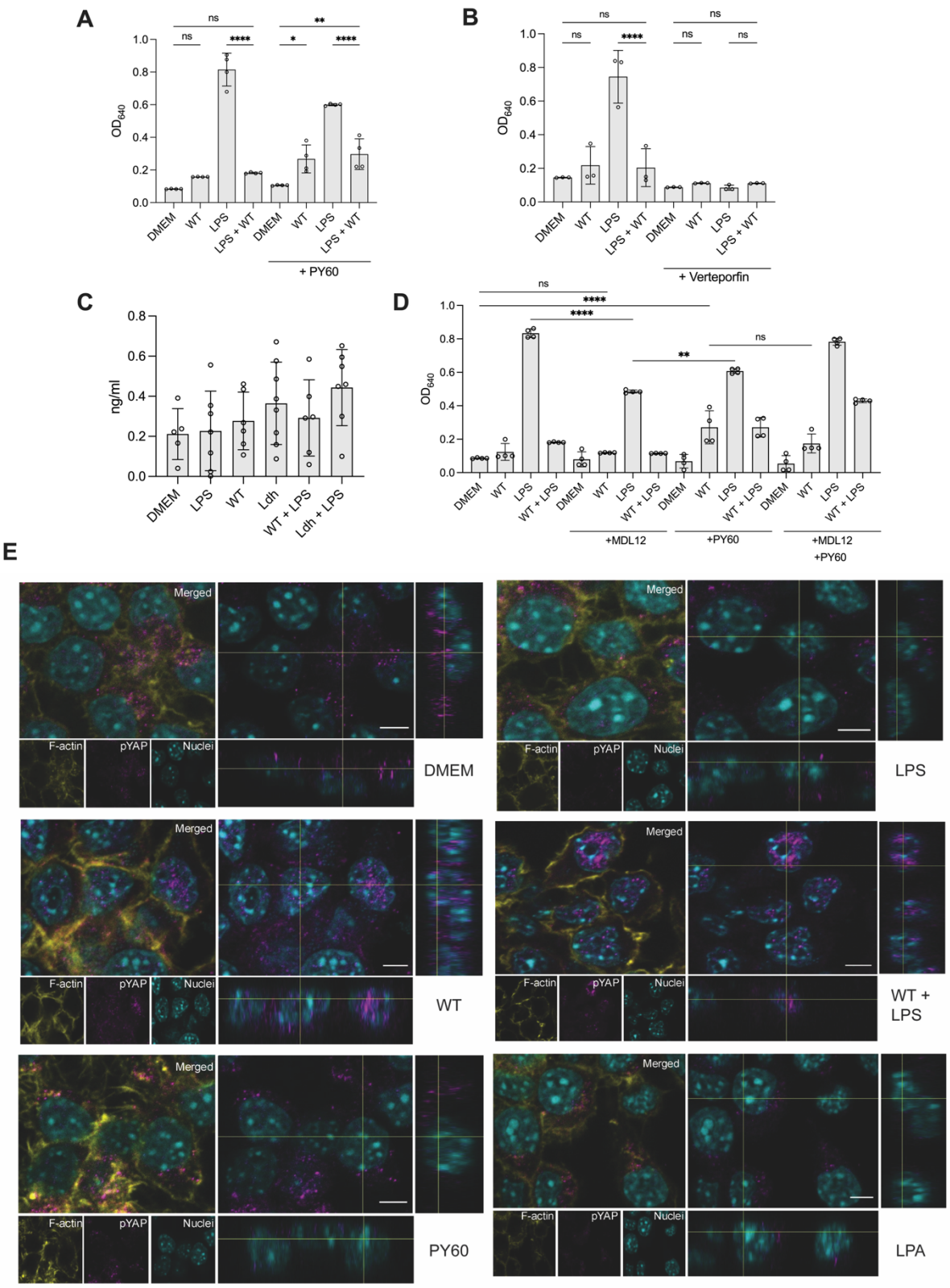

Figure S13 - *E. faecalis* infection disturbs pYAP function and localization.

RAW 264.7 macrophages were infected with the WT *E. faecalis* and incubated in cell culture media in the presence or absence of LPS and **(A)** PY-60 (10 μM), **(B)**

verteporfin (10 μM), **(D)** MDL-12 alone or in combination with either PY-60 or verteporfin for 6 h prior to measurement of NF-κB-driven SEAP reporter activity. The compounds were added 30 min before the beginning of the experiment. Data (mean ± SEM) are a summary of at least three independent experiments. Statistical analysis was performed using one-way ANOVA with Tukey's multiple comparison tests where NS, p>0.05, *p<0.05, **p<0.01, and ****p<0.0001. **(C)** Intracellular cAMP quantification of RAW264.7 cells uninfected or infected with WT or Ldh in presence or LPS. **(E)** CLSM orthogonal view of RAW264.7 macrophages at 6 hpi with WT in the presence or absence of LPS. Magenta, p-YAP; cyan, dsDNA stained with Hoechst 33342; yellow, F-actin stained with phalloidin. Images are representative of 2 independent experiments. Scale bar: 5 μm.

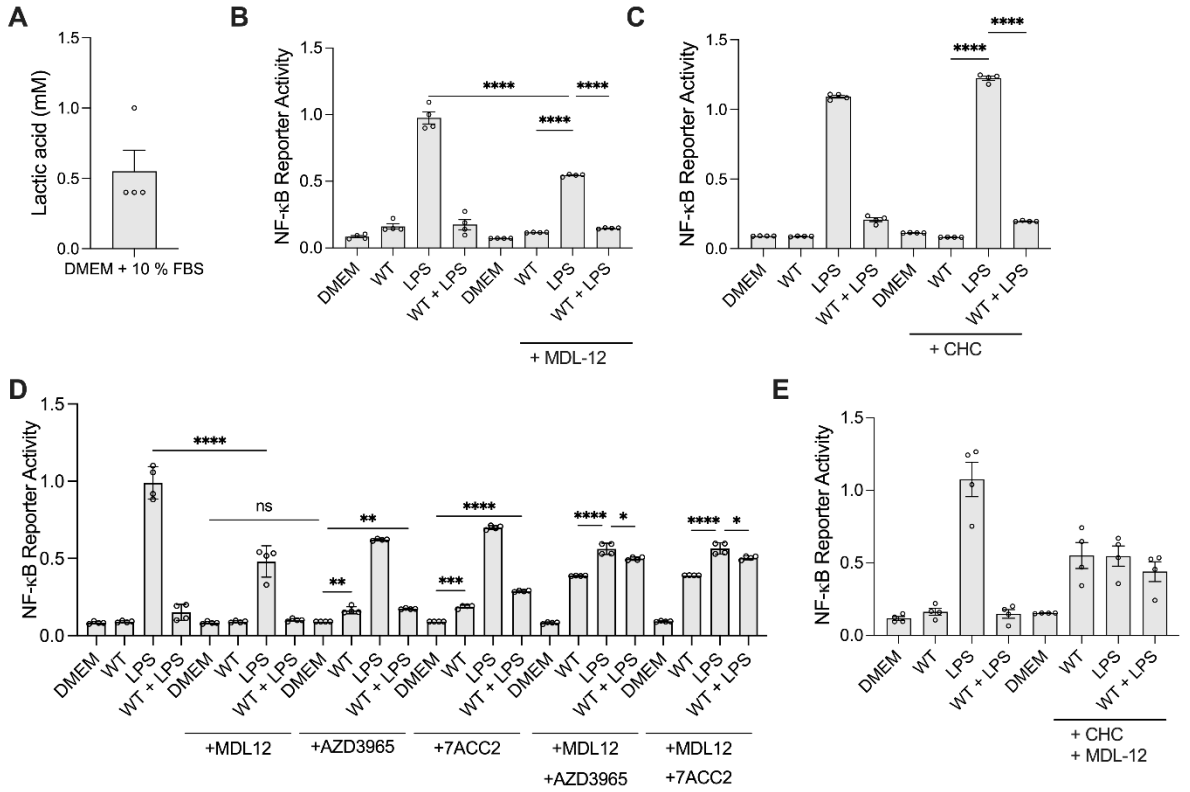

1762 **Figure S14 – MCT1 mediate *E. faecalis* suppression of NF-κB activation in**
1763 **macrophages. (A)** Lactic acid concentration of DMEM + 10 % FBS media. RAW 264.7
1764 macrophages were infected with the WT *E. faecalis* and incubated in cell culture media
1765 in presence or absence of LPS and **(B)** CHC (5 mM) and **(C)** MDL-12 (20 μM),**(D-E)**
1766 AZD3965 (1μM), 7ACC2 (1μM) and CHC alone or in combination with MDL-12 for 6 h
1767 prior to measurement of NF-κB-driven SEAP reporter activity. The cell cultures were
1768 treated with compounds for 30 min before the beginning of the experiment. Data
1769 (mean ± SEM) are a summary of at least three independent experiments. Statistical
1770 analysis was performed using one-way ANOVA with Tukey's multiple comparison
1771 tests where NS, $p>0.05$ and ****$p<0.0001$.
1772
1773

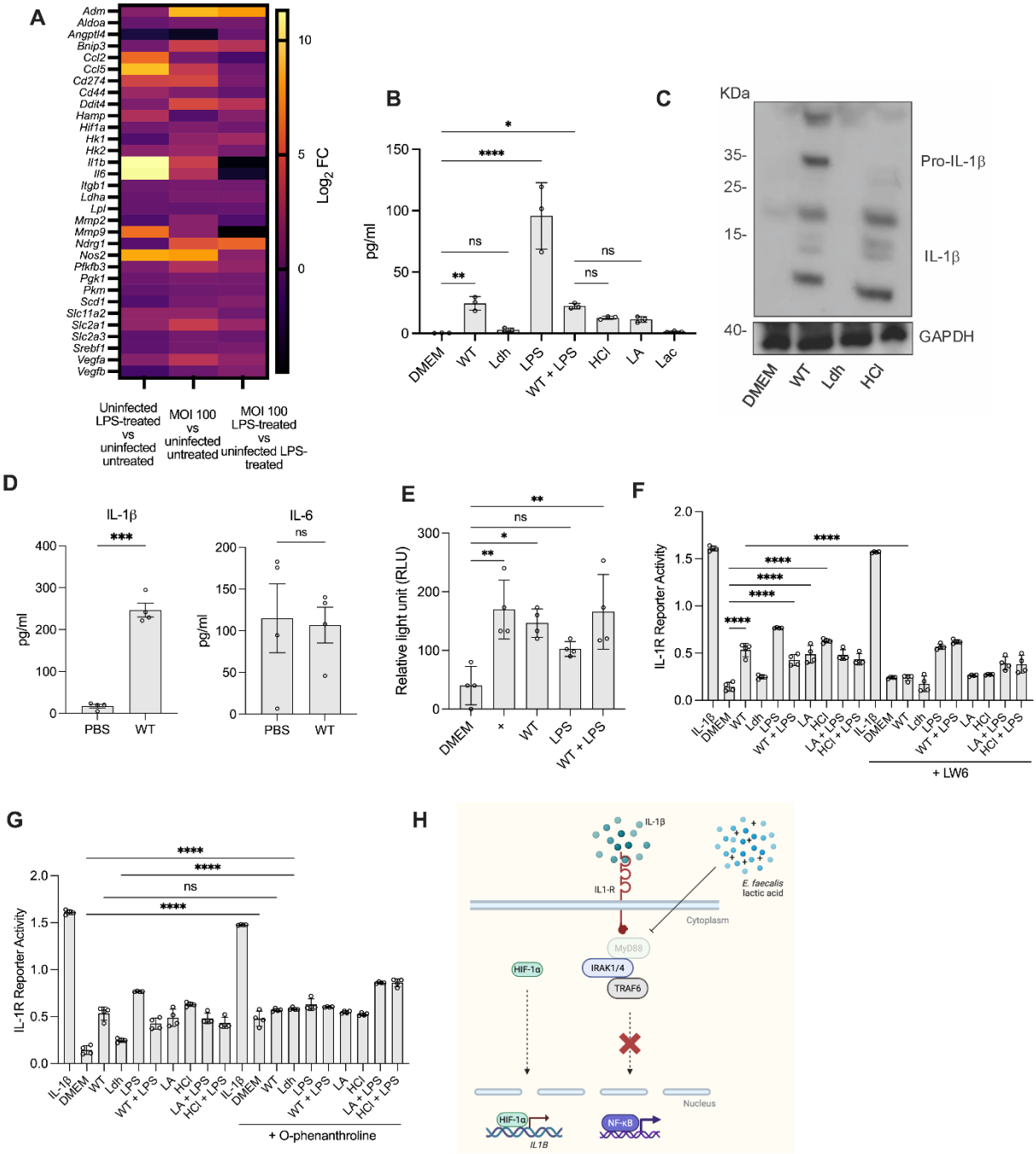

Figure S15 – *E. faecalis* prevents IL-1β activation of NF-κB in RAW264.7 macrophages

(A) Heatmap of differentially expressed HIF-1α-related genes. **(B)** Levels of IL-1β from the supernatants of uninfected or infected with WT or Ldh RAW264.7 macrophages treated with LPS, HCl, LA or sodium lactate (Lac). **(C)** Immunoblot performed on protein extracted from RAW 264.7 macrophages infected with WT or Ldh for 6 h and

1781 probed with antibodies specific for IL-1β and GAPDH. **(D)** Levels of IL-1β and IL-6
1782 from uninfected or WT-infected wound lysates at 24 hpi. Each dot represents one
1783 mouse. **(E)** HIF-1α reporter activity assay in RAW264.7 macrophages that were
1784 uninfected or infected with WT treated with O-phenanthroline (+) or LPS. **(F-G)** IL-1R
1785 reporter activity assay with HEK-Blue IL-1R cells treated with 20 μl bacteria-free
1786 supernatants from uninfected or infected with WT or Ldh RAW264.7 macrophages that
1787 were left untreated or treated with LPS, HCl, or LA for 6 h. Some RAW264.7 cells pre-
1788 treated with LW6 or O-phenanthroline for 30 min prior to the beginning of the assay.
1789 **(H)** IL-1β activation of NF-kB signaling pathway. Data (mean ± SEM) are summary of
1790 at least 2 independent experiments **(B-G)**. Statistical analysis was performed using
1791 unpaired t test with Welch's correction **(D)**, ordinary one-way ANOVA followed by
1792 Tukey's multiple comparison test **(B, E)** or Fisher's LSD **(F-G),** ns, $p>0.05$; *$p\leq0.05$;
1793 **$p<0.01$, ***$p<0.001$, and ****$p<0.0001$.
1794

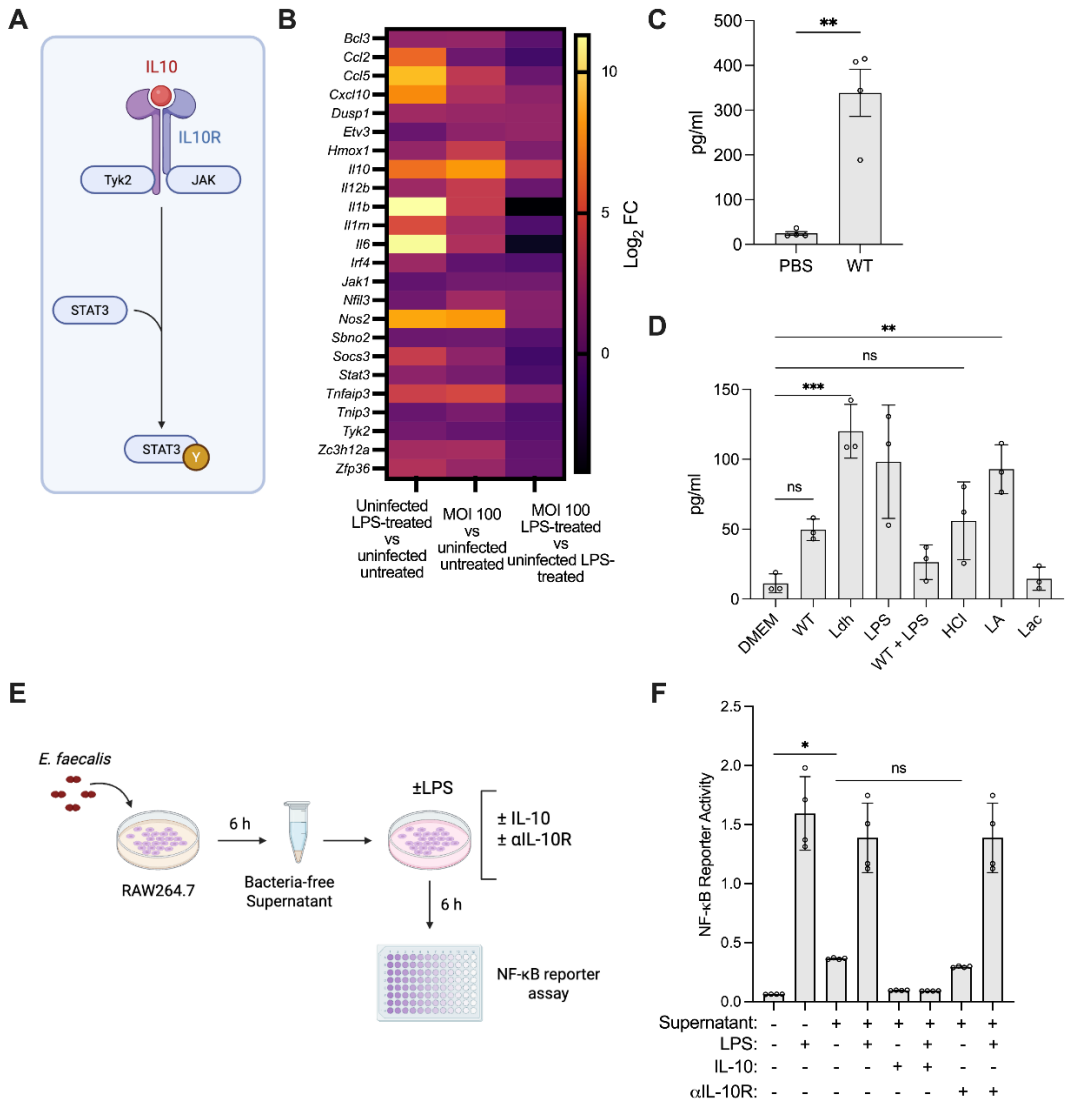

Figure S16 – IL-10 from *E. faecalis* infected macrophages does not suppress NF-κB during enterococcal infection.

(A) IL-10 signaling pathway. **(B)** Heatmap of differentially expressed IL-10-related genes. **(C)** IL-10 levels from uninfected or WT-infected wound lysates at 24 hpi. Each dot represents one mouse. **(D)** Levels of IL-10 from the supernatants of uninfected or infected with WT or Ldh RAW264.7 macrophages treated with LPS, HCl, lactic acid (LA) or sodium lactate (Lac). **(E-F)** NF-κB reporter activity assay with RAW264.7 cells treated with 20 μl bacteria-free supernatants from uninfected or 6 h WT infected RAW264.7 macrophages that were left untreated or treated with LPS. RAW264.7 cells

1805 were pre-treated with IL-10 or antibody αIL-10R for 30 min prior to the beginning of
1806 the assay. Data (mean ± SEM) are summary of at least 3 independent experiments
1807 **(C-D and F)**. Statistical analysis was performed using unpaired t test with Welch's
1808 correction **(C)**, ordinary one-way ANOVA followed by Tukey's multiple comparison test
1809 **(D)** or Fisher's LSD **(F),** ns, p>0.05; *p≤0.05; **p<0.01, ***p<0.001, and ****p<0.0001.

1810
1811
1812

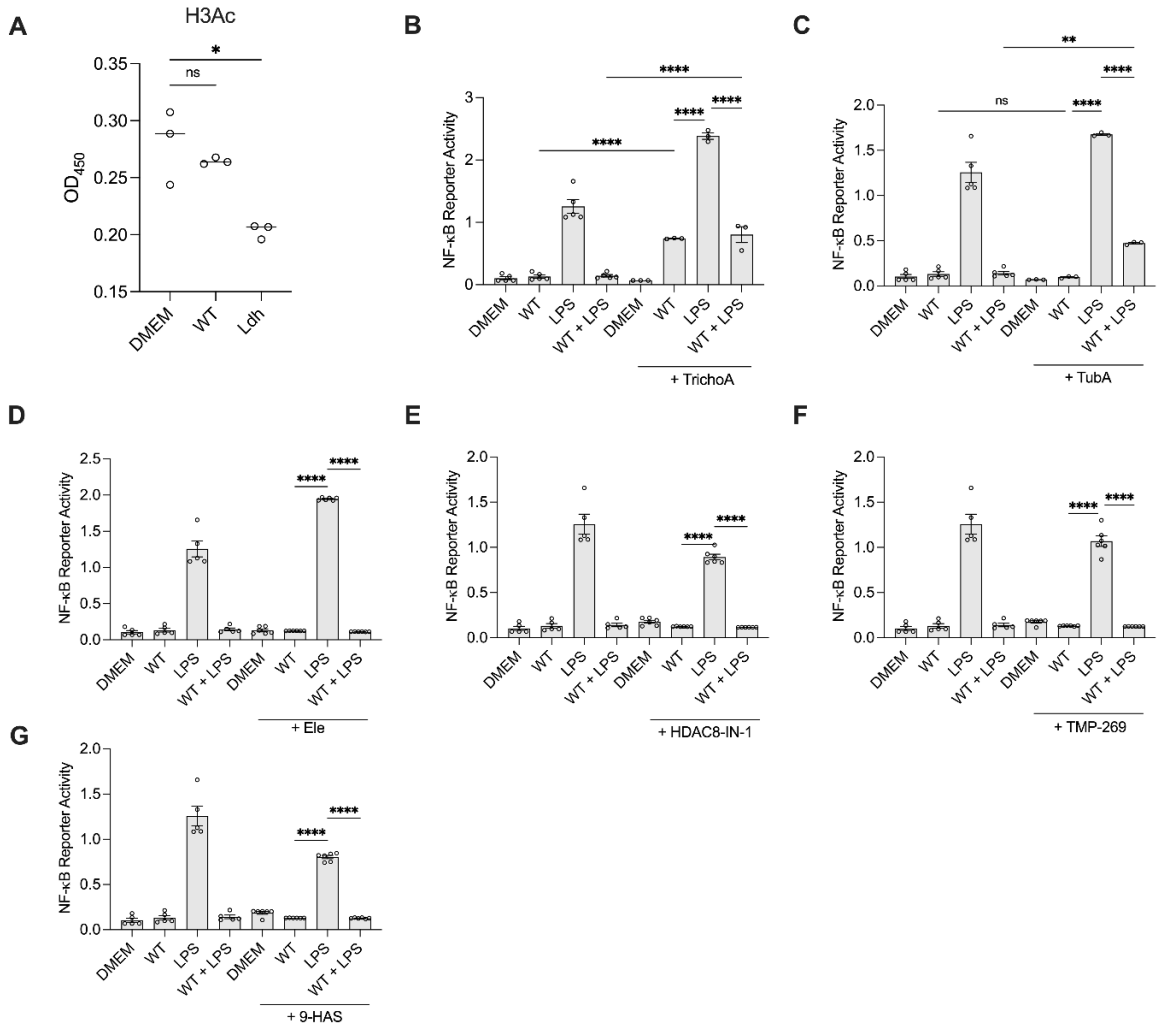

1813
1814 **Figure S17 – HDACs likely play a partial role in mediating *E. faecalis* suppression**
1815 **of NF-kB activation in macrophages. (A)** Relative abundance of H3Ac by ELISA of
1816 uninfected or WT and Ldh infected macrophages. RAW 264.7 macrophages were
1817 infected with the WT strain and incubated with cell culture media in the presence or

1818 absence of LPS and **(B)** TrichoA (10 nM) and **(C)** TubA (15 nM), **(D)** Ele (1 μM), **(E)**
1819 HDAC8-IN-1 (100 nM), **(F)** TMP-269 (10 μM) and **(G)** 9-HAS (100 μM) for 6 h prior to
1820 measurement of NF-κB-driven SEAP reporter activity. The compounds were added
1821 30 min before the beginning of the experiment. Data (mean ± SEM) are a summary of
1822 at least three independent experiments. Statistical analysis was performed using one-
1823 way ANOVA with Tukey's multiple comparison tests where ns, $p>0.05$; *$p\leq0.05$; and
1824 ****$p<0.0001$.

1825
1826
1827

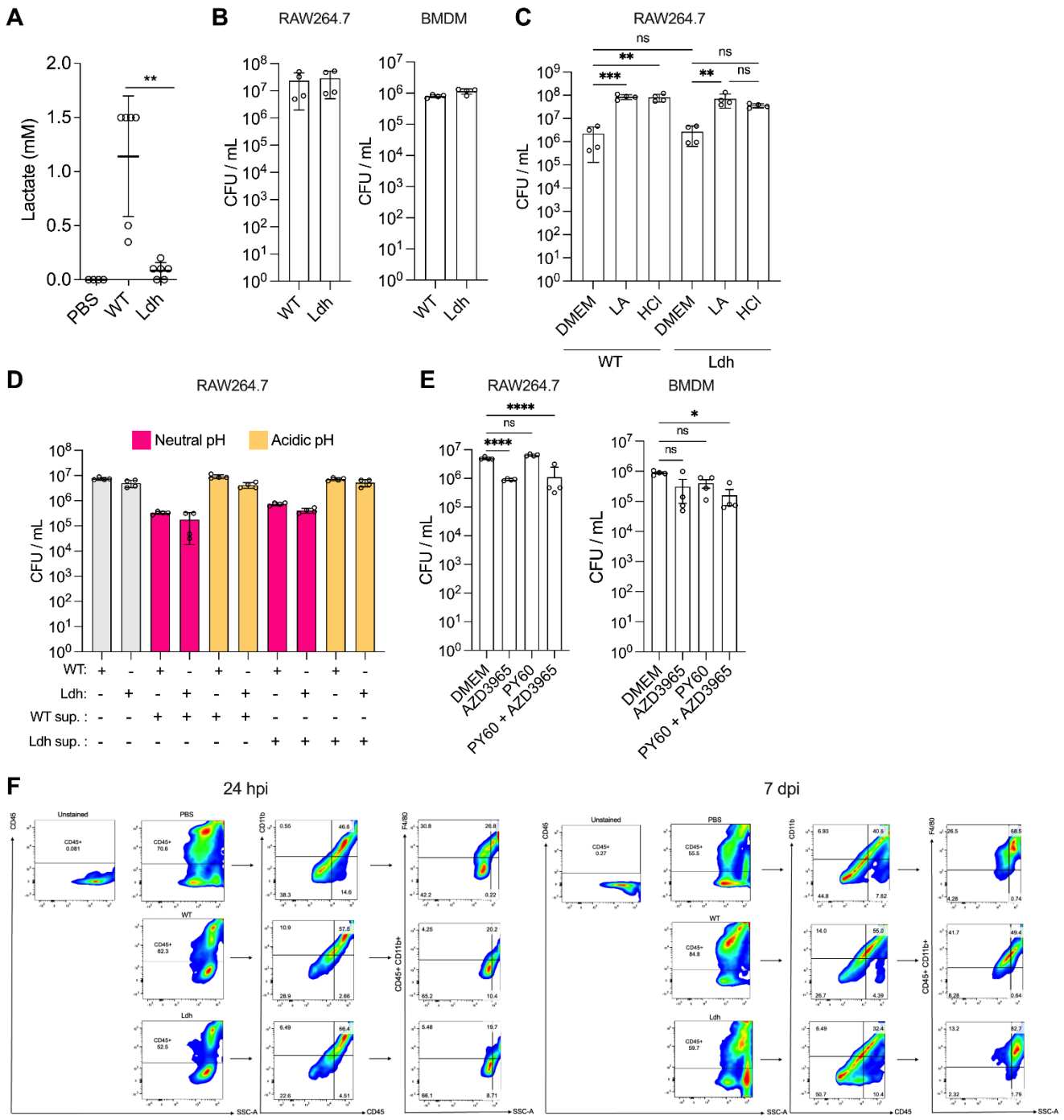

Figure S18 – Lactic acid reduces macrophage killing of bacteria.

(A) Lactate concentration of wound measured at 24 hpi for the indicated condition. **(B-E)** RAW264.7 cells or BMDMs were infected with either WT or Ldh without any other treatment **(B)**, in the presence of LA (40 mM) or HCl to lower the extracellular pH **(C)**, bacterial free supernatant from WT or Ldh cultures that were neutralized with NaOH or acidified with HCl **(D)**, or in the presence of AZD3965 (10 μM), PY60 (10 μM), or

both **(E).** Intracellular bacterial CFU was quantified. Statistical analysis was performed using one-way ANOVA with Tukey's multiple comparison tests where p>0.05; *p≤0.05; **p<0.01, ***p<0.001, and ****p<0.0001**. (F)** Representative gating strategy for macrophages (CD45$^+$ CD11b$^+$ F4/80$^+$) from wounds that were treated with PBS or infected with WT or Ldh strains at 24 hpi or 7 dpi. The number indicate percentages of cells within the gated areas. Recorded MFI levels of MyD88 and p-ERK derived from this group.

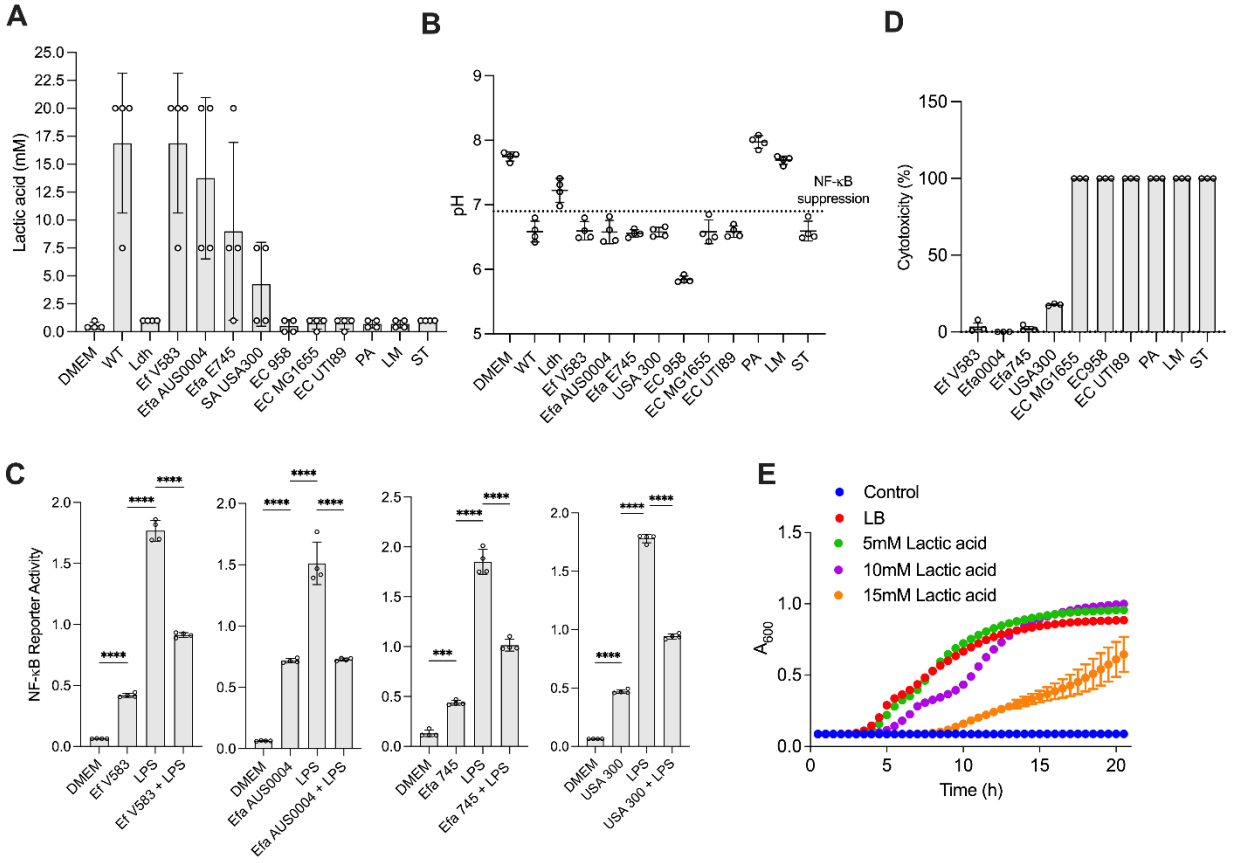

1855 **Figure S19 – Lactic acid-producing species acidify the medium and suppress**
1856 **macrophage NF-κB activation at high MOI.**
1857 **(A)** Lactic acid concentration of several bacterial species grown in cell culture media
1858 at initial MOI 100 measured after 6 hpi. **(B)** Extracellular pH following bacterial growth
1859 in cell culture media with starting inoculum equivalent to MOI 100 measured after 6
1860 hpi. **(C)** RAW 264.7 macrophages were infected with the non-cytotoxic bacterial
1861 species of *E. faecalis* strain V583, *E. faecium* strains AUS0004 and E745 and *S.*
1862 *aureus* strain USA300 at initial MOI 100 for 6 h prior to NF-kB reporter assay. **(D)** RAW
1863 264.7 macrophages were infected with different bacterial species at initial MOI 100 for
1864 6 h prior to LDH assay to measure cytotoxicity. Data (mean ± SEM) are summary of
1865 at least 2 independent experiments **(A-D)**. Statistical analysis was performed using
1866 ordinary one-way ANOVA followed by Tukey's multiple comparison test **(C)** ***$p<0.001$,
1867 and ****$p<0.0001$. **(E)** Growth curve for *E. coli* strain UTI89 grown overnight in LB
1868 media supplemented with different concentration of lactate.
1869
1870
1871
1872
1873
1874
1875
1876
1877
1878
1879
1880

Supplementary Tables

1914

1915

1916

1917 **Table S1 –** Differentially expressed NF-κB/ AP-1-related genes

		Condition					
		Uninfected LPS-treated vs uninfected untreated		MOI 100 untreated vs uninfected untreated		MOI 100 LPS-treated vs uninfected LPS-treated	
Gene	**Gene product**	**Log2FC**	**Significant?**	**Log2FC**	**Significant?**	**Log2FC**	**Significant?**
NF-κB							
Tlr4	TLR4	-0.84	No	-0.66	No	-1.33	No
Cd14	CD14	2.15	Yes	0.31	No	-2.13	Yes
Myd88	MyD88	1.11	No	-1.06	No	-1.86	Yes
Tirap	TIRAP	0.38	No	-1.03	No	-1.16	No
Ly96	MD-2	0.89	No	0.29	No	-0.14	No
Ticam1	TRIF	1.84	No	1.59	Yes	0.28	No
Ticam2	TRAM	-1.35	No	1.28	No	2.48	Yes
Traf6	TRAF6	0.46	No	0.57	No	-0.09	No
Map3k7	TAK1	-0.06	No	0.07	No	0.17	No
Chuk	IKKα	0.32	No	0.35	No	0.004	No
Ikbkb	IKKβ	0.37	No	-0.02	No	-0.13	No
Nfkbia	IKBα	2.95	Yes	3.01	Yes	0.95	No
Rel	c-Rel	1.60	Yes	1.70	Yes	0.29	No
Rela	p65	-0.07	No	0.41	No	0.59	No
Relb	RelB	1.26	No	2.33	Yes	1.01	No
Nfkb1	p105	3.20	Yes	2.33	Yes	0.11	No
Nfkb2	p100	1.98	Yes	1.84	Yes	0.89	No
AP-1							
Mapk14	p38	-0.62	No	-1.87	Yes	-0.94	No

Mapk8	JNK	0.28	No	0.54	No	0.40	No
Jun	cJun	0.47	No	0.82	No	-0.34	No
Fos	cFos	0.39	No	-0.65	No	-1.79	Yes
Common							
Rps6ka5	MSK1	-2.58	Yes	-1.87	Yes	-0.99	No
Rps6ka4	MSK2	0.29	No	-0.30	No	0.22	No
Mapk3	ERK1	0.22	No	0.87	No	1.00	No
Mapk1	ERK2	-0.09	No	0.11	No	0.05	No

1935 **Table S2-** List of hits after transposon screen for genes that contribute to suppress

1936 NF-κB activation in macrophages

Gene	Gene product	Locus tag
OG1RF_10013	Adenylosuccinate synthase	OG1RF_10013
mptD	Mannose PTS enzyme IID component	OG1RF_10021
ldh1	L-lactate dehydrogenase 1	OG1RF_10199
OG1RF_10329	PaaI family thioesterase	OG1RF_10329
OG1RF_10418	YlbF family regulator	OG1RF_10418
pptB	ABC-family peptide pheromone efflux transporter, membrane protein	OG1RF_10427
rpoN	RNA polymerase factor sigma-54	OG1RF_10514
pgmB	β-phosphoglucomutase	OG1RF_10682
dapA	4-hydroxy-tetrahydrodipicolinate synthase	OG1RF_10956
yycH	YycH protein	OG1RF_10967
trpX	Tryptophan ABC transporter substrate-binding protein	OG1RF_11022
OG1RF_11023	ABC transporter permease	OG1RF_11023
OG1RF_11036	Putative transporter, P-type ATPase family	OG1RF_11036
OG1RF_11131	ABC transporter ATP-binding protein/permease	OG1RF_11131
nrnA	5'-3' exonuclease NrnA	OG1RF_11161
OG1RF_11270	Hypothetical protein	OG1RF_11270
aroE	Shikimate dehydrogenase	OG1RF_11280
aroC	Chorismate synthase	OG1RF_11283
tkt	Transketolase	OG1RF_11300
pflB	Formate C-acetyltransferase	OG1RF_11329
lepB	Signal peptidase I	OG1RF_11391

pbp1B	putative bifunctional peptidoglycan glycosyltransferase/DD-transpeptidase, penicillin-binding protein 1B	OG1RF_11450
OG1RF_11602	Putative transporter, P-type ATPase family	OG1RF_11602
dcm	DNA (cytosine-5-)-methyltransferase	OG1RF_11622
relA	Bifunctional (p)ppGpp synthase/hydrolase	OG1RF_11636
OG1RF_11669	DUF1033 family protein	OG1RF_11669
efaC	Mn^{2+} ABC transporter ATP-binding protein	OG1RF_11677
efrE	ABC family efflux transporter ATP-binding protein/permease EfrE	OG1RF_11766
OG1RF_11854	Metalloregulator ArsR/SmtB family transcription factor	OG1RF_11854
OG1RF_11923	Hypothetical protein	OG1RF_11923
OG1RF_12024	ABC transporter ATP-binding protein	OG1RF_12024
OG1RF_12033	ATP-dependent RecD-like DNA helicase	OG1RF_12033
OG1RF_12043	ClpXP adapter SpxH family protein	OG1RF_12043
OG1RF_12058	SMC family ATPase	OG1RF_12058
OG1RF_12066	5-bromo-4-chloroindolyl phosphate hydrolysis family protein	OG1RF_12066
OG1RF_12113	ABC transporter permease	OG1RF_12113
OG1RF_12190	YkuJ family protein	OG1RF_12190
OG1RF_12284	Putative transporter, sulfate permease family	OG1RF_12284
ireP	PP2C-type protein-serine/threonine phosphatase	OG1RF_12385
def	Peptide deformylase	OG1RF_12388
OG1RF_12401	Gluconate-specific PTS enzyme IID component	OG1RF_12401
OG1RF_12446	ArgE/DapE family deacylase	OG1RF_12446

OG1RF_12459	Isochorismatase/nicotinamidase	OG1RF_12459
menA	1,4-dihydroxy-2-naphthoate polyprenyltransferase	OG1RF_12507
croS	HAMP domain-containing sensor histidine kinase	OG1RF_12536
citE	Citrate (pro-3S)-lyase subunit beta	OG1RF_12565
citC	[citrate (pro-3S)-lyase] ligase	OG1RF_12567

1937

1938

1939

1940

1941

1942

1943

1944

1945

1946

1947

1948

1949

1950

1951

1952

1953

1954

1955

1956 **Table S3 –** Cytotoxicity as measured by LDH assay of compounds used in this

1957 study.

Condition	% Cytotoxicity	Source
DMEM (Baseline)	5.15	Gibco
Stattic (10 μM)	14.92	MedChemExpress
ML115 (1 μM)	12.01	MedChemExpress
2NP (45 μM)	25.34	MedChemExpress
Selu (1 μM)	15.33	MedChemExpress
Fluda (40 μM)	12.01	MedChemExpress
CHC (5 mM)	15.54	MedChemExpress
MDL-12 (20 μM)	11.58	MedChemExpress
TrichoA (10 nM)	19.47	MedChemExpress
TubA (15 nM)	4.92	MedChemExpress
Ele (1 μM)	5.54	MedChemExpress
HDAC8-IN-1 (100 nM)	5.01	MedChemExpress
TMP-269 (10 μM)	26.12	MedChemExpress
9-HAS (100 μM)	27.80	MedChemExpress

1958

1959

1960

1961

1962

1963

1964

1965 **Table S4-** Strains used in this study

1966

Strain	Reference
E. faecalis OG1RF	[102]
E. faecalis OG1RF Ldh (Δldh1Δldh2)	This study
E. faecalis OG1RF Δldh1	This study
E. faecalis OG1RF Δldh2	This study
E. faecalis OG1RF pldh1 (+ pGCP123::*ldh1)*	This study
E. faecalis V583	[103]
E. coli MG1655	[104]
E. coli EC958	[105]
E. coli UTI89	[106]
S. aureus USA300	[107]
S. *typhimurium* 14028S	[108]
P. aeruginosa PAO1	[109]
E. faecium E745	[110]
E. faecium AUS0004	[111]
Listeria monocytogenes ATCC19115	[112]

1967
1968

1969

1970

1971 **Table S5-** List of primers used in this study

Gene	Oligo Name	Sequence 5' to 3'
ldh deletion		
ldh1	dLDH1_For	CATGCTCGAGCGGCCATTATATGTTGGCACATCCAGG
	dLDH1_Rev	CAGTGTGCTGGAATTAATTTAACGCACTCACTCGAT
	dLDH1_SewF	AAGCGGAGTAACAATAGTGGGTAGCTCTTACATGTGCGTAAT
	dLDH1_SewR	ATTACGCACATGTAAGAGCTACCCACTATTGTTACTCCGCTT
	LDH1_F	GAAGAATAAATTAACCATTGCTTCTTCATC
	LDH1_R	CTTATCTCACGCATTAGCATTTAC

ldh2	dLDH2_For	CATGCTCGAGCGGCCGTCGTTTACTCTGTCCATCATTT
	dLDH2_Rev	CAGTGTGCTGGAATTTTTTCATTGTCCAGACCGAT
	dLDH2_SewF	ATAATCGCGTTGTGTACTTCACACGAACTTTTTAGGTGTGGTT
	dLDH2_SewR	AACCACACCTAAAAAGTTCGTGTGAAGTACACAACGCGATTAT
	LDH2_F	GAGGCAATTACTAAAATTCCATCAAAAC
	LDH2_R	CAATTGACTTATTAGATGGTGTGTCTT
ChIP-qPCR		
Myd88 (R1)	M_STAT3_1_F	GGCCCCGTAGTCTAG
	M_STAT3_1_R	CGCCTGTGGAGTTTC
Myd88 (R2)	M_STAT3_2_F	GGAAGCCAATCGTAATG
	M_STAT3_2_R	AAGGGGAGGGACTCC
Myd88 (R3)	M_STAT3_3_F	GCATCGGTGAGGAAAC
	M_STAT3_3_R	CCTCCCTAGCGCACC
Gapdh	M_gapdh_F	GCCCTTCTACAATGCCAAAG
	M_gapdh_R	TTGTGATGGGTGTGAACCAC
siRNA RT-PCR		
Hcar1	GPR81_M_F	GGTGGCACGATGTCATGTT
	GPR81_M_R	GACCGAGCAGAACAAGATGATT
SLC16A1	MCT1_M_F	TTGTCTGTCTGGTTGCGGCTTGATCG
	MCT1_M_R	CACCTCCAATAACACCAATG
Gpr65	GPR65_M_F	TGCGGCACAACCAAGCCACGGA
	GPR65_M_R	ATGTCGCGCTCTAAAACGCAGCG

qRT-PCR		
Cd14	CD14_F	TTGAACCTCCGCAACGTGTCGT
	CD14_R	CGCAGGAAAAGTTGAGCGAGTG
Myd88	Myd88_F	ACCTGTGTCTGGTCCATTGCCA
	Myd88_R	GCTGAGTGCAAACTTGGTCTGG
Tlr4	Tlr4_F	AGCTTCTCCAATTTTTCAGAACTTC
	Tlr4_R	TGAGAGGTGGTGTAAGCCATGC
Tlr2	Tlr2_F	ACAGCAAGGTCTTCCTGGTTCC
	Tlr2_R	GCTCCCTTACAGGCTGAGTTCT
Il1b	Il1b_F	TGGACCTTCCAGGATGAGGACA
	Il1b_R	GTTCATCTCGGAGCCTGTAGTG
Hif1a	Hif1a_F	CCTGCACTGAATCAAGAGGTTGC
	Hif1a_R	CCATCAGAAGGACTTGCTGGCT
Stat3	Stat3_F	AGGAGTCTAACAACGGCAGCCT
	Stat3_R	GTGGTACACCTCAGTCTCGAAG
Rela	Rela_F	TCCTGTTCGAGTCTCCATGCAG
	Rela_R	GGTCTCATAGGTCCTTTTGCGC
p105	p105_F	GCTGCCAAAGAAGGACACGACA

	p105_R	GGCAGGCTATTGCTCATCACAG
p100	p100_F	TGCTGATGGCACAGGACGAGAA
	p100_R	GTTGATGACGCCGAGGTACTGA
Mapk1	Mapk1_F	TCAAGCCTTCCAACCTCCTGCT
	Mapk1_R	AGCTCTGTACCAACGTGTGGCT
Il10	Il10_F	CGGGAAGACAATAACTGCACCC
	Il10_R	CGGTTAGCAGTATGTTGTCCAGC

1972